

# OWTNM 2006

**XV International Workshop on  
Optical Waveguide Theory and Numerical Modelling Workshop**



**OPTICAL COMMUNICATION GROUP  
DIPARTIMENTO DI ELETTRONICA E INFORMAZIONE  
POLITECNICO DI MILANO**

## Preface

This year occurs the 15<sup>th</sup> Anniversary of the International Workshop on Optical Waveguide Theory and Numerical Modelling. In the last 15 years the world of optical communications, the required optical devices, the technological processes and the available computer capabilities have experienced a substantial development but this Workshop continues to maintain and even increase a prime interest.

The aim of the OWTNM Workshop is to promote personal contact and exchange of ideas among scientists working in the field of numerical modelling and theoretical description of optical waveguide structures and devices. The Workshop aims to put in evidence problems, doubts, difficulties and therefore stimulate cooperation and promote synergy and new contact among groups. This meeting has a strong focus on modelling and simulation in the optical domain and provides a forum for discussing the most up-to-date aspects within an international audience. Topics of interest include but are not limited to: *Theory of passive, active and nonlinear waveguides; Photonic bandgap structures and photonic crystals; Photonic nanostructures; Plasmons and metamaterials in optics; Advances in numerical methods; Progress in mode solvers; Mathematical models and numerical methods; Simulation and design of photonic devices and integrated systems; Input/output waveguide coupling aspects; Device and system-oriented modelling; Coupling of electronic, optical, elastic and thermal effects; Waveguide grating structures.*

The 15<sup>th</sup> OWTNM Anniversary is held in Varese - Italy, a quiet and convenient place near Milano. The organization has been entrusted to the Optical Communication Group of the Department of Electronic and Information of the Politecnico di Milano, under the supervision of Prof. Andrea Melloni. The previous editions took place in Sydney - Australia (2005), Grenoble - France (2005), Ghent - Belgium (2004), Prague - Czech Republic (2003), Nottingham - UK (2002), Paderborn - Germany (2001), Prague - Czech Republic (2000), St. Etienne - France (1999), Hagen - Germany (1998), Enschede - The Netherlands (1997), Roosendaal - The Netherlands (1995), Siena - Italy (1994), Vevey - Switzerland (1993) and in Teupitz - Germany in 1992 where OWTNM was born.

Hence, researchers, device engineers, software developers, students and whoever interested in theory, modelling, simulation, and analysis of optical waveguide structures and devices periodically meet to share recent results, improvements in the field and discuss doubts and problems. This progress is supervised by members of the OWTNM Technical Committee, including Trevor Benson (*University of Nottingham, UK*), Jiri Ctyroky (*IREE AS CR, Czech Republic*), Anand Gopinath (*University of Minnesota, USA*), Hans-Peter Nolting (*HHI Berlin, Germany*), Hugo J. W. M. Hoekstra (*University of Twente, Netherlands*), Olivier Parriaux (*University of Saint Etienne, France*), Reinhold Pregla (*FernUniversität Hagen, Germany*), Christoph Wächter (*Fraunhofer IOF, Jena, Germany*) and Peter Bienstman (*Ghent University, Belgium*).

This year, 7 invited contributions, 42 oral contributions and 30 posters form an attractive and high-level programme covering different areas and aspects. The 42 oral presentations have been organized in the following 7 sessions: *Photonic Crystal and Wires; Photonic Crystal and Plasmons; Circuits and fibers modelling; Photonic Crystal Fibre; Dissipative solitons and numerical techniques; Gratings and coupling; Nonlinear effects modelling.*

Editor:  
Andrea Melloni, PhD  
Associate Professor  
Politecnico di Milano  
Dipartimento di Elettronica e Informazione

Contact:  
Andrea Melloni  
Piazza Leonardo da Vinci, 32  
I - 20133 Milano, Italy  
e.mail: melloni@elet.polimi.it  
website: <http://www.elet.polimi.it/upload/melloni/index.html>

2006 Politecnico di Milano - Dipartimento di Elettronica e Informazione

ISBN 88-902405-0-4

Printed in Milano - Italy

The 7 invited talks, covering almost the whole spectrum of the topics of the Workshop, are given by: Wolfgang Freude (*Nanostrip and Photonic Crystal Waveguides: The Modelling of Imperfections*); Jerome Moloney (*Ultrashort Vectorial Pulse Propagators*); Georgios Veronis (*Frequency-domain modeling of photonic crystal and plasmonic devices*); Mauro Mongiardo (*Hybrid and network methods in electromagnetic simulation*); Yehuda Leviatan (*A source model technique (SMT) for the analysis of the modal fields of Photonic Crystal Fibers*); Falk Lederer (*Dissipative solitons*); Philippe Lalanne (*Grating and waveguide concepts in photonic crystal devices*).

This year, for the first time and in occasion of the 15<sup>th</sup> Anniversary, a CD collecting all the presentations, both oral and posters, has been prepared and delivered to the participants at the Workshop. This effort will permit to keep track of the details of the presentations that, sometimes, fade for ever in our busy days.

As tradition, some of the papers presented either as oral or poster from the Workshop will appear in a Special Issue of Optical and Quantum Electronics Journal on the topic "Optical Waveguide Theory and Numerical Modelling".

This booklet includes abstracts of all the contributions presented. The order follows the time schedule at the Workshop.

Information about the OWTNM 2006, including the programme and local travel information can be found at the Workshop's website [www.elet.polimi.it/conferences/owtnm06](http://www.elet.polimi.it/conferences/owtnm06).

Last but not least, we would like to thank all individuals and institutions that have contributed to the organization, the support and the success of the Workshop, invited speakers, authors of papers, sponsors and ...our families!

Varese, April 2006



**Chairman OWTNM  
2006**

## Proceedings

## Nanostrip and Photonic Crystal Waveguides: The Modelling of Imperfections

Wolfgang Freude\*, Christopher G. Poulton\*, Christian Koos\*, Jan Brosi\*, Masafumi Fujii†, Andreas Pfrang‡, Thomas Schimmel‡, Manfred Müller\*, Juerg Leuthold\*

\*Institute of High-Frequency and Quantum Electronics, University of Karlsruhe, Germany

†Department of Electrical, Electronic and System Engineering, University of Toyama, Japan

‡Institute of Applied Physics, University of Karlsruhe, Germany

w.freude@ihq.uni-karlsruhe.de — www.ihq.uni-karlsruhe.de

Scattering loss in rough rectangular high index-contrast nanostrips is predicted with a new semi-analytical model employing true 3D radiation modes. Surface roughness in photonic crystal line defect waveguides is treated with a fast 2D semi-analytical method, with 3D FDTD numerics, and with microwave measurements.

### Summary

*Nanostrip roughness* Even the most advanced waveguides exhibit sidewall deviations of several nanometers [1][2], and this leads to attenuation due to reflection and to scattering into the radiation field. Unfortunately, standard numerical techniques such as FDTD require large amounts of resources to accurately model these effects. We developed a new perturbation model [3], which accurately predicts the attenuation due to sidewall roughness in high-contrast integrated optical waveguides. Previous approaches [4][5] approximated the radiation field using radiation modes which were either two-dimensional or appropriate only for low-contrast materials, and this can lead to predictions which are incorrect by up to an order of magnitude. We construct here the fully 3D radiation modes which are appropriate for rectangular, high index-contrast waveguides, Fig. 1a.

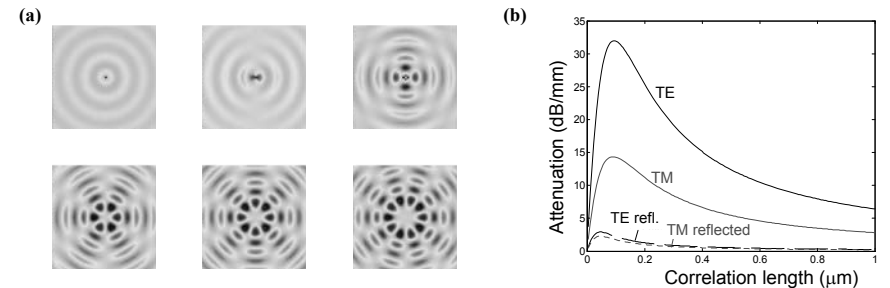


**Fig. 1** Square silicon nanostrip waveguide, operating wavelength 1.55 μm, width 420 nm, RMS sidewall roughness 5 nm (a) 3D radiation modes representing the scattered fields (b) Attenuation vs. correlation length

We determined experimentally the statistical sidewall roughness characteristics of an InGaAsP/InP pedestal waveguide by atomic force microscopy. Using these parameters, the prediction by the perturbation model agrees well with the measured attenuation. Further, we developed a wavelet based FDTD collocation method [6], and implemented it on a parallel IBM cluster (SP-SMP) consisting of 256 processors, each with a clock rate of 375 MHz and an available memory of 1 GB. Because of “limited” computing resources we investigated a 30 μm long waveguide with a rather large RMS roughness of 50 nm. The simulated attenuation agrees well with the results predicted by our model.

*Photonic crystal disorder* High refractive index contrasts allows the creation of large band-gaps in photonic crystals, so that light becomes more tightly confined to guiding defect structures. The strong contrast, however, can markedly increase scattering due to crystal imperfections [7] [8].

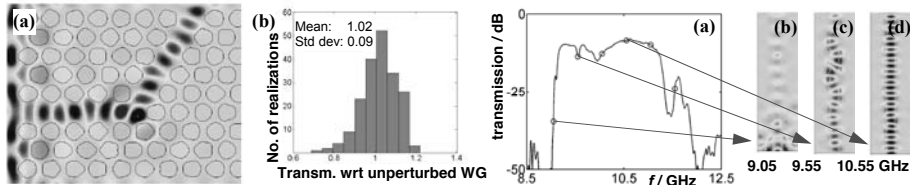


**Fig. 2** Line defect waveguide bend in a perturbed photonic crystal. (a) Magnitude of out-of-plane component of the magnetic field for a single realization. (b) Transmission histogram relative to unperturbed bend for 194 realizations

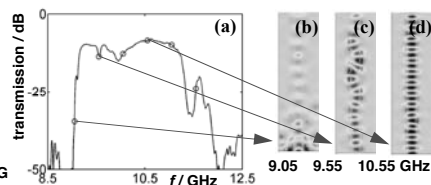


**Fig. 3** W1 line defect waveguide with 10% radial disorder (a) Measured transmission with random resonances (b)–(d) FDTD simulations of quasi-TE electric field for various frequencies

Fig. 2a shows a 2D photonic crystal line defect waveguide bend. It consists of a triangular array of infinitely long cylindrical air holes in InP with a period of  $a = 484$  nm, operated at a wavelength of  $1.55$   $\mu\text{m}$  within the bandgap. The air-holes are randomly deformed circles with a mean radius of  $r = 186$  nm and an RMS deformation of  $10$  nm ( $5\%$  of  $r$ ). We simulate this structure with a semi-analytical technique [9] treating the sidewall deviation as a small perturbation. The response of a single cylinder to an arbitrary external field can then be calculated, and the interactions between the cylinders are computed with a multipole method for successively higher perturbation orders, Fig. 2. — For disordered line defect *slab* waveguides, a 3D technique was published recently [10].

*Microwave modelling of photonic crystal disorder* Using a kind of “analogue computer”, we studied the influence of positional and radial disorder with a microwave model. We upscaled the structure by about 20 000 while decreasing the frequency by the same factor from 193 THz to about  $f = 10$  GHz [11]. The dielectric is a ceramic-filled plastic with  $\epsilon_r = 9.8$ , similar to silicon in the optical range. We measured amplitude and phase in transmission, Fig. 3a, and reflection. From the transmission phase factor the band diagram may be obtained. Interestingly, the bands are only slightly affected by the disorder which, however, leads to random resonances in transmission, Fig. 3a,b–d. This is connected to the concept of Anderson localization in solid state physics.

## References

- [1] P. Dumon et al., Low-loss SOI photonic wires and ring resonators fabricated with deep UV lithography, *IEEE Photon. Tech. Lett.*, 15, 1328–1330, 2004.
- [2] T. Tsuchizawa et al. “Microphotonics devices based on silicon microfabrication technology, *IEEE J. Sel. Top. Quantum Electron.*, 11, 232–240, 2005.
- [3] C. G. Poulton, C. Koos, M. Fujii, A. Pfrang, Th. Schimmel, J. Leuthold, W. Freude, Radiation modes and roughness loss in high index-contrast waveguides, *IEEE J. Sel. Topics Quantum Electron.* (submitted).
- [4] D. Marcuse, *Theory of dielectric optical waveguides*, Academic Press, London 1974, 95–172.
- [5] D. Lenz, D. Erni, W. Bächtold, Modal loss coefficients for highly overmoded rectangular dielectric waveguides based on free-space modes, *Optics Express*, 12, 1150–1156, 2004.
- [6] M. Fujii, W. J. R. Hofer, Interpolating wavelet Galerkin model of time dependent inhomogeneous electrically-large optical waveguide problems, *IEEE MTT-S Int. Microwave Symposium Digest*, June 2001. Paper WE3F-5.
- [7] W. Bogaerts et al., Scattering at sidewall roughness in photonic crystal slabs, *Opt. Lett.* 28, 689–691, 2003.
- [8] S. J. McNab, N. Moll, Y. A. Vlasov, Ultra-low loss photonic integrated circuit with membrane-type photonic crystal waveguides, *Opt. Expr.* 11, 2927–2939, 2003.
- [9] C. G. Poulton, M. Müller, W. Freude, Scattering from sidewall deformations in photonic crystals, *J. Opt. Soc. Am. B* 22, 1211–1220, 2005.
- [10] D. Gerace, L. C. Andreani, Low-loss guided modes in photonic crystal waveguides, *Opt. Expr.* 13, 4939–4951, 2005.
- [11] W. Freude, G.-A. Chakam, J.-M. Brosi, C. Koos, Microwave modelling of photonic crystals, In: K. Busch, S. Lölkes, R. Wehrspohn, H. Föll (Eds.): *Photonic Crystals — Advances in Design, Fabrication, and Characterization*. Wiley VCH, Berlin 2004, 198–214.

## Impairment of Photonic-Crystal Waveguide Taper due to Hole Inaccuracy

Lorenzo Rosa, Federica Poli, Matteo Foroni, Annamaria Cucinotta, Stefano Selleri  
 Dip. di Ingegneria dell'Informazione, Università di Parma, Parco Area delle Scienze, 181/A, Parma, Italy

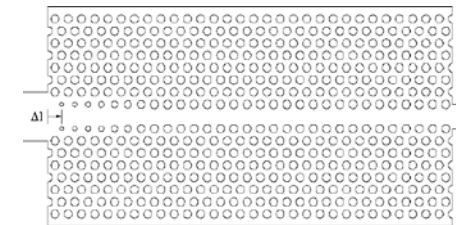
[stefano.selleri@unipr.it](mailto:stefano.selleri@unipr.it)

Tapers between photonic-crystal and  $2\sqrt{3}$   $\Lambda$ - and  $3\sqrt{3}$   $\Lambda$ -size wire-waveguides can have their transmission performance impaired by values as great as 35% if the taper holes are inaccurately etched.

## Summary

Photonic crystal waveguides (PCWs) are useful optical structures that can be obtained by introducing a line defect perturbing the refractive index of a periodic lattice constructed by etching air holes into a dielectric substrate. In developing PCWs it is fundamental to design adapting structures to interface them with optical fibers. Recently an approach has been proposed which, by tapering the air holes nearest to the interface and displacing them, can provide transmission higher than 90% over bandwidths of hundreds of nanometers [1,2]. However, performance is closely related to the hole diameter variation law, so it is important to investigate the sensitivity of the transmission spectra with respect to hole diameter variation caused by etching inaccuracy. The analysis is based on the optimal tapers presented in [2] for different input waveguide sizes and studies the performance impairments caused by varying the hole diameters in representative cases, up to the situation where there is no hole tapering at all.

The PCW parameters are the same as in [2], where substrate refractive index is 2.94, air index is 1, lattice period is  $\Lambda=430$  nm and unperturbed air-hole diameter is  $d=258$  nm. Wn denotes a PCW formed by removing n rows of air holes from the lattice, while  $\Delta z$  indicates the relative displacement of the first pair of holes centers in the taper from the wire-PCW interface, as shown in the figure.



Coupling is considered between input waveguides of  $W3$ -size, that is with an input width  $w = 2\sqrt{3}$   $\Lambda$ , and  $W5$ -size, that is  $w = 3\sqrt{3}$   $\Lambda$ , with a  $W1$  PCW, while the taper holes are progressively enlarged up to the diameter of the unperturbed ones. Results show a 8% to 35% additional loss for the  $2\sqrt{3}$   $\Lambda$  input waveguide width, while for the  $3\sqrt{3}$   $\Lambda$  input waveguide width the decrease is no worse than 15%. It is shown that tapers using a lesser number of different-diameter holes, as well as holes with diameters slightly reduced with respect to the unperturbed ones, are less sensitive to building errors. Related results will be shown at presentation time.

## References

- [1] L. Rosa, S. Selleri, and F. Poli, *IEEE J. Lightwave Technol.*, vol. 23, n. 9, pp. 2740–2745, 2005.
- [2] L. Rosa, F. Poli, M. Foroni, and S. Selleri, *ICTON 2005*, Tu.P.1, Barcelona, 2005.

## Damping of TE Waves in an InP Based Photonic Crystal Waveguide

Zsolt Szabó\* and György Kádár\*\*

\* Nanophysics Group, Nanomaterials Laboratory, National Institute for Materials Science, 1-1 Namiki, Tsukuba 305-0044, Japan

\*\*Research Institute for Technical Physics and Materials Science, H-1525 Budapest, POB 49, Hungary kadargy@mfa.kfki.hu

The damping of electromagnetic waves in a waveguide has been investigated by simulating the wave propagation with the Finite Difference Time Domain (FDTD) method. The waveguide consists of defect lines in an InP based two-dimensional photonic crystal. Both the loss due to the dispersive absorption of the material and the additional leakage loss from the waveguide to the photonic crystal were calculated and then their sum was compared to measured data.

### Summary

A two dimensional photonic crystal was studied which consists of a triangular array of holes (see Figure 1.) carved into the InP bulk material. The waveguide is formed by a defect line of the periodic structure leaving intact the bulk InP in the place of the middle three lines of holes. The dimensions of the photonic crystal are taken from an experimental work [1] and the dispersion curve of InP is considered. A band gap frequency is selected, the propagating energy density is computed along the length of the waveguide and then it is averaged for time and for the cross-section. The ratio between the cases with and without loss is calculated and illustrated in Figure 2. This same ratio is calculated in the bulk InP without photonic crystal structure too, and compared with that obtained in the photonic crystal waveguide. This is a way, how a distinction can be made between the losses caused by the conductivity of the material and losses due to the leakage of the electromagnetic waves into the photonic crystal.

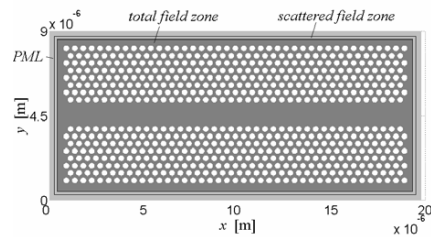


Figure 1. Geometry of the waveguide

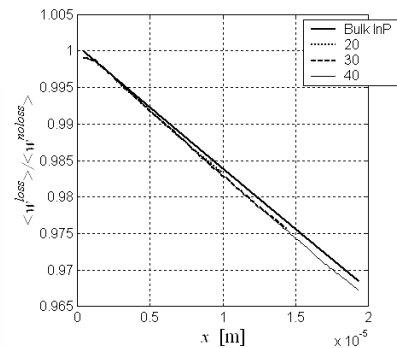


Figure 2. Damping of TE wave in the waveguide

The measured loss was given [1] as 110 dB/cm which should be compared with our calculated 75dB/cm value. The irregularities of the realized geometry and the imperfections of the experimental measurement might explain the rather higher measured than calculated damping.

### References

[1] A. Talneau, L. Le Gouezigou, N. Boudma, Optics Letters, 26 (16) 1259-1261 2001

## Modelling lossy photonic wires: a mode solver comparison

P. Bienstman<sup>(a)</sup>, S. Selleri<sup>(b)</sup>, H.P. Uranus<sup>(c)</sup>, W.C.L. Hopman<sup>(c)</sup>, A. Melloni<sup>(d)</sup>, R. Costa<sup>(e)</sup>, L.C. Andreani<sup>(f)</sup>, P. Lalanne<sup>(g)</sup>, J.P. Hugonin<sup>(g)</sup>, D. Pinto<sup>(h)</sup>, S.S.A. Obayya<sup>(h)</sup>

<sup>(a)</sup> Peter.Bienstman@UGent.be, Ghent University, Sint-Pietersnieuwstraat 41, 9000 Ghent, Belgium

<sup>(b)</sup> Università degli Studi di Parma, Parco Area delle Scienze 181/A, I-43100 Parma, Italy

<sup>(c)</sup> University of Twente, P.O. Box 217, 7500 AE, Enschede, The Netherlands.

<sup>(d)</sup> Dipartimento di Elettronica e Informazione, Politecnico di Milano, Via Ponzio 34/5, Milano, Italy

<sup>(e)</sup> CoreCom, Via G. Colombo 34/5, Milano, Italy

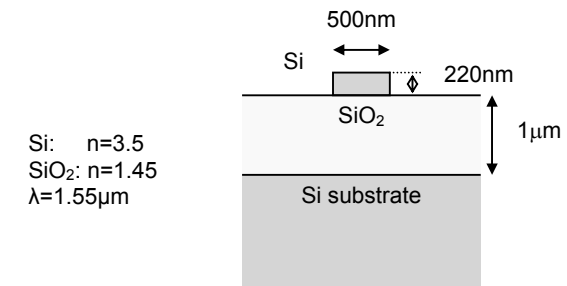
<sup>(f)</sup> Dipartimento di Fisica "A. Volta", Università degli Studi di Pavia, Via Bassi 6, I-27100 Pavia, Italy

<sup>(g)</sup> Institut d'Optique, Centre scientifique - Bâtiment 503, 91403 Orsay, France

<sup>(h)</sup> School of Engineering and Design, Brunel University, Uxbridge, Middlesex UB8 3PH, UK

During the past decade, there has been a tradition of comparing the current state-of-the-art optical mode solvers from time to time [1]. In the framework of the European COST P11 action [2], we performed such a comparison, but this time with an additional complication, namely the modeling of an extremely small loss in the propagation constant due to substrate leakage.

The structure we modeled is the following photonic wire structure in the SOI material system:



Because of the limited thickness of the oxide buffer, some part of the power in the fundamental mode will leak to the substrate. The aim of this exercise was to calculate the complex propagation constant of the fundamental mode of this structure as accurately as possible.

We will present results from a wide variety of models, ranging from different finite-elements solvers, effective index and perturbation methods, fourier modal methods and film mode matching methods.

### References

[1] J. Ctyroky, S. Helfert, R. Pregla, P. Bienstman, R. Baets, R. De Ridder, R. Stoffer, G. Klaasse, J. Petracek, P. Lalanne, J. P. Hugonin, and R. M. De La Rue, "Bragg waveguide grating as a 1D photonic band gap structure: COST 268 modelling task," OPT QUANT ELECTRON, vol. 34, pp. 455-470, 2002.

[2] COST P11 website: <http://w3.uniroma1.it/energetica/>

## Design optimisation for a generic planar scattering platform

Carl Styan, Ana Vukovic, Phillip Sewell, Trevor Benson  
George Green Institute for Electromagnetics Research, University of Nottingham, Nottingham, UK  
[exxcjs@nottingham.ac.uk](mailto:exxcjs@nottingham.ac.uk)

A methodology for the design of functional integrated optical components is presented.

### Introduction

The 2D slab photonic crystal (PhC) [1] has become popular due to its relative ease of fabrication and the availability of modeling tools that can simulate the approximate 2D structure. Many novel slab PhC configurations have been developed through user intuition; compact optical components including waveguides, tapers, resonators and filters. Increasingly to improve the operation of such structures and further reduce losses design optimisation techniques are being applied to the refinement of PhC structures. Rather than simply improve existing designs Håkansson et al have investigated Genetic Algorithm (GA) optimization used to create novel scattering components based upon regular PhC lattices with possible defects at each PhC lattice point [2]. In [3] Gheorma et al apply optimisation techniques to refine the relative position of scattering elements and generate aperiodic structures with tailored transmission characteristics. In reality there are restrictions on the size of structure that can be simulated and optimised and therefore in the majority of cases only a small section of the structure is chosen for refinement. While this approach allows shorter runtimes and ensures convergence of the optimisation routines it loses a level of generality.

We believe that we are now at a point where the potential exists for the development of a generic platform that can be optimised to provide one of a number of multiple functionalities and which is no longer constrained by the existence of a formal lattice. Building on our past expertise in the optimisation of photonic devices using adaptive accuracy within GA [4] we focus on the use of GA to find optimal 2D scattering structures. The particular layout is optimised so that the multiple scattering from the lattice elements provides a desired functional element between input and output ports, tailored to a given specification. A multiple scattering [5] technique is employed along with complex source point excitation to model the field within the device. The requirement for numerous highly accurate numerical simulations leads to increasingly long runtimes. We demonstrate how such problems can be tackled with large-scale parallel computing resources, distributing optimisation and how managing the existing simulation tools more effectively within the global optimisation can reduce overall design time. In this work we outline the required capabilities for enabling efficient design optimisation and provide illustrative examples.

### References

- [1] S. G. Johnson, J. D. Joannopoulos, "Photonic crystals: the road from theory to practice", Kluwer Academic, 2002.
- [2] A. Håkansson, J. Sánchez-Dehesa, and L. Sanchis, "Inverse Design of Photonic Crystal Devices," *IEEE J. Selected Areas in Comm.*, vol. 23, no. 7, 1365-1371, (2005).
- [3] I. Gheorma, S. Haas, and A. Levi, "Aperiodic nano-photonic design," *J. Appl. Phys.*, vol. 95, 1420-1426, (2004).
- [4] C. Styan, A. Vukovic, P. Sewell, T.M. Benson, "An Adaptive Synthesis Tool for Rib Waveguide Design", *Journal of Lightwave Tech.*, vol. 22, Issue 12, pp 2793- 2800, Dec. 2004.
- [5] D. Felbacq, G. Tayeb, and D. Maystre, "Scattering by a random set of parallel cylinders," *J. Opt. Soc. Am. A*, vol. 11, 2526-2538 (1994).

## Modeling of Membrane Photonic Crystal Defect Cavities for Semiconductor Quantum Wire Laser Applications

K.F. Karlsson, K.A. Atlasov, and E. Kapon  
Ecole Polytechnique Fédérale de Lausanne (EPFL), Laboratory of Physics of Nanostructures  
CH-1015 Lausanne, Switzerland  
[fredrik.karlsson@epfl.ch](mailto:fredrik.karlsson@epfl.ch)

Two-dimensional (2D) semiconductor photonic-crystal (PhC) membrane-based microcavities can provide a very tight confinement of the electro-magnetic field, making it possible to achieve very high Q-factors and small mode-volumes for certain resonant frequencies [1]. Such a microcavity allows control of the spontaneous emission for an incorporated internal light source, and is promising for attaining ultra-low or thresholdless lasing phenomenon if integrated with a high material gain active medium. A quantum wire (QWR) may serve as such an active medium [2]. In addition, extending a cavity in one direction will alter its behavior toward 1D photonic wire, and 1D-polariton formation may be expected as a result of the integration with such a QWR.

In the present contribution we study the  $L_x$ -cavity type ( $x$  missing holes in a row) in a hexagonal photonic lattice using fast 2D finite-difference (FD) eigenvalue calculations relying on the effective-index approximation. Final refinement and verification are done by full three-dimensional (3D) finite-difference time-domain (FDTD) simulations. The 2D FD model is much more time-effective than conventional 2D FDTD for finding cavity resonances and field distributions, in particular for degenerate or energetically close modes. This makes the model convenient for studying the evolution of the successive transition from a  $L_1$  cavity to a full 1D PhC-waveguide, which can host successively longer QWRs. Furthermore, the cavities have to be analyzed and optimized with respect to both the Q-value and the properties of the QWRs, i.e. modal distribution and polarization. For example, fig.1 shows a qualitative spectrum of the  $L_6$  cavity obtained by 2D-computation, which demonstrates potentially high-Q mode primarily polarized along the QWR. The potentially interesting modes are further analyzed and optimized by 3D FDTD with the aim of attaining high Q-values. It is found that on a geometrically modified  $L_6$  cavity,  $Q > 2 \cdot 10^5$  can be obtained while keeping a strong optical confinement with a mode volume  $\sim 0.86 a^3$ .

Our modeling effort has resulted in a design of high-Q  $L_x$ -cavities appropriate for QWR integration. The details of the mode evolution from a single lattice-point defect toward a 1D PhC-waveguide have also been studied. Based on this general approach, we discuss the design of a PhC-based QWR laser and its potential performance.

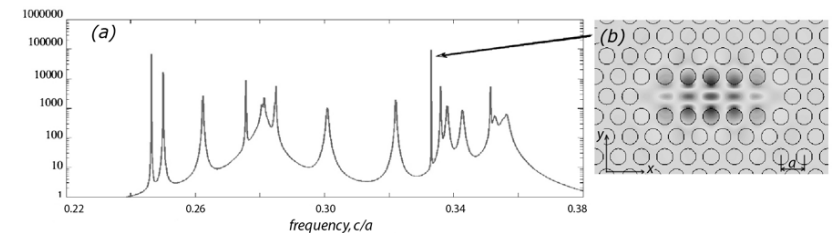


Fig.1. Qualitative spectrum for the  $L_6$  PhC-cavity (a), and the near-field distribution of  $E_x$  (b) of a mode suitable for efficient coupling with a QWR of a finite length.

### References

- [1] Y. Akahane, T. Asano, B.S. Song, and S. Noda, *Nature* **425**, 944-947, 2003.
- [2] E. Kapon, *Proc of the IEEE*, **80**(3), 398-410, 1992.

# Ultrashort Vectorial Pulse Propagators

J.V. Moloney

Arizona Center for Mathematical Sciences  
Department of Mathematics  
and  
Optical Sciences Center  
University of Arizona, Tucson 85721

## ABSTRACT

Rapid progress in recent years in the development of high power ultrashort pulse laser systems has opened up a whole new vista of applications and computational challenges. There currently exists a void in modeling pulse propagation phenomena that lie between computationally expensive 3D vector Maxwell solvers and much easier envelope models. The need to resolve the underlying optical carrier wave (carrier shocks) while simultaneously capturing ultra-broadband and large angle propagation phenomena requires special care when designing a model propagator.

In my talk, I will present a 3D unidirectional carrier-resolved vector pulse propagator that spans the void between full Maxwell and envelope models such as Nonlinear Schrödinger and its many variants and extensions. A novel aspect of our approach is that the pulse propagator is designed to faithfully capture the light-material interaction over the broad spectral landscape of relevance to the optical interaction. Moreover the model provides a seamless and physically self-consistent means of deriving the many ultrashort pulse propagation equations presented in the literature. Amongst those applications that are most challenging from a computational point of view are those involving explosive critical self-focusing with concomitant explosive growth in the generated light spectrum. Moreover, new experimental developments in the field of extreme nonlinear optics will require more rigorous propagation models beyond those existing in the current literature. Specific applications areas chosen for illustration in this talk will include atmospheric light string propagation, nonlinear X and O-wave generation due to nonlinear self-trapping in condensed media and supercontinuum shaping in photonics crystal/small core fibers. Figure 1 shows that a spatio-temporally chaotic self-trapped femtosecond pulse propagating in water has a dominant globally attracting X-shaped spectral feature when the central wavelength is in the normally dispersive regime. These examples exhibit rather different aspects of intense femtosecond pulse propagation and demonstrate the robustness and flexibility of our recently formulated unidirectional Maxwell propagator.

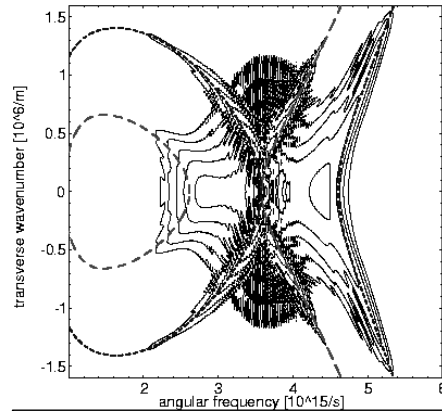


Figure 1 Spectrally-resolved far-field spectrum of a self-trapped femtosecond pulse in water.

At the 3D vector Maxwell level, I will discuss an adaptive space/time mesh scheme based on the well-known FDTD algorithm that significantly enhances computational performance over that of uniform and non-uniform mesh variants. The approach is particularly suited to modeling coupling of light to isolated nanostructures in an otherwise featureless landscape. The adaptive mesh refinement (AMR) algorithm works by cascading the mesh from relatively large scales needed to resolve the optical wavelength down to the finest mesh required to resolve the nanostructure. By requiring small time stepping only on the finest mesh, one simultaneously obtains a significant saving in computer memory storage and computation time. The key requirement of the approach is that the computational overhead imposed by grid management is more than offset by savings in storage and computation time. Figure 2 shows a 3D cascaded mesh layout for a refined region about a quantum dot embedded within a defect in a 3D photonic crystal film (not shown). Stability and convergence of the AMR scheme requires proper treatment of interpolation in space and time between grid levels and imposition of flux boundary conditions.

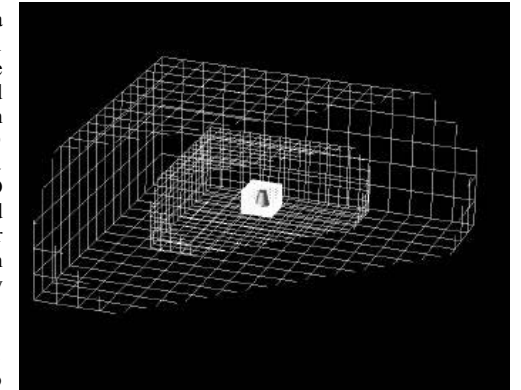


Figure 2 Three levels of mesh refinement about an isolated quantum dot.

As an illustration of this approach, we will discuss applications of linear and nonlinear light coupling to a quantum dot via a nanometer scale metal bowtie antenna and computed linear and nonlinear optical properties of metamaterials created from metallic nano cut-wire and plates embedded in a host dielectric.

## Strong Control of Radiation States in a Slab Waveguide sandwiched between two Omni-Directional Mirrors

H.J.W.M. Hoekstra\*, D. Yudistira\* and R. Stoffer<sup>o</sup>

\*Integrated Optics Micro Systems group and <sup>o</sup>AAMP group, University of Twente, P.o. box 217, 7500 AE Enschede, The Netherlands,  
[h.j.w.m.hoekstra@ewi.utwente.nl](mailto:h.j.w.m.hoekstra@ewi.utwente.nl)

The paper shows theoretically that radiative losses, due to imperfections and field mismatch, in freestanding slab waveguides can be strongly reduced by the application of omni-directional mirrors.

### Summary

Field enhancement is quite relevant for all kind of applications requiring a strong matter-optical field interaction like in lasers or sensors. A large number of different structures showing field enhancement has been proposed and studied in the literature, such as cavities, photonic crystal (PhC) structures and slow-light devices. Efficient excitation in such structures is in general hampered by optical losses due to field mismatch at transitions between different structures and by impurity scattering due to structural imperfections.

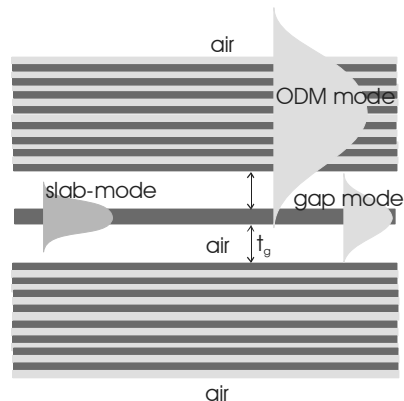


Figure 1. Sketch of a slab waveguide sandwiched between two ODMs.

without ODMs, can be obtained by structural optimization, suppressing the effect of ODM modes and quasi-guided gap modes. The effect of the latter on the LDOM depends critically on the thickness of the air layers between slab and ODMs. This may be used to rapidly turn off and on part of the gap modes micro-mechanically. Possible implications of the effect will be discussed during the presentation.

### References

- [1] Y. Fink, J.N. Winn, S. Fan, C. Chen, J.D. Joannopoulos and E.L. Thomas, *Science* 282, 1679, 1998.  
 [2] P.St.J. Rusell, S. Tredwell and P.J. Roberts, *Opt. Comm.* 160, 66, 1999.

## Time-Domain Full-Wave Solver for Integrated Optical Waveguides

Luca Pierantoni, Alessandro Massaro, Andrea Di Donato, Davide Mencarelli, Tullio Rozzi  
 Dipartimento di Elettromagnetismo e Bioingegneria, Univ. Politecnica delle Marche, Ancona, Via Brecce Bianche, Ancona - Italy  
[luca.pierantoni@univpm.it](mailto:luca.pierantoni@univpm.it)

**Abstract** – In this contribution we introduce the 3D full-wave TLMIE method for the analysis and design of complex devices in the area of integrated optics. Theoretical results are compared to measured data, showing very good agreement. We then provide design criteria for the optimization of the devices.

### Summary

Photonic circuits based on multilayer waveguides are suitable for several integrated optical architectures such as directional couplers, filters, switches, microelectromechanical systems (MEMS), optical interconnections in RF systems, photodetectors, laser. We perform the electromagnetic (EM) analysis by using a full-wave 3D-solver based on the Transmission Line Matrix-Integral Equation (TLMIE) method [1]. The TLM is a time-domain space-discretizing method in which the dynamics of the EM field is described by applying Huygens' principle. This is a powerful method that allows the numerical full-wave modeling of 3D structures with nearly arbitrary geometry. Its disadvantage appears in dealing with wide homogeneous (i.e. bulk, free-space) where the 3D-spatial domain of computation is large, thus increasing the number and the size of the elementary cells. This problem is overcome by using the hybrid TLMIE method, which combines the advantages of the TLM technique with the advantages of the IE method, where the analytical or numerical Green's functions are used for describing homogeneous (bulk/free-space) regions. The TLMIE method is the kernel of a 3D-solver equipped by pre-and post-processing tools, which are helpful for giving physical insight to the dynamics of EM propagation [1]. As an example, we present the EM modeling of a widely used optical polymeric modulator (Fig.1).

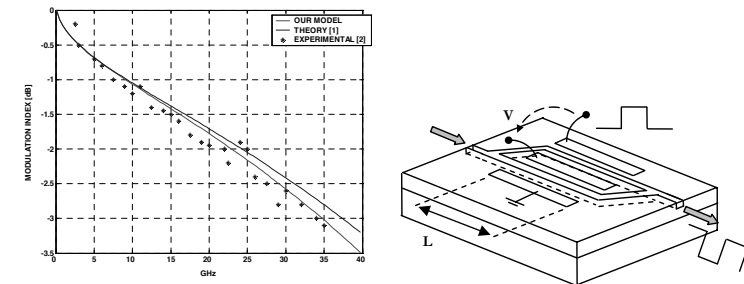


Fig1: Full-wave modelling of a polymeric modulator. Results from TLMIE (in red) are compared to measures and to data from literature.

### References

- [1] L. Pierantoni, A. Massaro and T. Rozzi, "Accurate Modeling of TE/TM Propagation and Losses of Integrated Optical Polarizer", *IEEE Transaction on Microwave Theory and Technique*, vol.53, Issue 6, June 2005, pp.1856-1862.

## Frequency-domain modeling of photonic crystal and plasmonic devices

Georgios Veronis\*, Shanhui Fan\*

\*Department of Electrical Engineering, Stanford University, Stanford, California 94305, USA  
gveronis@Stanford.edu

We use the finite-difference frequency-domain (FDFD) method to investigate the properties of subwavelength plasmonic waveguides based on slots in thin metal films. We also introduce a new method for sensitivity analysis of nanophotonic devices based on FDFD.

### Summary

Several problems in nanophotonics are uniquely suitable for frequency-domain modeling methods. Frequency-domain methods are essential in modeling of plasmonic devices due to the complicated dispersion properties of metals at optical frequencies. Here we first demonstrate the existence of a bound optical mode supported by a slot in a thin metallic film deposited on a substrate, with slot dimensions much smaller than the wavelength. The modal size is almost completely dominated by the near field of the slot. Consequently, the size is very small compared with the wavelength, even when the dispersion relation of the mode approaches the light line of the surrounding media. In addition, the group velocity of this mode is close to the speed of light in the substrate, and its propagation length is tens of microns at the optical communication wavelength. Thus, such a waveguide could be potentially important in providing an interface between conventional optics and subwavelength electronic and optoelectronic devices.

We also investigate the performance of bends and power splitters in plasmonic slot waveguides. We show that, even though the waveguides are lossy, bends and splitters with no additional loss can be designed over a wavelength range that extends from DC to near-infrared, when the bend and splitter dimensions are much smaller than the propagation length of the optical mode. We account for this effect with an effective characteristic impedance model based upon the real dispersion relation of the plasmonic waveguide structures. In addition, we show that by using optimization techniques we can design structures that couple light efficiently from dielectric waveguides to plasmonic slot waveguides.

Finally, we present a new method for sensitivity analysis of nanophotonic devices. The algorithm is based on the finite difference frequency-domain method and uses the adjoint variable method and perturbation theory techniques. We show that our method is highly efficient and accurate and can be applied to the calculation of the sensitivity of transmission parameters of resonant nanophotonic devices.

## Guiding Light in Plasmon-Polariton Waveguides

A.N.Kireev and Olivier J.F. Martin

Nanophotonics and Metrology Laboratory  
Swiss Federal Institute of Technology Lausanne  
EPFL - STI - ITOP - NAM, Station 11, CH-1015 Lausanne, Switzerland

[alexandre.kireev@epfl.ch](mailto:alexandre.kireev@epfl.ch)

The guiding properties of sub-wavelength metal-dielectric waveguides based on surface plasmon-polariton excitations are investigated numerically with the help of Green's tensor formalism and FDFD method.

### Summary

Surface plasmon-polariton-based waveguides can confine the light to very small dimensions [1] overcoming traditional diffraction limit for minimal spot size. Recently they attracted extensive interest due to their potential nano-photonics applications in optical data storage, near-field optical microscopy and bio-photonics. The propagating waves in these waveguides are associated with surface plasmon-polariton (SPP) collective excitations resulting from a coupling of charge oscillations and electromagnetic fields on metal surfaces. The SPP waves are transversally evanescent and bound to interfaces between dielectrics and metals.

Among the most promising SPP waveguides actively studied nowadays effectively one-dimensional thin metal film waveguides, rectangular slab metallic waveguides embedded in dielectric media and inverted SPP slot waveguides made of a thin dielectric film sandwiched between two metal slabs. Also attractive are metallic wedge waveguides allowing high concentration of electromagnetic field in the region of highest curvature of the waveguide surface.

The fundamental  $TH_y$  state of SPP slab waveguide is shown in

Fig.1. The magnetic field is mostly localized in the vicinity of metallic surfaces and its normal derivative has discontinuity at the interface. Due to this feature the method of integral equations based on the Green's tensor formalism [2] was found to be especially effective to investigate SPP waveguides. A system of coupled FDFD equations for two transversal components of the magnetic field has also been derived and used for a search of waveguide eigenmodes and their classification. The modes localization and their polarization properties have been investigated. As a direct application, the optimization of waveguides in order to reduce the high propagation losses associated to SPP is considered.

Together with other important plasmon-polariton effects taking place on the nano-structured surfaces, like enhanced light transmission through a sub-wavelength apertures and nano-focusing, the sub-wavelength guiding can serve as a basis for novel integrated photonic technologies.

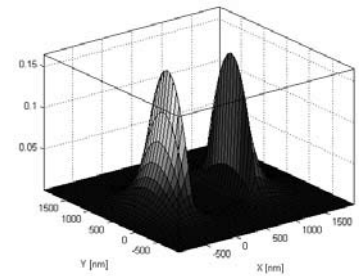


Figure 1 Fundamental state of SPP slab waveguide.

### References

- [1] E. Ozbay, Science, **311**, 189-193, 2006.
- [2] Olivier J. F. Martin and Nicolas B. Piller, Phys.Rev., **E58**, 3909-3915, 1998.

## Improved ASR convergence for the simulation of Surface Plasmon Waveguide Modes

Peter Debackere, Peter Bienstman, Roel Baets  
 Photonics Research Group, INTEC, Ghent, Belgium  
 Peter.Debackere@intec.UGent.be

In order to simulate surface plasmon waveguide structures we have utilized and improved the adaptive spatial resolution technique and combined it with PML boundary conditions.

### Summary

The convergence of the Fourier Modal Method for metallic structures is a problem, particularly in TM. One of the techniques proposed to increase convergence is adaptive spatial resolution. This basically consists of a parametric representation of the coordinate axis, which allows a spatially adaptive resolution, increasing the sampling in the neighbourhood of the discontinuities of the permittivity function[1]. The original technique was later extended to multilevel profiles [2]. We modified the parametric reformulation so the formalism could be used to provide reliable estimates for a two-stage method in a eigenmode solver (CAMFR [3]). PML boundary conditions were also integrated into the formalism. Four different possibilities for the parametric representation have been compared, of them, only one shows a dramatic increase in convergence in combination with PML.

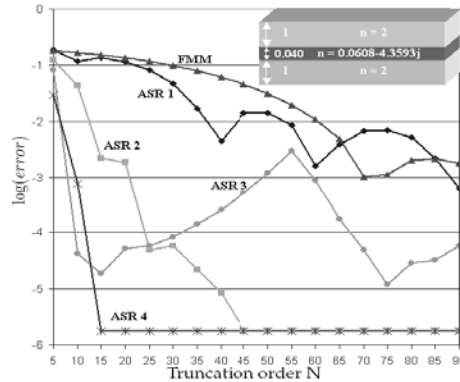


Fig. 1.: Convergence of the ASR methods, the setup is depicted in the inset of the figure.

We are currently working towards a 2D version of the adaptive spatial resolution algorithm.

### References

- [1] Granet G, *JOSA A- Optics Image Science and Vision* **16**(10): 2510–2516, 1999.
- [2] Vallius T, Honkanen M, *Optics Express* **10** (1): 24–34, 2002.
- [3] Bienstman P and Baets R, *Opt. Quantum Electron* **33**(4–5):327-341 2001.

## Efficient simulation of metals in the finite-difference time-domain method

W.H.P. Pernice\*, F.P. Payne\* and D.F.G. Gallagher<sup>†</sup>

\*Department of Engineering Science, University of Oxford, 17 Parks Road, Oxford OX1 3PJ  
 wolfram.pernice@eng.ox.ac.uk

<sup>†</sup>Photon Design, 34 Leopold Street, Oxford OX4 1TW, UK

The purpose of this paper is to present an efficient framework for the integration of dispersive metallic elements into the finite-difference time-domain method. Simulation of dielectric structures containing metals is of particular interest for the design of surface plasmonic devices such as metal nano-particle arrays. As metals show strong dispersive behavior in the optical wavelength range it is

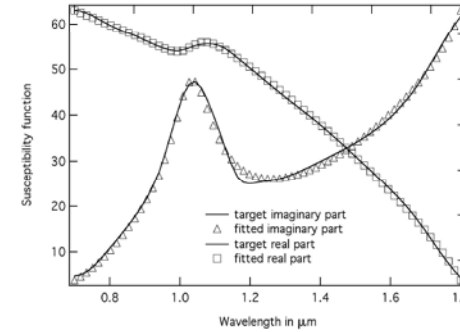


Fig 1. Fitting result for the complex susceptibility function of aluminium.

necessary to take the frequency dependency of the refractive index into account. Introducing an additional differential equation for the macroscopic polarization resulting from a time domain formulation of the complex susceptibility is one way to handle dispersion. In order to maintain numerical stability it is necessary to express the susceptibility in terms of functions that obey the Kramers-Kronig relations. We found that combinations of Lorentzian functions describing harmonic electronic oscillators are suitable functions and the susceptibility then takes the form

$$\chi(\omega) = \epsilon_\infty - \frac{\omega_p^2}{\alpha(j\nu + \omega)} + \sum_{p=1}^P \frac{(\epsilon_{stat} - \epsilon_\infty) A_p}{\alpha_p + 2j\omega\Gamma_p - \omega_p^2} \quad (1)$$

When refractive index data is available the susceptibility function of a metal can be fitted to equation 1 using a non-linear least squares algorithm which considers the real and the imaginary

parts simultaneously. In Figure 1 we show the result of our fitting routine for the susceptibility of aluminium. Equation 1 must then be transformed into the time domain to yield a differential equation linking the macroscopic polarisation and the electric fields. By selecting appropriate finite-difference operators for the temporal derivatives an updating scheme is derived to propagate EM fields in time and space. To confirm the correctness of the approach we computed the reflection coefficients for thin metal sheets. The results give very good agreement with analytical calculations as shown in Figure 2.

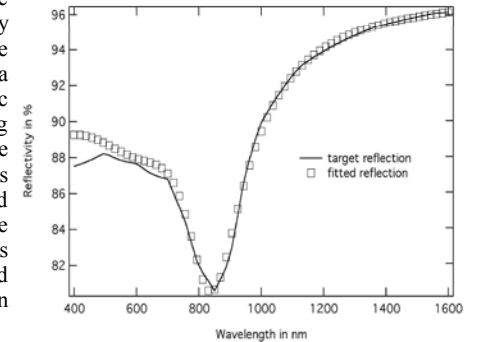


Fig 2. Reflection coefficient computed for a gaussian pulse incident on a 40 nm thick aluminium sheet surrounded by air.

## Numerical optimization of cascaded Y-branches in Ti:LiNbO<sub>3</sub>

Andrea Guglielame\*, Stefano Balsamo\*

\*Avanex Corporation, Via Fellini 10, 20097 San Donato Milanese, Italy

[stefano\\_balsamo@avanex.com](mailto:stefano_balsamo@avanex.com)

This work is focused on optimization of cascaded 3-dB Y-branches fabricated in Ti-indiffused Lithium Niobate. Numerical analysis is performed through a 3-D factorized Beam Propagation Method (BPM) with transparent boundary conditions. Application to a nested dual-parallel modulator is described.

### Summary

The 3-dB optical splitter is a key component for integrated optics, and the Y-branch in particular allows for precise splitting ratio control with low excess loss, particularly when a broad wavelength range must be covered. When working with Mach-Zehnder modulators (MZM) for optical fiber transmission, a power splitting as close as possible to 3 dB guarantees high extinction ratio and very low residual chirp, thus a strong emphasis is put on the Y-branches optimization.

Advanced modulation formats such as DQPSK, which have become very popular recently, require more complicated optical structures, known as “nested” or “dual parallel” modulators, capable of multilevel signal generation. Basically, these devices consist of cascaded Y-branches and combiners (see figure below): therefore, any non-ideal behaviour is amplified by cascading the optical building blocks leading to strong performance degradation (i.e., strong optical losses due to radiation modes, low extinction ratio, high chirp): this imposes strong constraints on the optical structures.

We describe here a comprehensive numerical study performed on a nested device formed by two identical, parallel MZM's. The whole structure has been simulated using a 3-dimensional Beam Propagation Method [1], with transparent boundary conditions [2], which allows us to simulate accurately and efficiently the optical propagation along the interferometers. The simulator has been “calibrated” by simulating and verifying the experimental data obtained on optical test structures.

By focusing separately on the most critical building blocks (namely, wide-angle splitters, waveguide bends and interconnecting transition waveguides), the main causes of performance degradation have been investigated and the suitable design corrections have been addressed leading to an optimized device. Moreover, wavelength sensitivity has been verified carefully.

The optimized nested interferometer shows nearly ideal optical response (Fig. 1b), with very high extinction ratio (better than 30 dB) and very low excess loss (lower than 0.1 dB) over the whole wavelength range of operation (1530-1630 nm).

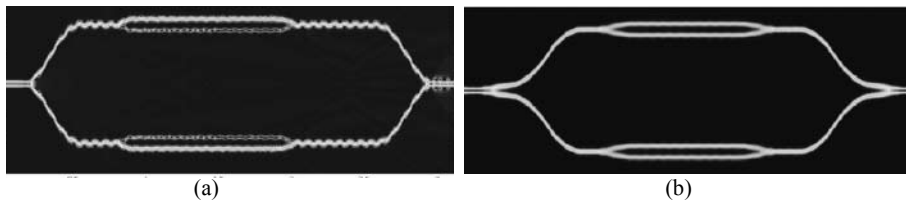


Fig. 1. Comparison of optical propagation in standard (left) and optimized (right) optical structure.

### References

- [1] M.J. Robertson, P.C. Kendall, S. Ritchie, P.W.A. McIlroy, M.J. Adams, IEEE J.Light.Tech. Vol. 7, N. 12, 1989
- [2] G.R.Hadley, IEEE J. Quantum Electron., Vol. 28, N. 1, 1992

## The Modelling of Segmented MMI Structures

Laurence Cahill

Department of Electronic Engineering, La Trobe University, Melbourne, Australia 3086

[l.cahill@latrobe.edu.au](mailto:l.cahill@latrobe.edu.au)

This paper investigates the mathematical modelling of multimode interference (MMI) structures where the geometrical layout is modified by changing the refractive index of segments of the multimode guiding region.

### Summary

MMI devices are widely used as splitters, couplers and switches. The usual MMI layout comprises a rectangular, uniform guiding region with single mode access waveguides. The analytical and numerical solutions to the wave equation for these structures are well established<sup>1</sup>.

In this study, the requirement of a uniform guiding region is relaxed and we consider introducing a step change in the refractive index over a segment or segments of the multimode guiding region. The step change in refractive index can be achieved if the multimode guiding region comprises an active electro-optic polymer or semiconductor and the segments are subjected to a step voltage<sup>2</sup>. Simple examples of segmented MMI couplers are shown in Figure 1.



Figure 1. Simple examples of segmented MMI structures (plan views)

By applying a voltage to some segments and not others, it is possible to change the refractive index of those first segments and hence modify the refractive index profile of the guiding region(s).

If the segmented MMI structure has a complicated geometry, then a numerical solution is mandatory. However, for the case of simple geometries, approximate analytical solutions can provide insight into the behaviour of the structures. For example, if the width of an MMI region is reduced by means of the electro-optic effect, then the imaging locations will be changed. Judicious choice of the dimensions of the segments may enable the switching of the input beams to different output waveguides. Concurrently, use can also be made of the different interference phenomena (general, paired and symmetric) to achieve desirable switching characteristics with segmented structures.

This paper investigates the use of approximate field solutions to a variety of segmented MMI structures in order to identify useful transmission and switching characteristics.

### References

- [1] L.B. Soldano, E.M. Pennings, IEEE J.Lightwave Technol. 13, 615-686, 1995.
- [2] S. Nagai et al, IEEE J. Lightwave Technol. 20, 675-681, 2002.

## Imaginary distance BPM as an efficient tool for modelling optical waveguide fabrication by ion diffusion

G. Lifante, E. Cantelar, F. Cussó, M. Domenech  
Depto. Física de Materiales, C-IV. Universidad Autónoma de Madrid. 28049-Madrid (Spain)

A.C. Busacca, A. Cino and S. Riva Sanseverino  
CRES-Centro per la Ricerca Elettronica in Sicilia, Via Regione Siciliana 49, 90046-Monreale (Italy)

Optical waveguide fabrication is accomplished nowadays by a variety of techniques which in many cases include one or several diffusion processes, such as Titanium indiffusion, proton exchange (PE) and reverse proton exchange (RPE). Ionic diffusion is described by the Fick equation, which has a formal analogy with the paraxial wave equation for electromagnetic waves. Therefore using the scalar approximation, the temporal variable (time) in the diffusion equation is directly correlated with the propagation position along the imaginary z-axis.

In this work, the imaginary distance propagation BPM [1] is used to model proton diffusion in LiNbO<sub>3</sub> and the results are compared with RPE LiNbO<sub>3</sub> channel waveguides, where two successive diffusion processes are performed [2-3]. The first one implies the exchange of lithium from the substrate by protons from a weak acid, such as benzoic acid. The Li<sup>+</sup> → H<sup>+</sup> exchange increases the extraordinary index of the substrate, whereas the ordinary index decreases. Thus, in a z-cut substrate the waveguides support only TM-propagation. To obtain useful guides for TE-propagation, a reverse process must be performed following a second diffusion stage, in which the original matrix is recovered by subjecting the substrate in a source of lithium ions, such as lithium benzoate. After the final processes (PE & RPE) an ordinary guide is formed at the substrate surface, whereas a buried extraordinary waveguide is also obtained. The precise refractive index profiles of both the ordinary and extraordinary indices are needed in many applications, particularly when simultaneous propagation of TE and TM modes is required and their overlap becomes critical. The results indicate that the imaginary distance beam propagation method is a precise method to model diffusion processes in two dimensions adequate to calculate refractive index profiles in ion diffused-channel waveguides.

- [1] G. Lifante, *Integrated Photonics* (J. Wiley & Sons, Chichester, England, 2003).  
[2] E. Lallier, J. P. Pocholle, M. Papuchon, C. Grezes-Besset, E. Pelletier, M. De Micheli, M. J. Li, Q. He and D. B. Ostrowsky, *Electron. Lett.* **25**, 1491-1492 (1989).  
[3] A. Parisi, A. Cino, A.C. Busacca, and S. Riva-Sanseverino, *Appl. Optics* **43**, 940-943 (2004).

## Single-Mode Volume Waveguides in Ferroelectrics Written by Bright Soliton Beams: Towards 3D Integrated Circuits

Eugenio Fazio<sup>o</sup>, Federico Pettazzi<sup>o</sup>, Grigore Leahu<sup>o</sup>, Massimo Alonzo<sup>o</sup>, Mathieu Chauvet<sup>+</sup>, Adrian Petris<sup>#</sup>, Valentin Ionel Vlad<sup>#</sup>, Nicola Argiolas<sup>§</sup>, Marco Bazzan<sup>§</sup>, Paolo Mazzoldi<sup>§</sup>, Cinzia Sada<sup>§</sup>

<sup>o</sup> *Ultrafast Photonics Lab, Dipartimento di Energetica, Università "La Sapienza"  
Via A. Scarpa 16 I-00161 Roma, ITALY*

[eugenio.fazio@uniroma1.it](mailto:eugenio.fazio@uniroma1.it)

<sup>+</sup> *Laboratoire d'optique P.M. Duffieux, Université de Franche Comte, Besançon cedex FRANCE*

<sup>#</sup> *Romanian Center of Excellence in Photonics Bucharest ROMANIA*

<sup>§</sup> *Dipartimento di Fisica "G. Galilei" Università di Padova, I-35131 Padova, ITALY*

Bright spatial solitons in pure and erbium doped lithium niobate are experimentally and theoretically demonstrated, both formed by CW and ultrashort pulses. In such materials spatial solitons leave a permanent trace that is acting as a volume, perfectly-single-mode, low-losses waveguide. This is a new low-cost technology that might open the possibility of realising 3D-integrated circuits

### Summary

The actual technologies for integrated circuits can only realise waveguides on the external surfaces of substrates, using different techniques. A possibility for over passing such limitation and indeed realise volume waveguides is the using of spatial solitons and associated soliton waveguides, which practically means a local modification of the refractive index induced by the propagation of self-confined beams. Recently we have demonstrated bright soliton formation in lithium niobate [1]. Peculiarity of such a material is the induced refractive index change that remains even after the writing procedure is switched off. Thus, a bright soliton in lithium niobate leaves a perfect single-mode waveguide. Such waveguides can be either channelled or planar, and more specifically present really low losses due to the nature of the writing process: soliton waveguides are self-written by self-confined light beams. Solitons and associated single-mode waveguides have been written both by ultralow power CW beams (from nW to mW) and by ultrashort laser pulses (about 100 fs) [2-3]: in the first case the waveguide can live for months and then can be washed out by a proper optical process, while in the second case the material is permanently damaged and the waveguide cannot be modified anymore. Soliton waveguides can be generated everywhere in the volume of the host material [4]: indeed, they are volume waveguides that could be adopted for the realisation of 3D passive and active integrated optical circuits, with simple or complex functionalities.

### References

- [1] E. Fazio, F. Renzi, R. Rinaldi, M. Bertolotti, M. Chauvet, W. Ramadan, A. Petris, V.I. Vlad, *Appl. Phys. Lett.* **85**, 2193 (2004)  
[2] E. Fazio, W. Ramadan, A. Petris, , M. Chauvet, A. Bosco, V.I. Vlad, M. Bertolotti, *Appl. Surf. Sci.* **248**, 972 (2005)  
[3] V.I. Vlad, E. Fazio, M. Bertolotti, A. Bosco, A. Petris, *Appl. Surf. Sci.* **248**, 484 (2005)  
[4] M. Chauvet, V. Coda, H. Maillotte, E. Fazio, G. Salamo, *Opt. Lett.* **30**, 1977 (2005)

## Balancing the grating excitation of slab waveguide modes for the highest accuracy retrieval of the slab parameters

M. Flury, N. Destouches, A.V. Tishchenko, O. Parriaux  
*Laboratoire Traitement du Signal et de l'instrumentation, UMR CNRS 5516,*  
*18 Rue Benoît Lauras, F-42000 Saint-Etienne*  
[o.parriaux@univ-st-etienne.fr](mailto:o.parriaux@univ-st-etienne.fr)

Using a grating coupling approach one can measure both the ordinary and the extraordinary refractive indices of a step index slab layer by measuring the effective index of TE and TM propagating modes. The conditions for the ultimate accuracy on the refractive index will be discussed.

### Summary

The industrial technology of dielectric multilayers is highly developed and can advantageously be used in advanced R&D fields such as femtosecond lasers, WDM telecoms, biosensors, etc. In most current applications the quantity of interest which requires post- or in-situ monitoring is the optical path through the deposited layers, i.e. the product of the layer thickness by the refractive index. High end applications however often require the control of the refractive index and layer thickness separately. Such information is not provided by vendors who most often ignore the third digit of the index of their layers and by how much the latter can vary amongst the samples of a given charge and between charges. There is therefore a metrology problem which we propose to solve by waveguide mode measurement. The most popular measurement technique is that of the “m-lines” created by prism excitation. There is even a commercial product making the best of what this technique can provide [1, 2]. The prism technique is however limited in accuracy for a number of reasons. A grating coupling approach has from the start major advantages: contactless measurement, perfect geometry, uniformity. The retrieval of the ordinary and extraordinary index  $n_o$  and  $n_e$  of a step index layer requires the propagation of at least three modes which can suitably be the  $TE_0$ ,  $TE_1$  and  $TM_0$  modes. The achievement of the ultimate accuracy on the refractive index rests on a number of conditions :

- \* The grating strength must be strong enough to couple a measurable optical power in the waveguide mode,
- \* The grating strength must be weak enough to represent a small perturbation of the waveguide,
- \* The possible non-uniformity of the grating coupler must have the least effect on the waveguide mode effective index.

These conditions lead to defining the grating corrugation in the substrate first, then to the deposition of the layer to be characterized. This is fortunate since it allows standard platforms to be supplied by a few reliable sources for corrugated substrate. The grating period and depth, and recommended layer thickness is adjusted so as to provide a resonance peak of comparable angular width for all three modes. This is achieved by means of analytical expressions obtained by resorting to the Rayleigh-Fourier method. In doing so one obtains classes of standard grating platforms devoted to three broad classes of layer refractive index and to the stable wavelengths available in most industrial and institutional laboratories. The paper will vividly explain what the resonance width depends on, and how the measurement conditions for the ultimate accuracy on the refractive index can intuitively be found.

### References

- [1] Metricon Corporation, 12 North Main Street, Pennington, New Jersey 08534, USA.
- [2] S. S. Hardaker, S. Moghazy, C. Y. Cha, R. J. Samuels, J. Polymer Sci. B. 31, 1951-1963, 1993.

## Oblique Coordinates for Computing Band-Diagrams in Photonic Crystals with Hexagonal Lattice

Stefan F. Helfert

*FernUniversität in Hagen, Universitätsstr. 27, 58084 Hagen, Germany*  
[stefan.helfert@fernuni-hagen.de](mailto:stefan.helfert@fernuni-hagen.de)

The elementary cells in hexagonal photonic crystals are not described by structures with a rectangular boundary but by parallelograms. We show in this contribution how oblique coordinates can be used to compute the band structure of such devices.

### Summary

Fig.1 shows the elementary cell of a photonic crystal (PC) with a hexagonal lattice. For computing the band structures oblique coordinates as in [1]-[3] were introduced. Since only the TE-case (2D) was examined in the given references, equations for the 3D-vectorial case were derived from Maxwell's equations. The expressions were applied in various algorithms: the method of lines (MoL) [4] the finite difference method and the Rayleigh-Ritz-Method. In all these cases the Floquet modes were determined from an explicit eigenvalue/eigenvector problem. The obtained results are compared with the literature to show the validity of the found expressions. Fig.1 shows the band structure of a hexagonal PC computed with the MoL. The values at the edge points were compared with those obtained in [5] showing a good agreement.

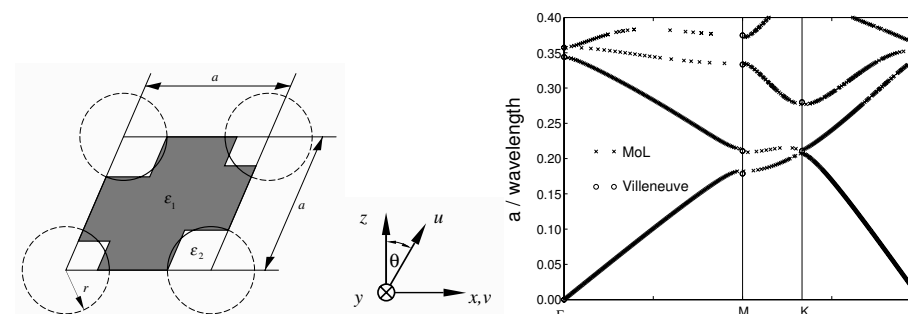


Fig.1: Elementary cell of a photonic crystal with a hexagonal cell and oblique coordinate system; band structure (TM) computed with the MoL

### References

- [1] J. Yamauchi, J. Shibayama, and H. Nakano, in *OSA Integr. Photo. Resear.* San Francisco, USA, 1994, pp. 19-21.
- [2] T. M. Benson, P.Sewell, S.Sujecki, and P.C. Kendall, *OQE*, **31**, pp. 689-703, 1999
- [3] P. Sewell, T. M. Benson, S. Sujecki, and P.C. Kendall, *JLT.*, **17**, pp. 514-518, 1999.
- [4] R. Pregla and W. Pascher, in *Numerical Techniques for Microwave and Millimeter Wave Passive Structures*, T. Itoh, (Ed.), pp. 381-446. J. Wiley Publ., New York, USA, 1989.
- [5] P. R. Villeneuve, S. Fan, S. G. Johnson and J. D. Joannopoulos, *IEE Proc.-Optoelectr.*, **145**, pp. 384-390, 1998.

## A simple coupled mode model for near band-edge phenomena in grated waveguides

H.J.W.M. Hoekstra, W.C.L. Hopman, J. Kautz, R. Dekker and R.M. de Ridder  
Integrated Optics Micro Systems group, University of Twente, P.o. box 217, 7500 AE Enschede, The Netherlands,

[h.j.w.m.hoekstra@ewi.utwente.nl](mailto:h.j.w.m.hoekstra@ewi.utwente.nl)

The paper presents a simple coupled mode model to describe near band-edge phenomena in the transmission spectra of waveguides with a section containing a rectangular grating.

### Summary

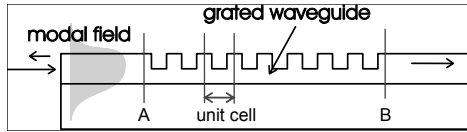


Figure 1. Sketch of a waveguide with a grating section; A and B are reference planes for defining the cavity, defined by the grating section.

Fabry-Perot cavity for the grating mode(s) (strong reflection at the boundaries of the grating section), together with the dispersive properties of these modes which are composed of forward and backward moving fields.

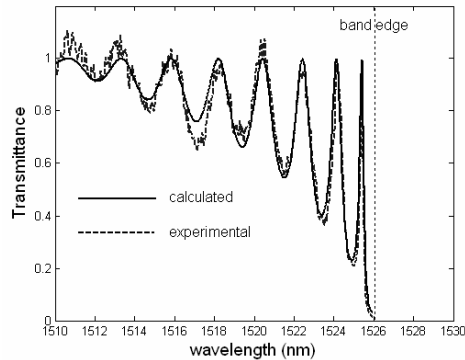


Figure 2. Experimental transmittance of a grating waveguide and results calculated with the presented model

device parameters, such as width of the peaks, field enhancement, modal group velocity, group delay and peak position as a function of the length of the grating section can be derived in good approximation. The presented theory is illustrated with numerical calculations and results of experiments on waveguides with grating sections.

It is well known that the features of the near band-edge transmission spectrum of a waveguide with a partly grating section (see figure 1) are dominated by the effects of strong dispersion. In this wavelength region sharp transmission peaks (see figure 2) are found corresponding to strong field enhancement inside the cavity, defined by the grating section. These phenomena can be explained by

considering the grating section as a Fabry-Perot cavity for the grating mode(s) (strong reflection at the boundaries of the grating section), together with the dispersive properties of these modes which are composed of forward and backward moving fields. It is the aim of the paper to show that from the wavelength position of the near band-edge transmission peaks most of the relevant parameters of the grating device can be deduced. First it is argued that, due to the symmetry of the grating (with rectangular grooves) the modal reflection and transmission coefficients for the transitions are nearly real. Using the latter, the approximate shape of the near band-edge dispersion curve, defined by  $\beta(\lambda)$  with  $\beta$  the propagation constant and  $\lambda$  the wavelength, of the propagating grating modes can be deduced from the positions of the transmission peaks for a structure with a given grating length. Next, from the dispersion curve most of the relevant

## Molding the Emission of Photonic Nanojets by Different Particle Shapes

Tahmineh Jalali<sup>1,3</sup>, Daniel Erni<sup>1</sup>, Christian Hafner<sup>2</sup>

<sup>1</sup>Communication Photonics Group, <sup>2</sup>Computational Optics Group, Laboratory for Electromagnetic Fields and Microwave Electronics, ETH Zurich, Gloriastrasse 35, CH-8092 Zurich, Switzerland

<sup>3</sup>Physics Department, Shahid Chamran University, Ahvaz, Iran

[jalali@photonics.ee.ethz.ch](mailto:jalali@photonics.ee.ethz.ch)

Particles shaped as e.g. spheres and ellipses with different refractive indices have been studied under plane wave illumination using simulation tools such as 2D-FDTD and 3D-MMP. For specific conditions the power distribution in the vicinity of the particle's opposite boundary has resulted in a tightly-focused photonic nanojet.

### Summary

The emergence of photonic nanojets that appear on the shadow-side of illuminated cylindrical particles have been recently studied in very detail [1-2]. The possibility of undergoing the diffraction limit [3] can be useful for various applications such as scanning near-field optical microscopy (SNOM), high-resolution lithography, advanced optical (and magnetic) data storage schemes, for immersion lens microscopy and for the fluorescence imaging of living cells [4].

In this paper, we report on the optimization of various dielectric particle shapes with respect to a highly confined power distribution in the resulting nanojet. The latter has been parameterized according to the beam waist and its beam divergence. The simulations have been performed using an advanced 2D finite-difference time-domain (FDTD) scheme (with a tailored material dispersion model and accurate boundary averaging features), whereas 2D and 3D reference simulations were carried out with the semi-analytical multiple multipole (MMP) method. Circular and elliptical particles with different refractive indices have been extensively analyzed, rendering elliptical particles as a promising candidate for highly directed nanojets (c.f. Fig. 1). Spherical shapes to obtain optimal 3D nanojets pose an additional challenge in order to find the associated refractive indices to the particle sizes involved. Other than symmetrical particle shapes are now under further investigation.

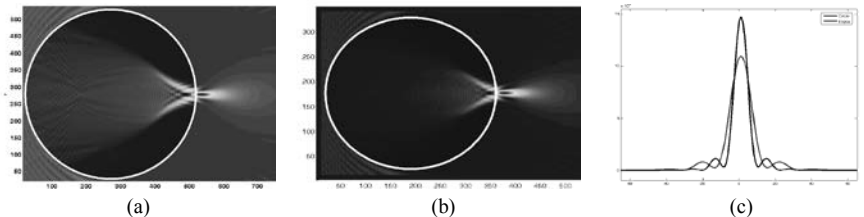


Fig. 1: Nanojets for two different particle shapes illuminated by a plane wave from the left ( $\lambda = 500$  nm; E-polarization): Time-averaged Poynting field for the (a) circular shape with  $d = 5 \mu\text{m}$ ,  $n = 1.54$ ; (b) elliptical shape with  $d_2 = 0.9 \cdot d_1 = 4.5 \mu\text{m}$ ,  $n = 1.4$ . (c) Transversal beam profile of the resulting nanojets (red: circular shape, blue: elliptical shape) where the elliptical particle yields a beam waist of  $W_{FWHM} = 240$  nm.

### References

- [1] A. V. Itagi, W. A. Challener, *J. Opt. Soc. Am. A*, 22(12), 2847, 2005.
- [2] S. Lecher, Y. Takakura, P. Meyrueis, *Opt. Lett.* 30, 2641-2643, 2005.
- [3] Z. Chen, A. Taflove, *Opt. Express* 12, 1214-1220, 2004.
- [4] E. Betzig, *Opt. Lett.* 20, 237, 1995.

## Measurements of effective index in channel SiON waveguides

Yu. Larionov, S.Kuzmin, V.Svetikov, V. Sychugov

*A.M.Prokhorov General Physics Institute, Russian Academy of Sciences,  
Vavilov St.38, 199911, Moscow, Russia, E-mail: luv@fo.gpi.ac.ru*

A higher accuracy of measurement of index value in a channel SiON waveguide can be achieved by diminution of average induced index at writing Bragg gratings in it using 193 nm irradiation.

### Summary

Silicon oxynitrid (SiON) offers wide opportunities for fabrication of integrated optical circuits (IOC) due to a potential of index modification from 1.45 (SiO<sub>2</sub>) to 2.0 (Si<sub>3</sub>N<sub>4</sub>). A number of works shows a possibility of development of various IOC on a base of the material, for example [1], and our work [2] dealing with an integrated optical demultiplexer. The main element of these IOC is a channel waveguide, an effective index of it being appreciably differ from its value for a planar one.

A known method of measurement of effective channel index  $n_{eff}$  is based on writing a weak Bragg grating in the waveguide and measurement of a spectral position of the reflection peak from it  $\lambda_{refl}$  [3]. If a period of the Bragg grating is  $\Lambda$  one can compute index as follows:

$$n = \lambda_{refl} / 2\Lambda \quad (1)$$

Induced index is small in a weak channel Bragg grating so  $n$  computed from (1) is practically coincides with  $n_{eff}$ .

Due to a comparatively poor photosensitivity of SiON, one usually writes the Bragg gratings in the waveguides by pulse irradiation of an eximer UV-laser using a phase mask, the period of it being known with a great accuracy. A spectral position of the reflectivity peak can be measured with a great accuracy by a spectroanalyser.

However, the writing of Bragg gratings in channel waveguides brings out induced index not only in irradiated parts of the channel but results in a change of physical state of a local part of the substrate where Bragg gratings are disposed. Maybe it is due to rather high density of power (~600 mJ/cm<sup>2</sup>) and great dose of UV- up to 12 kJ/cm<sup>2</sup> at an irradiation wavelength of 248 nm [4]. As a result an average induced index  $\Delta n_{ave}$  can have a value one order of magnitude larger than the modulated induced one [4], the last being contribute only a little to a difference between  $n$  and  $n_{eff}$ . This can affect an appreciable error in value of  $n_{eff}$ .

For decrease of the error we have diminished a dose loading on channel waveguides by writing Bragg gratings using an irradiation at wavelength of 193 nm. Apart for decrease of  $\Delta n_{ave}$  we used some methods of sensitization including a pre-exposure procedure of some H-loaded films with homogeneous beam of light. A type of recorded Bragg gratings is discussed in our work.

### References

- [1] G.L.Bona, *Microsystem technologies*. 9, 291-294, 2003.
- [2] A.Goncharov, et al., *Quatum Electron*. 35, 1163-1166, 2005.
- [3] C.V.Poulsen, et al., *El. Lett.*, v.31, n.17, 1437-1438, 1995.
- [4] D.Wiesmann, et al., *El. Lett.* v.34, n.4, 1998.

## Finite Difference Time Domain (FDTD) studies of an electrically pumped integrated microdisk laser

Xavier Letartre, Pedro Rojo-Romeo, Christian Seassal

*\*Laboratoire d'Electronique Optoélectronique et Microsystèmes LEOM, UMR CNRS 5512, Ecole Centrale de Lyon, 36 avenue Guy de Collongue, 69134 Ecully Cedex, FRANCE  
[xavier.letartre@ec-lyon.fr](mailto:xavier.letartre@ec-lyon.fr)*

The aim of this paper is to theoretically investigate the optical properties of an InP based electrically pumped microdisk laser, integrated in a waveguided microphotonic circuit.

### Summary

Very low threshold microlasers can be realized using III-V based microdisk resonators [1], as they supports high quality factor (Q) low volume modes. However, when a microlaser has to be integrated into a microphotonic circuit, it must be electrically pumped and optically coupled to a waveguide. This leads to a more complex device and the optical properties of the microresonator can be strongly modified.

As an example, we studied an InP microdisk laser reported onto a SOI (Silicon On Insulator) wafer through a SiO<sub>2</sub>/ SiO<sub>2</sub> bonding. In this case the Si layer is devoted to build passive dense microphotonic circuits based on high refractive index Si wave guides [2,3]. Such an architecture is used to integrate microphotonic devices over CMOS circuits in an "above IC approach".

The simulated structure is described in figure 1. An InP bottom contact layer (~ 100nm thick) is used to electrically pumped the microlaser (the effect of the top contact is not investigated here). Using 3D FDTD simulations, we show that the influence of this contact layer strongly depends on the vertical symmetry of the laser mode and that very high Q modes can be maintained. The monomode character of the microlaser is also discussed.

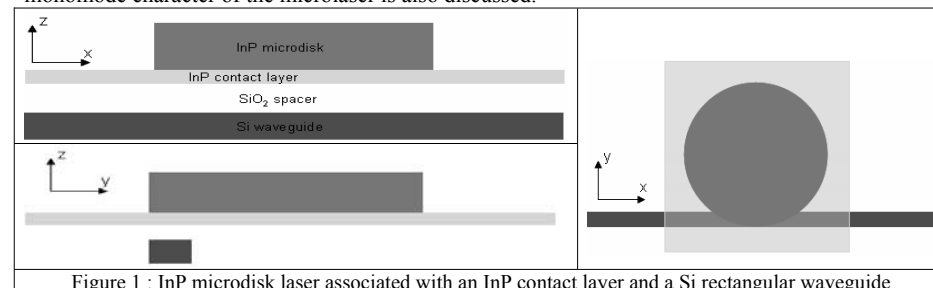


Figure 1 : InP microdisk laser associated with an InP contact layer and a Si rectangular waveguide

The laser signal is collected into a Si rectangular waveguide. The competition between radiated losses and guided light is numerically investigated, depending on the geometrical parameters (spacer thickness, misalignment...).

This work has been supported by the French Research Network in Micro and Nano Technologies and the European project FP6-2002-IST-1-002131-PICMOS.

### References

- [1] Toshihiko Baba and Daisuke Sano, *IEEE J. of Select. Topics in Quantum Electron*. 9, 1340 (2003)
- [2] R. Orobtcchouk, A. Layadi, H. Gualous, D. Pascal, A. Koster, and S. Laval, *Applied Optics* 39, 5773 (2000).
- [3] A. Kazmierczak, M. Brière, E. Drouard, P. Bontoux, P. Rojo-Romeo, I. O'Connor, X. Letartre, F. Gaffiot, R. Orobtcchouk, T. Benyattou, *IEEE Phot. Tech.Lett.* 17, 1447 (2005)

## Improved Finite-Difference Time-Domain Modelling of Surface Plasmons

Ahmad Mohammadi<sup>1,2</sup>, Mario Agio<sup>1</sup>

<sup>1</sup>Nano-Optics Group, Laboratory of Physical Chemistry, ETH Zurich, CH-8093 Zurich, Switzerland

<sup>2</sup>Department of Physics, Shiraz University, 71454 Shiraz, Iran  
[ahmad.mohammadi@phys.chem.ethz.ch](mailto:ahmad.mohammadi@phys.chem.ethz.ch)

We propose a scheme to reduce the *staircasing* error in the Finite-Difference Time-Domain (FD-TD) method for modelling surface plasmons in metallic nanostructures.

### Summary

Bringing optical communication down to the chip scale would have a tremendous impact on the photonics and microelectronic industries. Recent developments demonstrate that systems like photonic crystals[1] and metallic nanostructures[2] could effectively guide light in an integrated layout. Metals are particularly attractive because they support surface propagating modes, called surface plasmons, that are able to guide light in an even more compact way[2].

Designing metallic nanostructures often requires numerical solution of Maxwell's equations. Among the available methods, FD-TD[3] has gained popularity thanks to its flexibility in solving arbitrary shapes and to the steadily increasing power of computers. However, its application to the study of surface plasmons is not mature, and issues concerning its accuracy are still partly unsolved[4]. In the FD-TD algorithm space and time are discretized such that the electric and magnetic fields are not defined on the same grid location. Because of that, in presence of a material discontinuity, the field components will experience different boundaries, which do not always correspond to the original shape. While this problem can have a relatively small effect for dielectrics, it could be detrimental for electromagnetic excitations confined at a metal-dielectric interface. We have recently proposed a method that addresses this issue for dielectrics[5], which is based on the proper inclusion of the electromagnetic boundary conditions at a discontinuity. We are currently extending these ideas to the case of metals, with particular interest on surface plasmons. Fig. 1 shows the improvement in the calculation of the dispersion relation of surface plasmons using our FD-TD algorithm (smoothing) instead of *staircasing*.

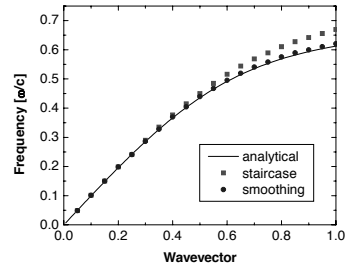


Fig. 1. Dispersion relation for surface plasmons at a metal-air interface.

### References

- [1] M. Notomi et al., *Opt. Express* 12, 1551-1561, 2004.
- [2] E. Karalis et al., *Phys. Rev. Lett.* 95, 063901(4), 2005.
- [3] A. Taflov, and S.C. Hagness, *Computational Electrodynamics: The Finite-Difference Time-Domain Method* (Artech House, Norwood, MA), 2005.
- [4] C. Oubre, and P. Nordlander, *J. Phys. Chem. B* 108, 17740-17747, 2004.
- [5] A. Mohammadi, H. Nadgaram, and M. Agio, *Opt. Express* 12, 10367-10381, 2005.

## Self-Phase Modulation in Slow-Wave Structures: a comparative numerical analysis

Francesco Morichetti<sup>o\*</sup>, Andrea Melloni<sup>\*</sup>, P. Bienstman<sup>+</sup>, G. Priem<sup>+</sup>, and J. Petráček<sup>§</sup>

<sup>o</sup>CoreCom, Via G. Colombo 81, 20133 Milano, Italy, [morichetti@corecom.it](mailto:morichetti@corecom.it)

<sup>\*</sup>Dipartimento di Elettronica e Informazione, Politecnico di Milano, Via Ponzio 34/5, 20133 Milano – Italy

<sup>+</sup>Department of Information Technology, Ghent University, Sint-Pietersnieuwstraat 41, 9000 Ghent, Belgium

<sup>§</sup>Institute of Physical Engineering, Brno University of Technology, 616 69 Brno, Czech Republic

### Summary

Recently increasing interest has been focused on optical Slow-Wave Structures (SWSs) made of cascaded coupled resonators, because of their interesting potentialities especially in nonlinear regime. The interplay of nonlinearities with the amplitude and phase spectral response of SWSs leads to a variety of novel phenomena that require accurate modelling and computationally efficient numerical techniques to be studied. In this contribution, Self-Phase Modulation effects in SWSs are investigated by means of several 1D approaches, operating either in time or frequency domain, being respectively: (1) a nonlinear extension of the Mode Expansion (ME) method that calculates iteratively nonlinear index changes inside the structure; (2) a Time Domain (TD) nonlinear method exploiting an effective equivalent circuit of the nonlinear Bragg reflector; (3) direct solution of Maxwell's equations in the Frequency Domain (FD) after suitable transformation in the form of coupled ordinary differential equations. The accuracy, computational efficiency (time and memory consume), versatility and limits of the proposed techniques are analysed and compared.

The SWS under investigation was proposed in the framework of COST P11 action [1] and consists of  $N$  Fabry-Pérot cavities, with optical length  $\lambda_0=1550\text{nm}$ , coupled each other by means of an intermediate quarter-wave layer, as shown in Fig. 1(a) for the case  $N = 2$ . The materials of the distributed Bragg reflectors ( $n_b=2.36$ ,  $n_a=2.6$ ) and the medium  $n_a$  filling the cavities are assumed to have the same Kerr nonlinearity ( $n_2 = 0.6 \cdot 10^{-13} \text{ cm}^2 / \text{W}$ ). Fig. 1(b) shows the spectral response of the double-cavity SWS of Fig. 1(a) for increasing input power, calculated by means of the proposed methods. A good agreement is found, with the only exception of the bistability region where the TD method appears less accurate in following sharp amplitude transitions versus frequency. On the other side, the TD method can be straightforwardly used to investigate nonlinear temporal effects occurring in SWS, such as optical limiting, solitary waves propagation and modulation instability.

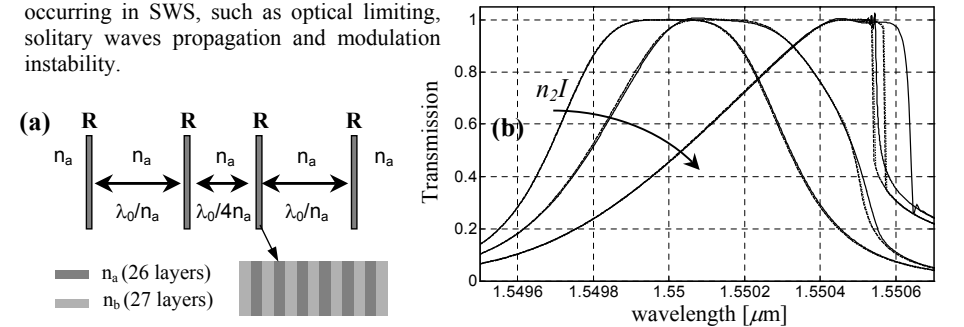


Fig 1: (a) Schematic of a double-cavity SWS. (b) Nonlinear response of the SWS shown in (a) for increasing input intensity  $n_2I$  ( $0, 2.4 \cdot 10^{-6}, 9.6 \cdot 10^{-6}$ ): TD (continuous lines), ME (dotted lines), FD (dashed lines).

### References

- [1] COST P11 website: <http://w3.uniroma1.it/energetica/>

## Hurst's Index and Complexity of Wave in Modulated Dielectric Medium

Alexander Nerukh, Nataliya Ruzhytska, Dmitry Nerukh

Kharkov National University of RadioElectronics, 14 Lenin Ave., Kharkov, 61166 - Ukraine  
nerukh@ddan.kharkov.ua

Correlation between Hurst's index of an electromagnetic signal and its complexity in time-varying medium is shown.

### Summary

Properties of the wave transformation under medium modulation can be investigated by modelling this process with time-varying medium, which is modulated by a finite packet of rectangular periodic change of the medium permittivity. Each change of the permittivity leads to appearing of backward and forward waves with changed amplitudes and frequency. The ratio between the amplitudes of the forward and backward waves, which is governed by a sequence  $r_i$ , has monotone or irregular behaviour. The latter can be investigated by virtue of the Hurst exponent  $H$  [1], which equals to  $H=0.5$  for white noise (a completely uncorrelated signal). The value  $H > 0.5$  ( $H < 0.5$ ) is associated with the long-range correlation when the time series exhibits persistence (antipersistence). It has been shown in [2] that the character of  $r_i$  behaviour is determined by the generalised parameter  $u$ . Irregularity is absent if  $u > 1$  and in this case index  $H$  differs from the value 0.5 significantly. The  $r_i$  behaviour can be characterised also

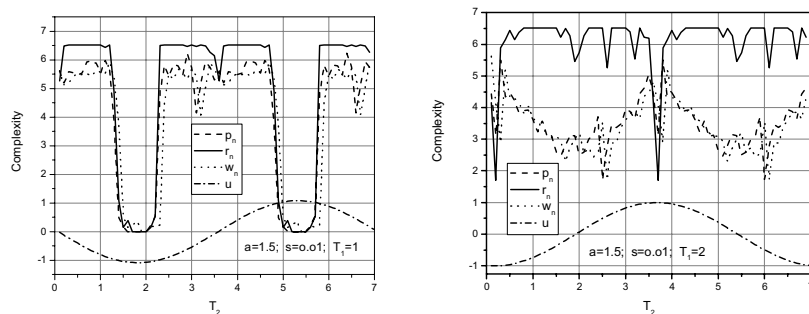


Fig. 1

by the complexity measure [3, 4]. This measure dependence (Fig.1) on the on-off time ratio for various modulation periods shows the correlation between the complexity and the index  $H$ . It is seen that the complexity drops to zero when the parameter  $u$  (the dash-dot sine-like line) becomes greater than 1 and  $H$  has values which are typical for regular behaviour.

### References

- [1] Hurst H E, Black R P and Simaika Y M, 1965 Long-Term Storage: An Experimental Study (London: Constable)
- [2] Nerukh A.G., J. of Physics D: Applied Physics, **32**, pp. 2006-2013, 1999.
- [3] Crutchfield J. P. and K. Young, Phys. Rev. Lett., **63**, pp. 105-108., 1989.
- [4] Ruzhytska N.N., A.G.Nerukh, D.A.Nerukh, Optics and Quantum Electronics, **35**, 347-364, 2003

## Semi-analytical diagnostics and design of gradient refractive index profile waveguides

Nikolai Nikolaev\*, Victor V. Shevchenko<sup>o</sup>

\*Peoples' Friendship University of Russia, 6 Miklukho-Maklaya St., Moscow, 117198 Russia  
ne\_nikolaev@mail.ru

<sup>o</sup>Institute of Radio Engineering and Electronics, Russian Academy of Sciences, Build.7, 11 Mokhovaya St., Moscow, 101999 Russia

Planar optical waveguides with gradient refractive index profile are modelled using an accurate semi-analytical method. Inverse problem for designing such waveguides and diagnosing their properties is solved and its application shown.

### Summary

Gradient index profile waveguides, like, for example, polymer ones, has many applications due to possibilities to provide advanced propagation properties or field profile and being more sensible to their surrounding. Their fabrication and usage widened during last few years [1]. However, as the fabrication process is too complicated to make an exact profile, some further adjustments are often needed to provide the required propagation properties.

We propose a new approach to design the waveguides with complex gradient profiles of refractive index, including the advantage of the best design from already fabricated gradient materials. We use the Shift Formulae Method (SFM) described in [2]. This method allows solving the problem of synthesis by using the results of direct problem solution. The essence of Shift Formulae Method is special integral relationships derived from wave equations; they are named shift formulae and describe changes of dispersion characteristics of waves at changes of waveguide parameters or their structure. Preliminary results of the method application were shown in [3].

Numerical procedure can be applied to waveguides of different types, most common of which are buried waveguides. We consider here waveguides, the permittivity profile of which is represented by a smooth function modeled by truncated exponential-power function. Analytical solution is followed by a program, elaborated to solve the inverse problem, which do not only allow to synthesize the right waveguide, but also to solve diagnostic problems to retrieve refractive index profile inside the material after measured propagation characteristics. The values of propagation constants and the position of dispersion curves depend on permittivity profile parameters. Applications to diagnosing changes in surrounding media are analyzed and discussed.

### References

- [1] K. Kuriki, T. Kobayashi, N. Imai, T. Tamura, S. Nishihara, A. Tagaya, Y. Koike and Y. Okamoto, IEEE Photonics Technology Letters, Vo. 12, No. 8, 989-991, 2000.
- [2] V.V. Shevchenko, N. Espinosa-Ortiz, J. of Commun. Technology and Electronics, **38**, N16, 121, 1993.
- [3] N.E. Nikolaev, V.V. Shevchenko, Proc. Xth International Workshop on Optical Waveguide Theory and Numerical Modelling. April 5-6, 2002. Nottingham, UK.

## Bragg Diffraction in Bounded Homogeneous System of Coupled Channel Waveguides

J. Kh. Nurligareev\*, V.A. Sychugov\*, K.M. Golant<sup>o</sup>

\*Laser Materials and Technology Research Center, General Physics Institute, Russian Academy of Sciences, Vavilova str. 38, Moscow, 199911 Russia

jamil@kapella.gpi.ru

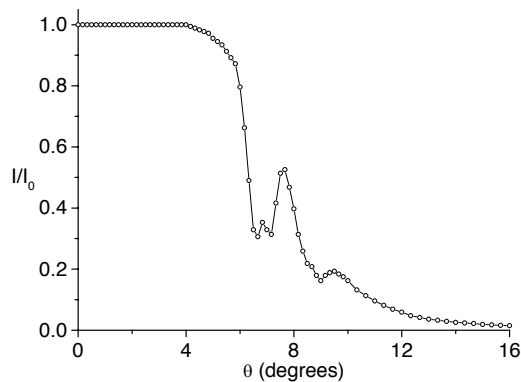
<sup>o</sup>Fiber Optics Research Center, General Physics Institute, Russian Academy of Sciences

The bounded homogeneous system consisting of  $N$ -channel waveguides is studied. We show that the  $N^{\text{th}}$  and  $N+1^{\text{st}}$  modes (nearest to the Bragg reflection condition) suffer abrupt change in effective refractive index and exhibit small propagation losses even located between leaky modes.

### Summary

Nowadays, the channel-waveguide type systems have attracted particular interest in waveguide laser optics owing to the possibility of high-power continuous operation in them [1]. The light propagation processes in homogeneous systems have been investigated in the last few years [2,3] and the Bragg diffraction process is one of the most interesting features [3]. In this work we report an investigation of the bounded homogeneous system consisting of  $N$  channel straight waveguides. The number of modes travelling in this system was computed in relationship to the number  $N$  of channels, spacing between them and number of individual channel modes. It was found numerically that the calculated wave vectors values for the  $N$  and  $N+1$ -order modes are close to the Bragg reflection condition and hence these modes may be called as Bragg modes.

The effective refractive indices  $n^*$  of these modes are different, i.e. the plot  $n^*(m)$  has a step. We found the dependence this step  $\Delta n^*$  on the spacing between the channels and the number of modes in the single waveguide. The system of  $N$  single-mode straight waveguides with guiding modes number  $M=34 < N=50$  was experimentally investigated. In this case, the Bragg modes of the system are located between the leaky modes and have small propagation losses relative to adjacent modes as shown in the figure. Location of the Bragg modes between leaky modes may be useful for its selection by semiconductor laser generation.



### References

- [1] R.J. Beach, M. Feir, R.H. Page, L.D. Brasure, R. Wilcox, S.A. Payne, J.Opt.Soc.Am.B., 1521-1534, 19(7), 2002.
- [2] T. Petsch, T. Zeutgraf, U. Streppel, A. Bräuer, U. Perchel, F. Lederer, Proc.ECIO-01, Paderborn, Germany, 21-24, 2001.
- [3] A.A. Goncharov, K.K. Svidzinsky, V.A. Sychugov, B.A. Usievich, Laser Physics, 1017-1023, 13(8), 2003.

## Time Domain Modelling of Nonlinear Optical Waveguides

S S A Obayya and D Pinto

Electronic and Computer Engineering, School of Engineering and Design, Brunel University, Uxbridge, Middlesex, UB8 3PH, UK

Tel. +44 18952 65790, Fax +44 1895 258 728

email: Salah.Obayya@brunel.ac.uk

Nonlinear materials have attracted a great interest because of their potential to develop new devices in the field of optical systems. Their properties have led to an intense investigation on the possibility of utilising these materials for all-optical ultrafast applications. As shown in [1], their power-dependent properties have been usefully applied for “switching” operation with all-optical systems. The formulation of FDTD for nonlinear problems, as presented in [2] where FDTD has mainly been used to investigate soliton generation in nonlinear material, has made this method of general applicability and it can be used to simulate a wide variety of devices. Moreover, this method can take into account all order of nonlinearity in order to make it suitable to simulate all types of nonlinear effects. In this paper, a numerically efficient FDTD code has been developed in order to analyse the nonlinear waveguide and nonlinear Bragg Gratings Reflector (BR), whose schematic diagram is shown in Fig. 1, was analysed using the developed FDTD code. The reflection coefficient was calculated for different numbers of periods  $N$ , and for different levels of power of the incident pulse. For all simulations the  $TE_0$  fundamental mode profile was used, with a Gaussian pulse in time modulated by a sinusoidal function with centre wavelength fixed to  $\lambda_0 = 0.99 \mu\text{m}$ . The results are shown in Fig. 2. From this figure, it may be seen that for a fixed value of the number of periods  $N$  the reflection coefficient value increases as the power of the incident source increases. Furthermore, the reflection coefficient seems to reach a saturation value as the power of the incident source is higher than  $10 \text{ W/m}$ . Moreover, for a fixed level of power it can be noted that the reflection coefficient increases as the number of periods  $N$  increases. An explanation to values of the reflection coefficient greater than unity can be attributed to the Self-Phase Modulation (SPM) effect in nonlinear media. The spectrum broadening and the shift of the reflection coefficient peak towards lower frequencies induce to an amplitude gain within a certain frequency band of the incident signal. In the workshop, more results will be presented on the FDTD simulation of nonlinear optical waveguides and BR showing their potentially useful “tuneable” characteristics.

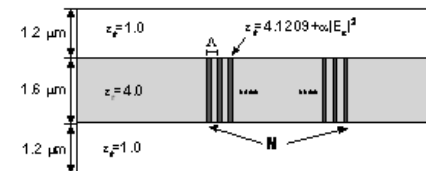


Fig. 1

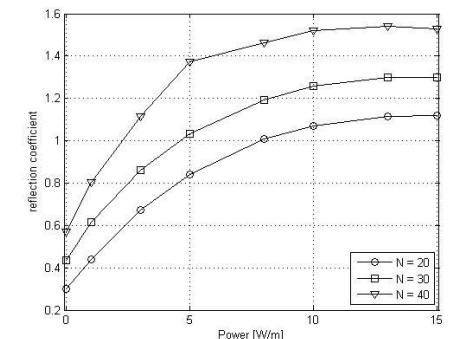


Fig. 2

### References

- [1] H. Murata, M. Izutsu and T. Sueta, J. Lightwave Technol., 16, 833-840, 1998.
- [2] R.M. Joseph and A. Taflove, IEEE Trans. Antennas Propagat., 45, 364-374, 1997.

## Modeling of an Optical Ring Resonator Electric Field Sensor

Francesco De Leonardis\* and Vittorio M. N. Passaro°

\*Dipartimento di Ingegneria dell'Ambiente e per lo Sviluppo Sostenibile, Politecnico di Bari, Taranto - Italy

°Dipartimento di Elettrotecnica ed Elettronica, Politecnico di Bari, Bari - Italy, [passaro@deemail.poliba.it](mailto:passaro@deemail.poliba.it)

The modeling of a novel concept of electric field photonic sensor based on a ring resonator is presented. Several modeling techniques have been applied, including finite element method and scattering matrix.

### Summary

The interest devoted towards optical approaches in sensing electric fields is due to their inherent tolerance to highly disturbing environments, possibility of remote monitoring, passive sensor head and high sensitivity [1]. The photonic sensor in this paper is based on an integrated optical AlGaAs/GaAs ring resonator used as an electro-optic (EO) phase modulator (see Fig 1, showing the upper electrode connected to the antenna dipole). The light at  $\lambda = 1550$  nm is coupled to the input waveguide and, then, inside the ring resonator. Finally, the transmitted power is detected at the output by using a second waveguide. The electric field to be measured changes the ring resonance condition due to EO effect and, then, the detected power. The sensor sensitivity (of the order of 1-2 kV/m) depends on beam temporal coherence factor, coupling coefficient, ring sizes, optical losses and photodiode signal-to-noise ratio. It has been optimized by biasing the device in the spectrum point of maximum slope. In the range  $0.95 \pm 1$  of temporal coherence, a good device sensitivity and linearity can be easily achieved, with a bandwidth larger than 20 GHz for a ring radius of  $1500 \mu\text{m}$ . In Fig. 2 the shift of ring resonant wavelength can be observed, when an external electric field of 200 kV/m is applied. The point of maximum slope for the device bias is obtained from the spectrum in absence of any electric field (black curve). In Fig. 3 and 4 the 3D dependences of sensor sensitivity on the design parameters are sketched. For a ring of  $1500 \mu\text{m}$ , a coherence of 0.98 and a coupling coefficient of 0.25 can be easily obtained. In Fig. 5 the device sensitivity decreases by reducing the source coherence, but its linearity range is further improved.

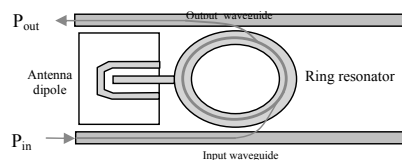


Fig. 1. Scheme of the sensor.

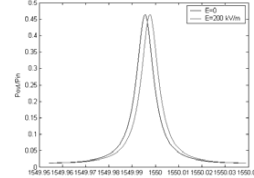


Fig. 2. Wavelength shift with applied electric field.

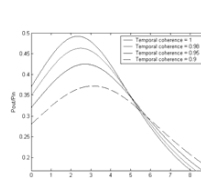


Fig. 5. Output power vs applied electric field.

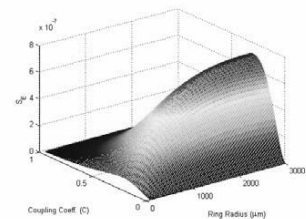


Fig. 3. Sensitivity vs coupling coefficient and ring radius.

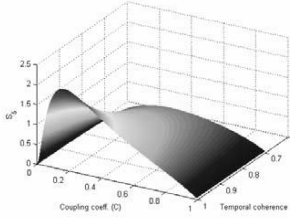


Fig. 4. Sensitivity vs coupling coefficient and temporal coherence (ring radius of  $1500 \mu\text{m}$ ).

## Simulation of Thermo-Optic Reconfigurable Optical Add/Drop Multiplexers in SOI Technology

Vittorio M. N. Passaro\*, Francesca Magno\*, and Andrei V. Tsarev°

\*Dipartimento di Elettrotecnica ed Elettronica, Politecnico di Bari,

via Edoardo Orabona n. 4, 70125 Bari, Italy

[passaro@deemail.poliba.it](mailto:passaro@deemail.poliba.it)

°Institute of Semiconductor Physics, Siberian Branch Russian Academy of Sciences

Prospect Lavrenteva n. 13, Novosibirsk, 630090, Russia

[tsarev@isp.nsc.ru](mailto:tsarev@isp.nsc.ru)

A novel reconfigurable optical add/drop multiplexer (ROADM) on Silicon-on-Insulator (SOI) that utilize multi-reflector beam expanders and thermo-optic tuning is described. Numerical results of computer experiments carried out by 3D FEM and 2D FDTD methods have demonstrated the device proof-of-concept.

### Summary

A preliminary examination of the multi-reflector (MR) technology has been recently completed by our international team [1] and proves the basic conception of the device and its applicability to Silicon-on-Insulator (SOI) structures. In this paper we propose an advanced multi-reflector reconfigurable optical add/drop multiplexer in SOI using an array of thermo-optic phase shifters, providing wide range tunability and remarkably high tuning rate (up to  $0.6 \text{ nm}/^\circ\text{C}$ ) for filtered optical wavelengths. To provide better tuning efficiency and thermal isolation in optical phase shifters, we propose and examine a novel double-rib SOI waveguide array (see Fig. 1). General device description is accompanied by a number of numerical results performed by 3D finite element method (FEM) and 2D finite difference time domain (FDTD) to demonstrate the device proof-of-concept (see Fig. 2). General limitation of FDTD approach makes very difficult to examine real devices that have very large number of reflectors ( $>100$ ) and thus too large dimensions. Nevertheless FDTD helps us to determine reflection and transmission coefficients that have to be used in further analysis of real devices.

Our results have proved the validity to conduct intensive investigations over multi-reflector filtering technology and new optical devices that can be manufactured on SOI waveguides and that could open a new horizon in the "optical age of silicon". This work was partially supported by Russian Fund for Basic Research under Grant No 05-02-08118-ofi-a.

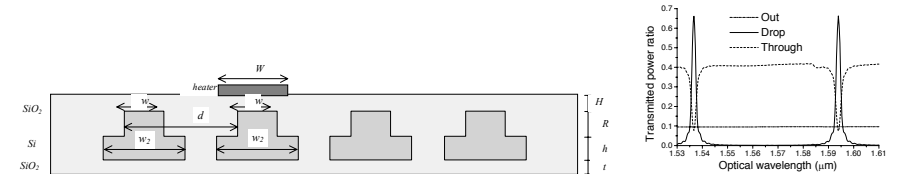


Fig. 1. General view of double-rib waveguide array with the heater on the top.

Fig. 2. Frequency response of ROADM simulated by FDTD with 32 slanted reflectors.

### References

[1] V. M. N. Passaro, F. Magno, and A. V. Tsarev, *Optics Express*, **13**, 3429, 2005.

[1] W. Johnstone et al., *IEE Proc.-Sci. Meas. Tech.*, **142**, 109, 1995.

# Efficient Phase Matched Second Harmonic Generation through Rotated Periodic Poling in LiNbO<sub>3</sub> Waveguides

F.M. Pigozzo, E. Autizi and A.-D. Capobianco

DEI Department, University of Padova, Via Gradenigo 6/b, 35131 Padova, Italy  
 superg@ray.dei.unipd.it

C. Sada, M. Bazzan, N. Argiolas and P. Mazzoldi

INFN and Physics Department, University of Padova, Via Marzolo 8, 35131 Padova, Italy

We present a new method to enhance the continuously phase matched second harmonic generation in 2D PPLN optical waveguides fabricated using the off-center Czochralski technique and proton-exchange. We show that a periodic variation of the nonlinear coefficient along the transverse coordinate permits for efficient energetic exchanges.

**Keywords:** Nonlinear optics, Integrated optics, Frequency conversion, Lithium niobate.

Recently we reported on the possibility of realize Periodically Poled Lithium Niobate (PPLN) crystals by means of the unconventional Czochralski technique, i.e. by off-centering the temperature field axis with respect to the growth one [1]. We have already shown the opportunity of performing efficient phase matched Second Harmonic Generation (SHG) using the PPLN in a novel different way, i.e. rotating the PPLN 90 degrees with respect to the propagation direction in a 2D waveguide made by ion-implantation on a periodically poled a-cut LiNbO<sub>3</sub> crystal [2] (see Fig. 1). In this work we extend our analysis and we report on the possibility of performing efficient interaction in a bidimensional waveguide made by proton-exchange. In addition, we show the effects of different poling periods and cutting offset on the conversion efficiency. Finally, we compare the effectiveness of a conventional generation when the first two modes at fundamental frequency and second harmonic are in Quasi Phase Matching (QPM) with the SH efficiency resulting from the new technique. Surprisingly whenever defects in the fabrication process are taken into account the rotated PPLN configuration exhibits a higher robustness in terms of achievable SHG.

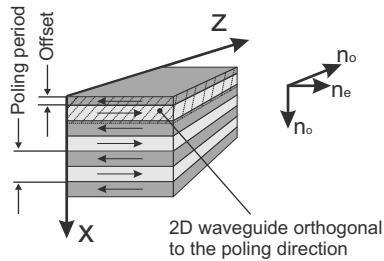


Fig. 1. Efficient phase matched SHG can be achieved increasing the modal overlap in a 2D waveguide through a rotated PPLN.

[1] E. Autizi, A.-D. Capobianco, F.M. Pigozzo, N. Argiolas, M. Bazzan, E. Cattaruzza, P. Mazzoldi and C. Sada, *OQE Special issue on OWTNM 2005*, to be published.

[2] F.M. Pigozzo, E. Autizi, A.-D. Capobianco, N. Argiolas, C. Sada, M. Bazzan and P. Mazzoldi, *Nonlinear Guided Waves and Their Application*, Dresden, Germany, September 2005.

# Solving Boundary Problem for Nonlinear Elliptic Equation By Successive Approximations Method

S.V. Kolosova, S. Ruzhytska

Kharkiv National University of RadioElectronics, 14 Lenin Avenue, Kharkov, 61166, UKRAINE: E-mail:  
 ruzhysk@ums.kharkov.ua

It is considered a 2D boundary value problem for a nonlinear Poisson equation, which can describe field distribution in a waveguide cross-section. Solution of this problem is made by method of successive approximations. It is shown that accuracy of the solution is controllable.

## Summary

The boundary problem for the field distribution in a nonlinear waveguide cross-section is given by the Poisson equation [1]

$$\Delta u + e^{-u} = 0, \quad \forall (x, y) \in \Omega \quad (1)$$

which is formulated in 2D domain for a function  $u$ . This function is assumed positive and satisfies to boundary conditions

$$u|_{\partial\Omega} = 0, \quad u(x, y) \geq 0, \quad \forall (x, y) \in \bar{\Omega}, \quad (2)$$

Solution to this problem is constructed by the ordinary successive approximations method that gives a chain of boundary problems

$$\begin{aligned} -\Delta u^{(1)} &= 1 & \forall (x, y) \in \Omega, & & u^{(1)}|_{\partial\Omega} &= 0, \\ -\Delta u^{(2)} &= e^{-u^{(1)}} & \forall (x, y) \in \Omega, & & u^{(2)}|_{\partial\Omega} &= 0, \\ & \dots & & & & \\ -\Delta u^{(k+1)} &= e^{-u^{(k)}} & \forall (x, y) \in \Omega, & & u^{(k+1)}|_{\partial\Omega} &= 0, \end{aligned}$$

where  $k = 1, 2, \dots$

Each boundary problem is solved by Ritz's method and calculation is implemented for two kinds of domains: rectangular and circular ones. The result for the rectangular domain is shown in Fig. 1, for circular domain in Fig. 2. Accuracy obtained solutions is compared with the solutions obtained by the quasilinearization method in [1] and the two-sided solutions in [2].

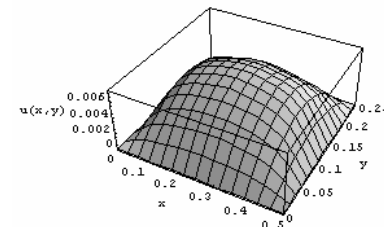


Fig. 1

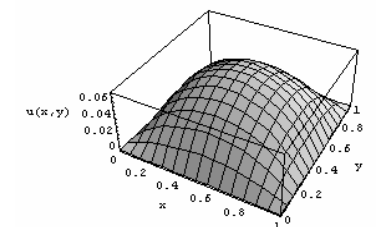


Fig. 2

## References

- [1] R. Bellman, R. Calaba, *Quasilinearization and nonlinear boundary value problems*, 1968.
- [2] S.V.Kolosova, A.V. Chaliy, *Reports of National Academy of Science of Ukraine*, No 11, 1999.

## Spontaneous Parametric Down Conversion Process in a Guided Wave Photonic Crystal

Letizia Sciscione\*, Marco Centini\*, Concita Sibilìa\*, Mario Bertolotti\*, Micheal Scalora<sup>°</sup>

\*Dipartimento di Energetica, Università "La Sapienza", Via Scarpa 16, 00161 Roma - Italy  
[letizia.sciscione@uniroma1.it](mailto:letizia.sciscione@uniroma1.it)

<sup>°</sup> Charles M. Bowden Research Center, AMSRD-WS-ST, RDERCOM, Readstone Arsenal, AL 35898-5000

We analyse and design a photonic crystal waveguide embedded between two corrugated waveguides in order to generate twin photons perpendicular to the pump field direction. We focused our attention on the study of the pump field as a mode of the photonic crystal wave guide.

### Summary

The generation of twin photons, arisen from a spontaneous parametric down-conversion (SPDC) process, has received attention for applications to quantum cryptography, teleportation, dense coding, and quantum communications. This interest is due to several properties, such as unimpeded propagation over relatively long distances and little interaction with the environment. The first sources of polarization-entangled photon pairs were non linear crystals such as BBO. Although the second order non linearity of these crystals is high, they present wide bandwidth and low brightness (per nanometer and single mode). Recently, photonic crystal fibres or PPLN waveguides have been proposed as sources of quantum-correlated photon pairs[1,2]. Considering that the interest is moving to different geometries combining small dimensions and high performance, we propose a photonic crystal waveguide composed of a planar layer embedded between two corrugated guides (as shown in Fig.1). We perform a modal analysis of the photonic crystals waveguide in order to minimize losses and to obtain a mirror-like behaviour for the pump field ( $\lambda_p=400\text{nm}$ ). All the analysis is performed with the aim to enhance the overlap among fields involved in the non linear process. Different geometries are proposed by changing the number of periods of the mirrors and the central slab length. The materials considered in our structures are InGaN for the guiding layer and GaN for the substrate, due to their outstanding properties in the visible spectral region. The study of the twin photon generation conditions in the direction perpendicular to the z-x plane and its efficiency will be presented.

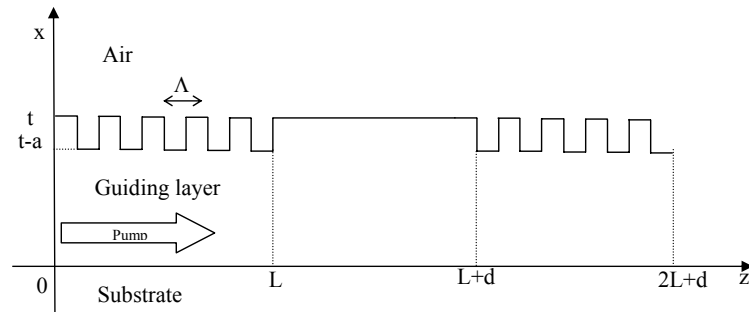


Fig. 1 Scheme of the proposed waveguide

### References

- [1] J.G. Rarity *et al.*, Opt. Exp.,13, 2, 534-544 (2005)
- [2] A . De Rossi *et al.*, Phys. Rev. Lett. 88, 43901 (2002)

## Square-lattice photonic crystal fiber cut-off analysis

Federica Poli, Matteo Foroni, Lorenzo Rosa, Annamaria Cucinotta, Stefano Selleri

Dipartimento di Ingegneria dell'Informazione, Università di Parma, Parco Area delle Scienze 181/A, Parma - Italy

[stefano.selleri@unipr.it](mailto:stefano.selleri@unipr.it)

The modal cut-off of square-lattice photonic crystal fibers has been accurately investigated, taking into account the effect of silica chromatic dispersion, by analyzing the leaky behavior of the second-order mode.

### Summary

Photonic Crystal Fibers (PCFs) are characterized by an array of air-holes running along their entire length which provides the confinement and guidance of light. Due to the huge variety of air-hole arrangements, PCFs offer a wide possibility to control the refractive index contrast between the core and the microstructured cladding and, as a consequence, novel and unique optical properties. Recently, the guiding and dispersion properties of PCFs with a square lattice of air-holes have been investigated [1]. It has been demonstrated that square-lattice PCFs have a wider effective area with respect to triangular PCFs with the same geometric parameters [1], that is the hole-to-hole spacing  $\Lambda$  and the air-hole diameter  $d$ , so they can be of practical interest as large mode area fibers for applications like high-power delivery. In order to successfully use square-lattice PCFs for this kind of applications, it is necessary to accurately define their single-mode operation regime.

In this work the cut-off analysis of square-lattice PCFs has been carried out through the Q parameter method, previously adopted for fibers with a triangular lattice [2]. In order to clearly decide at which wavelength  $\lambda^*$  the second-order mode is no more guided, that is it becomes a delocalized cladding mode, it is possible to take into account its leakage losses, which are related to the attenuation constant  $\alpha$ , the real part of the complex propagation constant  $\gamma$ . This has been calculated for the second-order mode by means of a full-vector modal solver based on the finite element method with anisotropic perfectly matched layer. The multipole method has been also used to confirm the simulation results, obtaining a good agreement.

In the present study the Q parameter has been calculated for different normalized wavelength  $\lambda/\Lambda$  values for square-lattice PCFs with  $d/\Lambda$  in the range  $0.45 \div 0.57$ . Differently from the previous cut-off analysis for triangular fibers [2], the chromatic dispersion of silica has been taken into account. Four different  $\lambda$  values, 633 nm, 1064 nm, 1310 nm and 1550 nm, have been considered, and  $\Lambda$  has been properly chosen to obtain the desired normalized wavelength values. It has been demonstrated that the choice of the guided-mode wavelength slightly influences the results of the cut-off analysis. In particular, by comparing the values of the normalized cut-off wavelength  $\lambda^*/\Lambda$  calculated with  $\lambda = 633$  nm and with  $\lambda = 1550$  nm, a mean relative difference of about 2.7% has been obtained for  $d/\Lambda$  is in the range between  $0.5 \div 0.57$ .

A phase diagram, which describes the regions of single-mode and multi-mode operation, as well as the endlessly single-mode regime, has been evaluated. It has been demonstrated that the single-mode regime of square-lattice PCFs is wider than that of triangular ones. Moreover, square-lattice PCFs can be endlessly single-mode in a wider range of the geometric parameter values with respect to triangular fibers. In fact, their endlessly single-mode operation region, described by  $d/\Lambda < 0.442$ , is larger than that of triangular PCFs, defined by  $d/\Lambda < 0.406$  [2].

### References

- [1] A. Bouk, A. Cucinotta, F. Poli, and S. Selleri, Optics Express 5, 941-946, 2004.
- [2] B.T. Kuhlmeiy, R.C. McPhedran, and C. Martijn de Sterke, Optics Letters 27, 1684-1686, 2002.

# Analytical Computation of the Propagation Matrix for the Finite-Difference Split-Step Non-Paraxial Method

Anurag Sharma\*, Debjani Bhattacharya\* and Arti Agrawal<sup>o</sup>

\*Physics Department, Indian Institute of Technology Delhi, New Delhi-110016, India  
asharma@physics.iitd.ac.in

<sup>o</sup>Department of Electrical, Electronic and Information Engineering, City University, London, UK

We describe a method for analytical computation of a propagation matrix, including the square-root operation, used in the finite-difference split-step non-paraxial method thereby reducing the computation time significantly. The method can also be used to compute diffraction of arbitrary fields efficiently.

## Summary

We have recently developed a finite-difference split-step non-paraxial method, which is based on the solution of the wave equation without paraxial or one-way approximation [1-3]. The method has been shown to give very good accuracy and stability, even with relatively large propagation steps. The algorithm of the method can be written as

$$\Phi(z + \Delta z) = \mathbf{P} \mathbf{Q}(z) \mathbf{P} \Phi(z) + O((\Delta z)^3) \quad (1)$$

where  $\Phi(z)$  is the column vector containing the field and its derivative,  $\mathbf{P}$  is a constant matrix representing propagation through a reference medium of index  $n_r$ ,  $\mathbf{Q}(z)$  is the sparse matrix defining the index distribution as a function of  $z$ , which is the direction of propagation. Thus, one single step requires only multiplication of a square (dense) matrix with a complex column vector and of a sparse matrix with a column vector, and hence, is computationally efficient. However, the one-time computation of matrix  $\mathbf{P}$  requires diagonalization and square root operation of a dense matrix  $\mathbf{S}$ , which is the finite-difference representation of the operator,  $k_0^2 n_r^2 + \partial^2 / \partial x^2$ . We have also used higher order finite-difference representation for  $\partial^2 / \partial x^2$ ; typically, the order  $M$  of this representation used is about 40. The effort for computation of  $\mathbf{P}$  increases linearly with  $M$  making it equivalent to the effort involved in propagating nearly 1000 steps. This computational overhead would further increase if the reference index were to be changed for some section of the device.

The purpose of this presentation is to report a procedure for analytical evaluation of the matrix  $\mathbf{P}$ . The starting point for the analytical evaluation is analytical diagonalization [4] of the tri-diagonal matrix representing the central difference approximation of  $\partial^2 / \partial x^2$ . This is used for obtaining the  $\mathbf{S}$  in the diagonalized form, which is then used to obtain  $\mathbf{P}$  analytically as all the sine, cosine and square root operations are carried out on diagonal matrices. This procedure also makes the evaluation of  $\mathbf{P}$  virtually independent of  $M$ . A typical comparison of computation times is shown in Fig. 1, which clearly demonstrates the advantage of the procedure being presented. It reduces the computation time for  $\mathbf{P}$  by a factor of 10 for  $M=40$ . It may be added that the new procedure makes the propagation in uniform media nearly analytical and hence, diffraction of arbitrary fields can be computed very efficiently. More examples will be presented.

## References

- [1] A. Sharma and A. Agrawal, *ECIO-2005*, Grenoble, France, April 5-8, 2005.
- [2] A. Sharma and A. Agrawal, *Opt. Quantum Electron.* (submitted, special issue on Theory and Modelling, 2006)
- [3] A. Sharma and A. Agrawal, *IEEE Photon. Technol. Lett.* (In press, 2006).
- [4] M.K. Jain *et al.*, Numerical Methods for Scientific and Engineering Computation, Wiley Eastern, New Delhi, 1985.

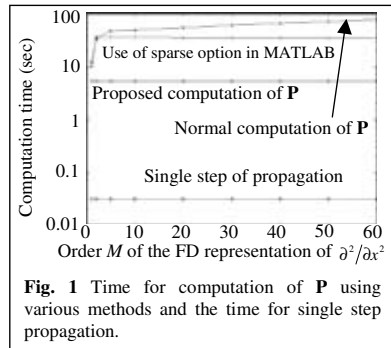


Fig. 1 Time for computation of  $\mathbf{P}$  using various methods and the time for single step propagation.

# Scale-Length Invariant Guided Modes in 1D Metamaterial Photonic Crystal Waveguides

Juan A. Monsoriu

Departamento de Física Aplicada, Universidad Politécnica de Valencia, 46022 Valencia, Spain

Ricardo A. Depine, María L. Martínez-Ricci

Departamento de Física, Universidad de Buenos Aires, C1428EHA Buenos Aires, Argentina

Enrique Silvestre, Pedro Andrés

Departamento de Óptica, Universidad de Valencia, 46100 Burjassot, Valencia, Spain  
enrique.silvestre@uv.es

In this contribution we study the guiding properties of 1D metamaterial photonic crystal waveguides. The unusual behavior of certain gaps shown by 1D metamaterial multilayered structures allows us to obtain guided modes that remain invariant under scaling of the cladding.

**Keywords:** guided-wave optics, photonic crystal, metamaterial

One-dimensional (1D) metamaterial photonic crystal waveguides (MMPCWs) are guiding structures with a planar dielectric core that acts as the defect (air in our case), surrounded by a perfect 1D layered cladding, which is formed by a set of alternating layers of metamaterial (MM) and a conventional dielectric material. These MMs are artificially constructed composites that can exhibit a negative electric permittivity and a negative magnetic permeability in the same frequency range.

The existence of “zero average refractive index” photonic band gaps (PBGs) and “zero permeability” and “zero permittivity” PBGs in 1D MM photonic crystals is demonstrated in Ref. [1] and [2], respectively. In contrast to Bragg PBGs, these new kinds of gap are invariant to scaling and very robust to disorder. We take advantage of these characteristics to design MMPCWs with guided modes located inside the above PBGs, which remain invariant to scale-length changes of the cladding (see Fig. 1).

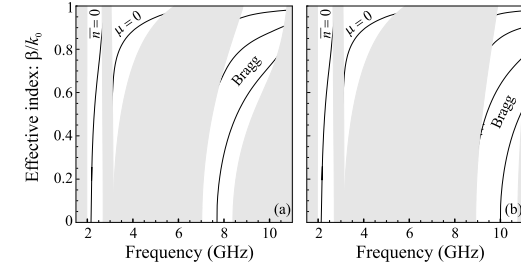


Fig. 1. TE guided modes in a MMPCW having a 6-cm-wide air core surrounded by: (a) a 1D MM photonic cladding with geometric and constitutive parameters as those used in Fig. 2, Ref. [1], and (b) the same structure but the lattice constant scaled by 2/3. White regions correspond to forbidden bands. Note that modal dispersion relations for the “zero average refractive index” guided mode and for the “zero permeability” guided mode remain unchanged.

- [1] J. Li, L. Zhou, C.T. Chan, P. Sheng, *Phys. Rev. Lett.* **90**, 083901, 2003.
- [2] R.D. Depine, M.L. Martínez-Ricci, J.A. Monsoriu, E. Silvestre, P. Andrés, *Phys. Rev. Lett.* (submitted).

## A simple low-dimensional model and efficient FEM calculations to determine the quality of photonic crystal cavities

A. Sopaheluwakan<sup>1</sup>, E. van Groesen

<sup>1</sup>*Applied Analysis and Mathematical Physics,*

*MESA+ Research Institute, University of Twente, The Netherlands*

[a.sopaheluwakan@math.utwente.nl](mailto:a.sopaheluwakan@math.utwente.nl)

We present a low-dimensional model to describe the decay of resonant modes of a photonic crystal with point defect. This model will be compared with calculations using a finite element scheme with fully transparent boundary conditions.

### Summary

Having the ability to control the propagation of light in a selected frequency range, photonic crystal structures have a number of potential applications: waveguides, junctions, couplers, resonant cavities, etc. By introducing a point defect in a periodic photonic crystal lattice, an optical resonant cavity is formed. For this type of structure, a localized mode can exist in the band gap, possessing a high quality ( $Q$ ) factor that can be utilized for many applications.

We use a finite element scheme in frequency domain to study numerically the decay of various resonant (defect) modes in a photonic crystal lattice with point defect. This (efficient) finite element scheme is equipped with transparent boundary conditions[1] that guaranty reflectionless boundaries of the computational domain. This approach can monitor efficiently the time variation of the field and the energy at a particular observation point inside the computational domain. However, for cavities with high  $Q$  factor, the decay of the field and energy is very slow, so to have an accurate result for  $Q$ , it is necessary to compute over a long time interval[2-4].

Using a simple low-dimensional model, we will derive analytical expressions describing the decay of the field and the energy, and also the  $Q$  factor. These are expressed in terms of the energy content of the resonant modes: the energy in the structure, normalized with some boundary value of the field. For a given structure, the result of the low dimensional model is compared with the numerical calculation.

### References

- [1] J. B. Nicolau, E. van Groesen, *J.of Nonl. Opt. Phys & Mat.* 14, 161-176, 2005.
- [2] O. Painter, J. Vuckovic, A. Scherer, *J. Opt. Soc. Am. B* 16, 275-285, 1999.
- [3] E. Miyai, K. Sakoda, *Opt. Lett* 26, 740-742, 2001.
- [4] V.F. Rodriguez-Esquerre, M. Koshiba, H.E. Hernandez-Figueroa, *IEEE Phot. Tech. Lett.* 16, 816-818, 2004.

## Numerical Approaches for the Analysis of Injection Locked Lasers

Giovanni Tartarini<sup>1</sup>, Lorenzo Rosa<sup>2</sup>, Stefano Selleri<sup>2</sup>, Pier Faccin<sup>3</sup>, Enrico Maria Fabbri<sup>3</sup>

<sup>1</sup>*Dip. Elettronica, Informatica e Sistemistica, Università di Bologna, Viale Risorgimento, 2, Bologna, Italy*

<sup>2</sup>*Dip. Ingegneria dell'Informazione, Università di Parma, Parco Area delle Scienze, 181/A, Parma, Italy*

<sup>3</sup>*Andrew Wireless Systems srl, Via de Crescenzi 40, Faenza, Italy*

[gtartarini@deis.unibo.it](mailto:gtartarini@deis.unibo.it)

Injection locked laser has been modelled though an accurate set of rate equations and analysed by means of two different numerical approaches. Results, which describe the time and spectral behaviour as a function of the detuning and of the master rate of injection, are compared as well as verified with experimental ones.

### Summary

The injection locking technique allows one or more oscillators, called slave lasers, to be tuned by a second oscillator with superior spectral properties, called master laser. This technique was first introduced for electronic and microwave devices and later on also for He-Ne and semiconductor lasers [1]. The master laser must provide a very high coherent radiation with a very narrow linewidth and low noise, while the slave one is a high power and low coherent laser. The spectral difference of their emitted field, typically, is of the order of GHz or tens of GHz. By injecting a fraction of the field generated by the master into the slave cavity, the slave field can be locked to the master one resulting in a high power radiation with spectral and noise properties improved with respect to the solitary working slave regime. In particular, this technique can narrow the slave linewidth, increase the modulation bandwidth and reduce noise and frequency chirping. It is therefore an extremely interesting solution, which can find application, for instance, in optical coherent systems, where an efficient and reliable method to synchronize an optical signal to a local oscillator is required, or in optical subcarrier modulated (SCM) systems, where the microwave signal must reach its destination exhibiting very low values of noise and distortion terms. In this work the master-slave configuration has been modeled by properly modifying the slave rate equations in order to take into account the radiation injected by the master laser [2]. Two modelling programs have then been developed: one of them is based on a commercial code based on the finite element method, while the other is based on own made Matlab scripts. The two approaches allow to evaluate the master-slave steady state regime, the locking band, the stability conditions and the solution behavior in time and spectral domain as a function of the detuning between the two lasers and of the master rate of injection. They can also describe the slave behaviour when injected by a chaotic radiation and, finally, its modulation properties and frequency chirping. Results provided by the two approaches are in excellent agreement in spite of the different rationale they are based on. Related aspects will be discussed at presentation time, as well as a comparison of the numerical results with those obtained from the experimental measurements of a master-slave laser set-up.

### Acknowledgments

Part of this work has been supported by Emilia-Romagna Region of Italy (Piano Telematico, *InSeBaLa* Project), and by the Italian Ministry of University and Research (MIUR).

### References

- [1] R. Lang, "Injection Locking Properties of a Semiconductor Laser," *IEEE-JQE*, **18**, 976-982.
- [2] V. Annovazzi-Lodi, A. Sciré, M. Sorel and S. Donati, "Dynamic behavior and locking of a semiconductor laser subjected to external injection", *IEEE-JQE.*, **34**, 2350-2357.

## Limited buffer waveguides: impact on leakage and coupling loss

R.Costa, G.Cusmai, A.Melloni and M.Martinelli  
 Corecom, via G.Colombo 81, 20133, Milano, ITALY  
 DEI Politecnico di Milano, via Ponzio 43/5, 20131, Milano, ITALY  
 e-mail: costa,cusmai@corecom.it

**Abstract:** The impairments on optical waveguides due to a limited buffer layer are mainly the leakage loss and a worse fiber-to-waveguide coupling efficiency. A numerical and experimental evaluation is proposed over SION waveguides with  $\Delta n=4.5\%$  for different buffer layer thicknesses.

**Key words:** Optical waveguide, Leakage loss, fiber coupling.

Working with optical waveguides having a limited buffer layer is nowadays a common constraint for many applications. A typical example is the fiber-to-waveguide dual-core mode adapter realized in [1], where the coupling of a si-wire waveguide to an optical fiber is obtained through an intermediate low index contrast waveguide well matched with the fiber and vertically coupled to the silicon waveguide. The main impairments on a moderately low index contrast waveguide due to the presence of a limited buffer layer are both on the propagation loss due to leakage to the substrate, and on the coupling loss to the optical fiber.

In the present contribution single-mode waveguides with an index contrast  $\Delta n=4.5\%$  and buffer layer thickness ranging from 2 to 5  $\mu\text{m}$  are analysed both theoretically and experimentally.

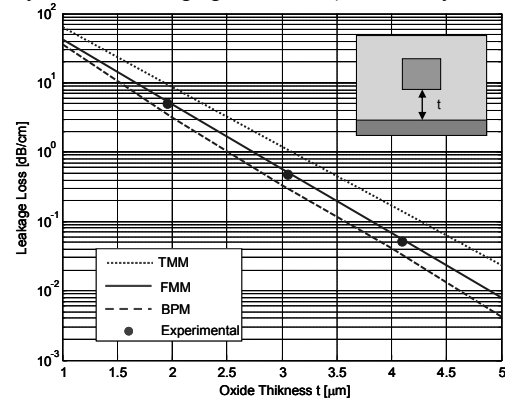


Fig.1: Experimental and theoretical TE leakage loss of a SION waveguide with  $\Delta N=4.5\%$ .

layer 2  $\mu\text{m}$  thick where the near-field acquisition is affected by a limited dynamic due to the high leakage. Finally, the results described so far are compared to those measured by the cut-back method, and it is evident that when high leakage losses dominate, even working with a well matched fiber, the resulting coupling losses are much higher than those expected by a simple mode-field superposition.

### References:

- [1] G. Roelkens, P. Dumon, W. Bogaerts, D. Van Thourhout and R. Baets, "Efficient silicon-on-insulator fiber coupler fabricated using 248-nm-deep UV lithography", IEEE Photon.Tech.Lett., VOL.17, NO.12, Dec. 2005, p.2613.
- [2] Fimmwave by Photon design [3] Beamprop by R-Soft.
- [4] A.K. Ghatak, K. Thyagarajan, and M.R. Shenoy, "Numerical analysis of planar optical waveguides using matrix approach", J.Lightwave Technol., Vol. LT-5, NO.5, May 1987, pp.660-667

## Simulation of New Integrated Optic Polarisation Controller in SOI Technology

Andrei V. Tsarev\*

\*Institute of Semiconductor Physics, Siberian Branch Russian Academy of Sciences  
 Prospect Lavrenteva n. 13, Novosibirsk, 630090, Russia  
[tsarev@isp.nsc.ru](mailto:tsarev@isp.nsc.ru)

A novel type of compact polarisation controller that utilizes multi-reflector technology is described. Numerical computer experiments carried out on Silicon-on-Insulator (SOI) waveguides by 2D FDTD method demonstrate the device proof-of-concept and its applicability in photonics and integrated-optics.

### Summary

This paper describes a new compact polarisation controller that is based on the beam expander technology [1, 2] and contains a set of proper adjusted reflector strips or deep grooves to be crossing optical waveguides at Brewster angle. Numerical computer experiments of polarization controller have been performed in Silicon-on-Insulator waveguides by 2D finite difference time domain (FDTD) software tool FullWAVE by RSoft Design Group, Inc. Device parameters have to be optimized in terms of number, width and position of reflectors, as well as by proper mismatch of optical waveguides to compensate the field distribution shift of transmitted guided waves (see Fig.1). This device architecture shows high anisotropy of optical power transmittance (0.02 and 0.94, respectively), for the two polarizations (see Fig.1a for TE and Fig.1b for TM) and is suitable for polarization control of optical elements in photonics and integrated-optics. This compact polarisation controller could be manufactured on different materials (silicon, polymer, etc.), having deep groove technology for reflector manufacturing and low optical losses in single-mode waveguides. This work was partially supported by Russian Fund for Basic Research under Grant No 05-02-08118-ofi-a.

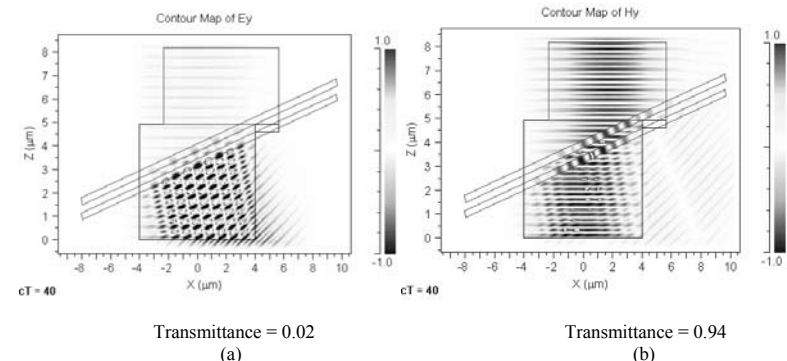


Fig.1. Simulation by FullWAVE FDTD of proposed polarization controller. a) TE guided wave propagation in 2D SOI waveguide (8  $\mu\text{m}$  width) crossed by two slanted deep grooves 0.3  $\mu\text{m}$  wide and spaced by 0.32  $\mu\text{m}$ ; b) same for TM guided wave propagation.

### References

- [1] A. V. Tsarev, "Beam-expanding device", USA Patent No. 6,836,601, Dec. 28, 2004.
- [2] V. M. N. Passaro, F. Magno, and A. V. Tsarev, Optics Express, **13**, 3429, 2005.

## Fabry-Perot Interferometer With Two Waveguide Grating Mirrors

*B.A.Usievich, V.A.Sychugov*

*Laser Materials and Technology Research Center, General Physics Institute, Russian Academy of Sciences,  
Vavilov str. 38, Moscow, 199911 Russia. e-mail: [borisu@kapella.gpi.ru](mailto:borisu@kapella.gpi.ru)*

Fabry-Perot interferometer with two mirrors using waveguide gratings is studied. Influence of various parameters on the interferometer performance is examined.

### Summary

Earlier we studied Fabry-Perot interferometer with one multilayer dielectric mirror and one waveguide grating mirror [1]. It was found that the transmission line of this interferometer could be two orders of magnitude narrower than that of ordinary interferometer. Now we analyse interferometer containing two identical waveguide grating mirrors taking losses into account. As the mirrors are identical then their reflection coefficients are equal at any given wavelength. So 100% transmission is possible in the resonance. Width of the resonance depends on its position and grows when the resonance moves away from the peak of waveguide grating mirror reflection. It was found that relative phase of the gratings affects strongly interferometer characteristics in the case of thin cavity and this effect disappears when the distance between mirrors is increased. We analysed interferometer in two variants of incidence: normal ( $0^\circ$ ) and close to normal ( $3^\circ$ ). The first case is of particular interest for practical applications and also interesting from theoretical point of view as two waveguide modes are excited simultaneously

### References

[1] B.A.Usievich, V.A.Sychugov, J.Kh.Nurligareev, O.Parriaux, *Optical and Quantum Electron.* 36, 109-117, 2004.

## Numerical Model of S-band depressed cladding EDFAs

Stefano Selleri\*, Annamaria Cucinotta\*, Federica Poli\*, Matteo Foroni\*, Moreno Maini<sup>o</sup>, Luca Vincetti<sup>o</sup>

*\*Dipartimento di Ingegneria dell'Informazione, Università di Parma, Parco Area delle Scienze 181A,  
Parma - Italy*

[stefano.selleri@unipr.it](mailto:stefano.selleri@unipr.it)

*<sup>o</sup>Dipartimento di Ingegneria dell'Informazione, Università di Modena e Reggio Emilia, Via Vignolese 905b,  
Modena - Italy*

A model of S-band depressed cladding EDFAs (Erbium Doped Fiber Amplifiers) which is able to predict the ASE suppression due to the bending loss has been developed. The comparison of numerical and experimental results has demonstrated the validity of the model.

### Summary

The optical amplification in the S band, 1450 nm ÷ 1530 nm, is very attractive to increase the transmission capacity of C (coarse)- and D (dense)-WDM systems. To realize S-band amplification, many techniques have been proposed in the recent years. One of the most promising is based on the use of a depressed-cladding Erbium-Doped Fiber (EDF). In fact it has been experimentally demonstrated that the Amplified Spontaneous Emission (ASE) in C band can be filtered by winding the depressed cladding EDF with proper bend diameters [1]. The depressed cladding fiber can be properly designed to have the fundamental mode cutoff at the desired wavelength  $\lambda_c$ . Beyond  $\lambda_c$  the guided mode becomes leaky and its leakage loss increases sharply as the wavelength increases. After that, by varying the bending diameter it is possible to change the leakage loss profile realizing a sort of tunable filter which suppresses the ASE in the C-band and allows S-band amplification. The refractive index profile determines  $\lambda_c$ , the slope of the leakage loss curve as well as the sensitivity to the bending. Thus a numerical model able to predict the main optical amplifier characteristics such as the gain and noise figure spectra is mandatory in order to find the optimal fiber refractive index profile.

Here a numerical model of S-band EDFAs is presented. The model is able to accurately calculate both the bending losses and the modal field distribution of a depressed cladding fiber by means of a full-vector complex modal solver based on the finite element method with perfectly matched layer as boundary conditions [2]. The bent fiber is replaced by a straight one with equivalent refractive index [3]. The population and propagation rate equations are then solved by means of a Runge-Kutta algorithm obtaining gain and noise figure spectra. The EDF input parameters are the refractive index profile, the dopant radius, the erbium concentration, the absorption and emission cross-sections. The pumps, signals and ASE beams are considered and the full ASE spectrum is resolved. The model has been applied to study a S-band EDFA. A gain of about 25 dB, almost constant in a 14 nm wavelength range around 1508 nm, has been measured with a 15 m-long EDF bent with a diameter of 15 cm, pumped by 120 mW laser at 980nm. The numerical results agree with experimental measurements.

### References

- [1] F. Poli, M. Foroni, A. Cucinotta, S. Selleri, P. Vavassori, ECOC2005, Glasgow, Scozia.
- [2] S. Selleri, L. Vincetti, A. Cucinotta, and M. Zoboli, *Opt. Quantum Electron.*, 33, 359-371, 2001.
- [3] M. Heiblum, J.H.Harris, *IEEE J.Quantum Electron.* QE-11, 75-83, 1975.

Summary

Network concepts have been applied recently to construct an architecture for field formulations in complex structures. The approach is based on the topological partitioning of the complex structure into several subdomains joined together by interfaces. In analogy with network theory, individual subdomains are characterized as circuit elements, obtained either analytically or numerically, and described in a unified format by using a generalized network formulation [1, 2, 3]. Network-oriented methods can add significantly to the problem formulation to their solution methodology, efficient parameterization, and to the generation of equivalent circuits.

The connection circuit represents the topological structure of the circuit and contains only the connections, including ideal transformers. In the connection circuit neither energy storage nor energy dissipation occurs. The connection circuit, governed by Tellegen's theorem and Kirchhoff laws, connects the circuit elements that may be one-ports or multiports. Topological relationships for fields state the continuity of the transverse component of the electromagnetic field and pose interesting constraints on the choice of independent and dependent fields with consequences for the connection network which represent the discretized form of the topological relationships. Figure 1(a) shows the segmentation of a problem space into subregions  $R_i$ . The subregions  $R_i$  and  $R_j$  are separated by a boundary with the two sides  $B_{ij}$  and  $B_{ji}$ . The equivalent circuit representation of different field expansions at the boundaries is depicted in Figure 1(b).

Also for each region of space with a finite volume it is possible to derive a rigorous network representation. This is done by considering the relative Green's function, of impedance or admittance type, expressed in terms of resonant modes. The Figure 2 illustrates the Foster canonical representation.

In free-space the complete electromagnetic field o may be expanded into a set of TM and TE spherical waves. Using the recurrence formula for spherical Bessel functions, Chu gave the Cauer representation of the equivalent circuits of the  $TM_n$  and the  $TE_n$  spherical waves. The equivalent circuit expansion of spherical waves also is shown in Figure 3.

Network representations provides *systematic* solution of field problems. In particular, the connection network maps different field representations at boundaries; inside regions alternative Green's function representation in terms of resonant/travelling modes provide network representation in terms of circuit/transmission line elements; free-space is accounted for by a spherical expansion with radial transmission lines.

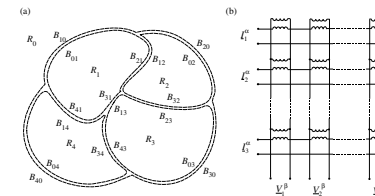


Figure 1: (a) Segmentation of an electromagnetic structure and (b) canonical form of the connection network.

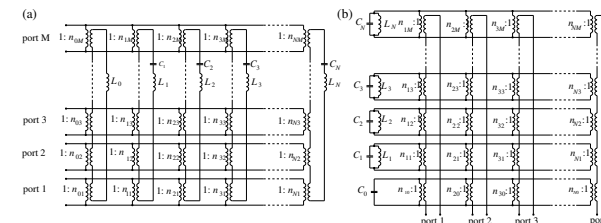


Figure 2: Foster (a) admittance and (b) impedance representations of a multiport.

References

- [1] L. B. Felsen, M. Mongiardo, and P. Russer, "Electromagnetic field representations and computations in complex structures I: Complexity architecture and generalized network formulation," *Int. J. Numer. Modeling*, vol. 15, pp. 93–107, 2002.
- [2] L. B. Felsen, M. Mongiardo, and P. Russer, "Electromagnetic field representations and computations in complex structures II: Alternative Green's functions," *Int. J. Numer. Modeling*, vol. 15, pp. 109–125, 2002.
- [3] P. Russer, M. Mongiardo, and L.B. Felsen, "Electromagnetic field representations and computations in complex structures III: Network representations of the connection and subdomain circuits," *Int. J. Numer. Modeling*, vol. 15, pp. 127–145, 2002.

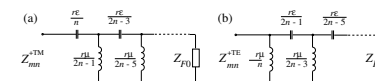


Figure 3: Equivalent circuit of (a)  $TM_{mn}$ , (b)  $TE_{mn}$  spherical wave.

## Dual resonance in a waveguide-coupled ring microresonator

Jiří Čtyrokový\*, Ivan Richter<sup>o</sup>, Milan Šiňor<sup>o</sup>

\**Institute of Radio Engineering and Electronics AS CR, Chaberská 57, 18251 Praha 8 – Czech Republic*  
*ctyrokovy@ure.cas.cz*

<sup>o</sup>*Dept. of Physical Electronics, FNSPE CTU, V Holešovičkách 2, 180 00 Praha 8 – Czech Republic*

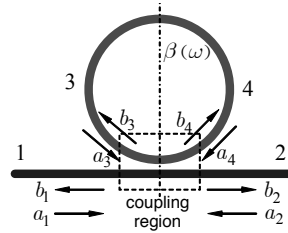
Coupling to a bus guide breaks the rotational symmetry of an isolated ring or disk microresonator. As a result, the degeneracy of sine and cosine azimuthal modes is lifted, and two resonant frequencies occur. It is shown that this effect can be easily described by taking back-reflections in the coupler into account.

### Summary

Ring and disk microresonators are very promising building blocks of large-scale integrated photonics devices [1]. They can be used in a number of applications like fixed and tuneable optical filters, add-drop de/multiplexors, sensors, *etc* [2, 3].

Most modelling work on microresonator devices makes use of the coupled-mode theory combined with appropriate mode solvers (see *e.g.*, [4]). In this approach, the resonance wavelengths of a single microresonator always appear as simple resonance peaks at the drop port or notches at the throughput port. From the physical point of view, however, coupling to a bus waveguide breaks the rotational symmetry of an isolated ring (or disk) microresonator. The degeneracy of sine and cosine azimuthal modes that takes place in any rotationally symmetric structure is thus lifted, and splitting of the resonant frequency occurs. The lower frequency corresponds to the mode field distribution for which the field is maximum at the position closest to the guide, and correspondingly, resonant frequency corresponding to the mode with the node closest to the bus guide is higher. The aim of this contribution is to show that this effect can be described by the conventional “optical circuit” model, too, provided that back-reflections and back-coupling are taken into account. The device under consideration is shown in the figure on the right below. The amplitudes of the forward waves ( $a_j$ ) and backward waves ( $b_j$ ,  $j = 1, 2, 3, 4$ , see figure) are related by

$$\begin{pmatrix} b_1 \\ b_2 \\ b_3 \\ b_4 \end{pmatrix} = \begin{pmatrix} r & t & \sigma & \kappa \\ t & r & \kappa & \sigma \\ \sigma & \kappa & r & t \\ \kappa & \sigma & t & r \end{pmatrix} \begin{pmatrix} a_1 \\ a_2 \\ a_3 \\ a_4 \end{pmatrix}, \quad \begin{aligned} a_3 &= e^{i\varphi(\omega)} b_4, \\ a_4 &= e^{i\varphi(\omega)L} b_3, \end{aligned}$$



where the matrix elements  $t$ ,  $\kappa$ ,  $r$  and  $\sigma$  are mutually constrained by reciprocity and (supposed) losslessness. The frequency splitting can be found to be  $\omega_{1,2} \approx \omega_0 \pm (c/N_g)(r/t)$ , where  $\omega_0$  is the originally degenerated frequency,  $c$  is the speed of light *in vacuo* and  $N_g$  is the group effective refractive index of the ring guide.

We are currently working on obtaining quantitative data about the size of the frequency splitting effect in real microresonator structures by FDTD and BEP modelling.

### References

- [1] A. Driessen, D. H. Geuzebroek, H. Hoekstra, *et al.*, AIP Conf. Proc. 709, pp. 1-18, 2004.
- [2] B. E. Little, S. T. Chu, P. Absil, *et al.*, IEEE Phot. Technol. Lett., vol. 16, pp. 2263-2265, 2004.
- [3] E. Klein, D. Geuzebroek, *et al.*, 12<sup>th</sup> ECIO'05, Grenoble, 6-8 Apr. 2005, Proc. pp. 180-183.
- [4] R. Stoffer, K. R. Hiremath, M. Hammer, *et al.*, Opt. Commun., vol. 256, pp. 46-67, 2005.

## Hybrid analytical/numerical coupled-mode modeling of guided wave devices

Manfred Hammer

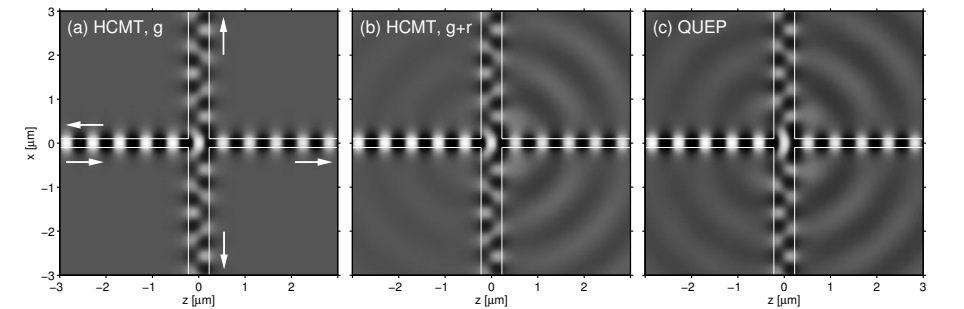
MESA<sup>+</sup> Institute for Nanotechnology, University of Twente, Enschede, The Netherlands  
*m.hammer@math.utwente.nl*

A general coupled-mode-theory version for integrated optical scattering/Helmholtz problems is proposed. Modes of optical channels and templates for radiated fields are combined with coefficient functions along arbitrary coordinates. Approximate solutions are obtained by 1-D FEM discretization of these amplitudes.

### Summary

Frequently, the light propagation through integrated optical structures is discussed in terms of interactions of a few well defined basis fields, typically the guided modes that are supported by the (local) optical channels of the device. Up to some remainder that represents radiated fields, it is then usually straightforward to write a reasonable ansatz for the optical field by superimposing the directional basis fields with coefficient functions that vary along the respective propagation coordinates, where position and orientation of these axes can be arbitrary. What remains is to determine the amplitudes, *i.e.* to compute the strength of the interactions. Here we propose to use numerical procedures: the amplitude functions are discretized by linear (1-D) finite elements. Then a variational (Galerkin) procedure is applied that permits to establish a dense, but small-size system of linear equations for the element coefficients, which is solved numerically. We show that it is also possible — with limitations — to incorporate radiation losses by suitable field templates, *e.g.* by properly placed Gaussian beams.

What concerns the field ansatz, the proposed approach may be regarded as a generalized (“hybrid”, analytical/numerical) variant of coupled mode theory (HCMT), but one where the familiar viewpoint of mode amplitude evolutions along a common axis of propagation has to be abandoned. Alternatively, this may be viewed as a numerical finite element technique with highly specialized, structure-adapted elements. A series of examples, including the waveguide crossing below, allows to assess the performance. The HCMT results are benchmarked versus a Helmholtz solver based on rigorous quadridirectional eigenmode expansion (QUEP). While so far only 2-D simulations have been carried out, the given formulation should permit a straightforward extension to 3-D.



2-D simulations of a perpendicular crossing of high contrast waveguides (refractive indices 1.45 : 3.40, core thicknesses 0.2  $\mu\text{m}$  (horizontal channel) and 0.45  $\mu\text{m}$  (vertical waveguide, bimodal)), illuminated from the left by the fundamental mode of the horizontal channel. The plots show snapshots of the electric field  $E_y$  for TE polarized light at a vacuum wavelength of 1.55  $\mu\text{m}$ . (a, b) HCMT simulations, basis fields: the guided modes supported by the horizontal and vertical cores, waves traveling in positive and negative directions along both axes (a). In (b), additionally four Gaussian beams (half-waist-width 0.5  $\mu\text{m}$ , origins at the inner corners, outgoing at 45° angles) represent radiated fields. (c) QUEP simulation with 120  $\times$  120 modal expansion terms on a 6  $\mu\text{m}$   $\times$  6  $\mu\text{m}$  computational window, reference.

## Fabrication Tolerant Design of Bent Singlemode Rib Waveguides on SOI

R. Halir<sup>o</sup>, A. Ortega-Moñux<sup>o</sup>, J.G. Wangüemert-Pérez<sup>o</sup>, I. Molina-Fernández<sup>o</sup>, P. Cheben<sup>\*</sup>

<sup>o</sup>Dpto. Ingeniería de Comunicaciones, Universidad de Málaga, Campus Teatinos s/n, 29071 Málaga, Spain

<sup>\*</sup>Inst. for Microstructural Sciences, National Research Council of Canada, Ottawa, ON K1A 0R6, Canada

A design procedure for the MBR (minimum bending radius) of both rectangular and trapezoidal singlemode rib waveguides on SOI (Silicon-on-Insulator), which takes into account fabrication tolerances, is presented. Special attention is paid to the sidewall-angle tapering that occurs in 90° turns of wet etched waveguides.

### Summary

SOI is a fabrication platform for PICs (Photonic Integrated Circuits) which has recently attracted a lot of attention [1], as it offers true CMOS compatibility as well as a high index contrast. In order to be of practical use, waveguides have to exhibit low guiding losses and are often required to support only one mode; presently, rib waveguides best fulfil both requirements [1,2]. Besides, miniaturisation of PICs requires the minimisation of their waveguides' curvature radii, for which it is necessary to control both the transition losses between the straight and the bent sections and the propagation losses in the latter [3]. Our design methodology combines semi-analytical methods and numerical simulations, allowing the determination of the MBR for a given level of total losses, for both rectangular and trapezoidal rib waveguides, while taking into account dimension fluctuations due to fabrication tolerances. Fig. 1 shows the MBR for both waveguide types as a function of tolerance parameters  $h$  and  $w$  ( $h$  is the slab height,  $w_{\text{rect}}$  and  $w_{\text{trap}}$  are the waveguides' top widths; the rib height is constant:  $H = 2.2\mu\text{m}$ ). On the other hand, the etching technique used to fabricate trapezoidal waveguides produces a sidewall angle tapering from the nominal  $54.74^\circ$  to  $45^\circ$  and back to  $54.74^\circ$  along  $90^\circ$  turns, which makes the waveguide multimode. However, the second order TE and TM modes that appear exhibit very large propagation losses, so that the waveguide is effectively singlemode. Fig. 2 shows the second order TM mode with worst-case waveguide dimensions; the TE mode has even higher losses.

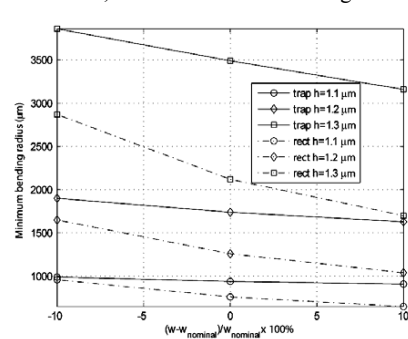


**Figure 1:** MBR for total allowable losses of 0.2dB per 90° turn ( $w_{\text{trap nominal}}=0.51\mu\text{m}$ ,  $w_{\text{rect nominal}}=1.75\mu\text{m}$ ,  $h_{\text{nominal}}=1.2\mu\text{m}$ ).

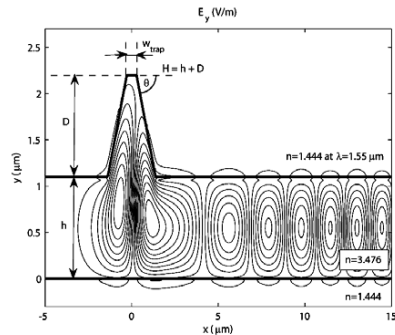


**Figure 2:** Leaky TM<sub>2</sub> mode with propagation losses of 44dB per 90° turn ( $h=D=1.1\mu\text{m}$ ,  $w_{\text{trap}}=0.56\mu\text{m}$ ,  $\theta=45^\circ$ ,  $R_{\text{curv}}=900\mu\text{m}$ ).

### References

- [1] I. Kiyat, A. Aydinli, and N. Dagli, Optics Express, vol. 13, pp. 1900–1905, March 2005.
- [2] O. Powell, Journal of Lightwave Technology, vol. 20, pp. 1851–1855, October 2002.
- [3] D. Dai, S. He, Journal of the Optical Society of America A, vol. 21, pp. 113–121, January 2004.

## High index-contrast multi-layer waveguides

Francesco Morichetti<sup>o\*</sup>, R. Costa<sup>o</sup>, Andrea Melloni<sup>\*</sup>, R.G. Heideman<sup>+</sup>, M. Hoekman<sup>+</sup>,

A. Borreman<sup>+</sup> and A. Leinse<sup>+</sup>

<sup>o</sup>CoreCom, Via G. Colombo 81, 20133 Milano, Italy, [morichetti@corecom.it](mailto:morichetti@corecom.it)

<sup>\*</sup>Dipartimento di Elettronica e Informazione, Politecnico di Milano,

Via Ponzio 34/5, 20133 Milano - Italy

<sup>+</sup>LioniX BV, P.O. Box 456, 7500 AH, Enschede, the Netherlands

A new approach for the realization of high-index contrast waveguides based on overlapped layers of different dielectric materials is proposed and investigated. Experimental results are also shown to demonstrate the feasibility and the potentialities of this new class of waveguides.

### Summary

High index-contrast waveguides are believed a key point to make integrated optics move in the direction of Very Large Scale of Integrations (VLSI). In this contribution non-conventional Multi-Layer Waveguides (MLWs) consisting of overlapped layers of dielectric media with different thickness and refractive index, are proposed as a way to merge the advantages of low index-contrast waveguides (low loss, low PDL, low birefringence) to the potentialities of higher index ones (high curvature and devices' compactness). With respect to conventional structures, in the presented MLWs additional degrees of freedom can be exploited for the optimization of the waveguide, whose effective index-contrast can be tailored by using only few (typically two) standard materials. The study of propagation in such MLWs, made of thick low-refractive-index layers (500nm-2000nm) encapsulated within much thinner high-index layers (50-150nm), also opens challenging tasks to electro-magnetic numerical solvers in terms of both accuracy and computational time. Several MLWs with different cross-sections have been numerically investigated. The presence of vertically oriented high-index layers, such as in the case of the "A-shaped" waveguide of Fig. 1(a), is found to add interesting features with respect to MLWs barely made of horizontally overlapped parallel strips. High index-contrast zero-birefringence single-mode MLWs can be designed for applications at the wavelength of 1550nm. In such waveguides, the field distribution of the quasi-TE and quasi-TM modes can be significantly different so as to lead to interesting novel effects. Preliminary MLWs have been realized by using  $\text{Si}_3\text{N}_4$  as higher index ( $n = 1.99$ ) material and TEOS  $\text{SiO}_2$  as lower index ( $n = 1.45$ ) material. Both low propagation losses ( $<0.1\text{dB/cm}$ ) and low PDL ( $<0.1\text{dB/cm}$ ) have been experimentally demonstrated. Measurements reported in Fig. 1(b) demonstrate also that birefringence can be reduced down to zero. MLWs with minimum bending radii down to few tens of microns can be designed, suitable for the realization of compact devices for wide-band applications, such as ring-resonators with Free Spectral Ranges in the THz scale.

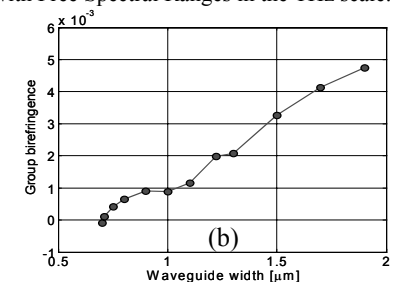
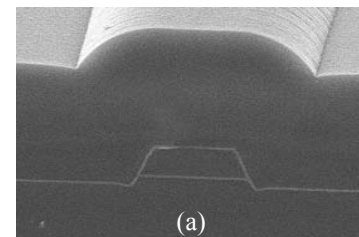


**Fig 1:** (a) SEM picture of the "A-shaped" MLW: the thin clear layers are made of  $\text{Si}_3\text{N}_4$  surrounded by TEOS  $\text{SiO}_2$ . (b) Experimental measurement of group birefringence versus channel width for the "A-shaped" MLW.

## Analysis of Propagation in Multimode Fibre and Waveguide Devices

John Love

*Optical Sciences Group, Australian Photonics Co-operative Research Centre, Research School of Physical Sciences & Engineering, Australian National University, Canberra ACT 0200, Australia*  
[jd1124@rsphysse.anu.edu.au](mailto:jd1124@rsphysse.anu.edu.au)

Many multimode optical fibre or waveguide devices such as tapers, couplers, X-junctions and splitters can be analysed quite accurately for their light-processing properties using simple modal or ray methods based on mode volume, statistical or length-scale arguments.

### Summary

In the early 1970's prior to the invention of methods for fabricating low-loss, single-mode optical fibres, considerable effort was expended on devising ray-based and quasi ray-based analyses for determining the long-distance propagation characteristics of large-core multi-mode fibres that were being introduced into inter-exchange telecommunications systems over distances of a few kilometres [1]. These analyses covered practical aspects such as excitation, transmission, absorption, scattering, dispersion and mode coupling. With the subsequent wholesale adoption of single-mode fibres in the 1980's into most systems and networks, interest in multi-mode fibres declined significantly.

More recently there has been some resurgence for the application of multimode fibres to local and metropolitan networks, aircraft networks, submarines, etc, mainly because of their simpler and therefore cheaper illumination, handling and splicing characteristics. As a consequence interest has been focussed in recent years on multimode fibre and planar waveguide devices such as tapers [2], couplers [3] and splitters [4].

A full modal analysis of light propagation through a multimode device can be undertaken formally but because of the very large number of core and cladding modes involved and the length dimension of these devices, the necessarily numerical quantification of the solution using e.g. BPM methods is time consuming and may not result in good accuracy because of the very large number of steps required.

Fortunately for a number of problems it is possible to generate reasonably accurate analytical solutions using one or more of the simpler techniques of mode volume conservation [2], statistical arguments [3,4,5] or length-scale comparisons [2,3]. The talk will cover examples of the use of these techniques used in tapered multimode fibres, multimode planar Y-junctions, multimode X-junctions and symmetric or asymmetric multimode fibre couplers.

### References

- [1] A.W. Snyder, J. D. Love, *Optical Waveguide Theory*, (Kluwer Academic Publishers, 2000)
- [2] J. Katsifolis, J.D. Love, L.W. Cahill, Proc Australian Conference of Optical Fibre Technology, 137-140, Melbourne, 1998,
- [3] R. Griffin, J.D. Love, P.R.A. Lyons, D.A. Thorncraft, S.C. Rashleigh, Journal of Lightwave Technology, 1508-1517, 1991
- [4] W.M. Henry, J.D. Love, J.D., Optical & Quantum Electronics, 379-392, 1997
- [5] D.R. Beltrami, J.D. Love, F. Ladouceur, F, Optical & Quantum Electronics, 307-326, 1999

## Cladding Mode Coupling Suppression in Bent Single-Mode Slab Waveguides

Céline Durniak, John Love

*Optical Sciences Group, Australian Photonics Co-operative Research Centre, Research School of Physical Sciences & Engineering, Australian National University, Canberra ACT 0200, Australia*  
[cjd124@rsphysse.anu.edu.au](mailto:cjd124@rsphysse.anu.edu.au) , [jd1124@rsphysse.anu.edu.au](mailto:jd1124@rsphysse.anu.edu.au)

We present analytical and numerical results that quantify core and cladding mode evolution and coupling with changing curvature on a single-mode slab waveguide with a finite cladding. We derive a delineation criterion that provides a boundary between approximately adiabatic and non-adiabatic bent waveguides.

### Summary

The next generation of devices for processing optically transmitted data based on optical fibre or planar waveguide technology needs to be more compact as light-processing systems become more miniaturized. A bent waveguide is an essential element for photonic integrated circuits. Earlier work using only numerical simulations indicated that bend loss could be minimized by imposing a uniform upper limit on the rate at which curvature is allowed to change anywhere along the bend [1]. Here we refine this coarser approach and investigate the minimization of bend loss in more detail by examining core and cladding mode evolution and coupling at each position along the entire bend.

We study TE modes of a simple bent slab waveguide consisting of a homogeneous core and a homogeneous finite cladding and for simplicity without coating. This also enables an analytical solution to be generated. The effective indices of the core and cladding modes are replaced by the equivalent tilted step profile on the straight waveguide [2]. We determine the effective indices of the core and cladding modes from the eigenvalue equation in the weak guidance approximation.

As the curvature increases, the effective index of the fundamental and each cladding mode increases. We show that the Gaussian-shaped mode is associated with the  $m^{\text{th}}$  higher-order cladding mode whose order in turn depends on the bend radius; the order increases with decreasing the bend radius. This evolution is similar to the spectral evolution of the corresponding modes on a straight, depressed-cladding fibre [3].

Bending breaks the translational invariance of the guide and optical power is coupled between the core fundamental mode and various cladding modes. A simple delineation criterion has been established to determine the maximum rate at which the radius of curvature of a bend can be changed consistent with minimal propagation loss. The usefulness of this criterion has been quantified by solving the corresponding coupled mode equations. There is also a strong analogy between the bend loss problem and the approximately adiabatic tapering of a depressed-cladding, single-mode optical fibre [3].

### References

- [1] John Love, Adrian Ankiewicz and Jim Katsifolis, Proc Australian Conference on Optics, Lasers and Spectroscopy, Melbourne, 1-4 December 2003, p. 66.
- [2] Jun Lu, Sailing He and Vladimir G. Romanov, Fiber and Integrated optics 24, 25-36, 2005.
- [3] J.D. Love, W.M. Henry, R.J. Black, S. Lacroix and F. Gonthier, IEE Proceedings 138, 343-354, 1991.

## Rigorous analysis of the coupling between two non-parallel optical fibers

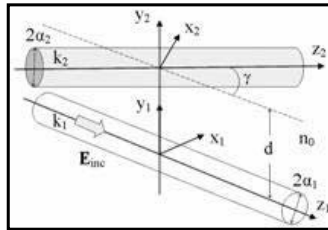
Ioannis Chremmos\*, Nikolaos Uzunoglu\*, George Kakarantzas<sup>o</sup>

\*Microwave and Fiber Optics Laboratory, <sup>o</sup>Photonics Communications Research Laboratory  
Department of Electrical and Computer Engineering, National Technical University of Athens  
9 Iroon Polytechniou Str., Zografos 15780, Athens, Greece  
jochremm@central.ntua.gr

The rigorous analysis of two coupled optical fibers with non-parallel (skew) axes is developed for the very first time, using the dyadic Green's function formulation and the generalized addition theorem for cylindrical waves under non-parallel axis translation, that was recently derived by the authors.

### Summary

Power coupling between parallel optical fibers is an extensively studied classical problem [1]. Recent advances in the field of wavelength-scale optical fiber elements [2] create, however, the need to revisit the problem in the most generic form, i.e. the coupling between fibers with non-parallel (skew) axes, which remains, with the exception of a single study [3], untouched in the electromagnetic literature. In present paper, the problem is addressed for the very first time, by using the rigorous Integral Equation (IE)



formulation for scattering, based on dyadic Green's functions. Since the boundary conditions on both fibers must be satisfied at the same time, Green's function of the fiber guiding the incident mode is used. The resultant electric field IE inside the second fiber

$$\mathbf{E}(\mathbf{r}) = \mathbf{E}_{inc}(\mathbf{r}) + (k_2^2 - k_0^2) \iiint \mathbf{G}_f(\mathbf{r}, \mathbf{r}') \cdot \mathbf{E}(\mathbf{r}') dV'$$

is treated through the entire-domain Galerkin technique, by expanding the unknown field over the spectrum of TE, TM ( $\mathbf{M}, \mathbf{N}$ ) cylindrical vector wave functions (CVWFs). The complexity of the problem then lies in the presence of CVWFs referring to the two skew cylindrical coordinate systems. To proceed in purely analytical fashion, the generalized addition theorem for CVWFs under non-parallel axis translation, recently derived by the authors [4], is utilized. This powerful tool allows us to reduce the IE into a coupled system of IEs for the field spectral components, where the Fourier transform of the incident field and the kernel of inter-fiber coupling are determined analytically. The final derived system can be numerically treated through any standard method of moments to compute the far-field scattering coefficients of guided fiber modes, or even the total field anywhere. Furthermore, with the aim to provide sufficiently accurate, analytical expressions for the scattering coefficients, under weak coupling conditions, the Neumann-series iterative procedure is employed. These analytical results, reported for the first time, are expected to be of great utility in applications involving coupled wire-waveguide structures [2] or fiber sensors [5].

### References

- [1] A. Jones, J. Opt. Soc. Am. 55, 261-271, 1965.
- [2] L. Tong, R. Gattass, J. Ashcom, S. He, J. Lou, M. Shen, I. Maxwell, E. Mazur, Nature 426, 816-819, 2003.
- [3] N. Uzunoglu, P. Mandis, Int. J. Infr. Millim. Waves 8, 535-547, 1987.
- [4] I. Chremmos, N. Uzunoglu, "Transformation of radially traveling cylindrical waves between two skew cylindrical coordinate systems," to be published by the J. Opt. Soc. Am. A.
- [5] T. Birks, J. Knight, T. Dimmick, IEEE Photon. Techn. Let. 12, 182-183, 2000.

## A source model technique (SMT) for the analysis of the modal fields of Photonic Crystal Fibers

Yehuda Leviatan\*

Department of Electrical Engineering  
Technion-Israel Institute of Technology  
Haifa 32000, Israel

A source-model technique (SMT) for the analysis of the modal fields of Photonic-Crystal Fibers (PCF) is described. The formulation is for a general cylindrical waveguide, made of a piecewise homogeneous dielectric. This geometry is adequate for the description of a variety of PCFs that have been suggested in the literature. The advantages of the SMT, as well as its limitations, compared to other methods that have been applied to the analysis of PCFs will be dwelt upon.

In the SMT formulation, the field in each homogeneous dielectric is simulated by the fields of an array of elementary sources located outside the region, near its boundaries. The array radiates in a homogeneous medium with the same parameters as the dielectric. The amplitudes of the sources are adjusted for the continuity conditions across the media boundaries, which are enforced at discrete set of points. This procedure leads to a homogeneous matrix equation for the amplitudes of the sources. Non-trivial solutions to this equation are found for specific pairs of angular frequency and axial propagation constant. When these solutions are found, the modal fields can be readily obtained by evaluating the fields of the arrays.

\* Joint work with Amit Hochman

The SMT has a number of appealing features: it does not require a mesh for discretization, as in FEM, it is a frequency domain method, which is well-suited to narrow-band problems, and it does not involve evaluation of reaction integrals as do surface-formulation based Method of Moments solutions. In summary, it is simple to implement, it is as efficient as other frequency-domain methods, and flexible enough to analyze complex geometries.

A few examples of the application of the SMT will be presented. These include solid and hollow-core PCFs, which have a photonic crystal cladding, consisting of a triangular lattice of circular air veins running parallel to the PCF axis. Results for PCFs with elliptical veins, which exhibit strong birefringence, will be also be shown. Strictly-bound modes, which have received little attention in the literature, as well as the more widely analyzed leaky modes, have been considered. For the leaky modes, calculation of the confinement losses is of interest, and will be shown by a rigorous method and by a perturbational one. The use of symmetry to both classify the modes, and reduce the computational burden will be explained. The modal dynamics of PCFs with elliptical veins will also be discussed in some detail. Finally, applying the SMT to realistic geometries, like PCF with veins of more complex cross sectional shapes, requires some extensions, which we will describe. In particular, a parametric representation of the boundaries has to be determined, and this is done with spline functions. This representation is then used in an automatic location scheme we devised for the sources and testing points. A PCF which was fabricated by Zheltikov's group will be analyzed. Plots of the phase refractive index, birefringence, group refractive index, and dispersion parameter will be presented.

## Differential toolbox to model microstructured-fiber behaviour

Juan J. Miret

*Departamento de Óptica, Universidad de Alicante, Apdo. 99, 08080 Alicante, Spain*

Enrique Silvestre, Teresa Pinheiro-Ortega, Pedro Andrés

*Departamento de Óptica, Universidad de Valencia, 46100 Burjassot, Valencia, Spain*

*enrique.silvestre@uv.es*

We present a differential algorithm to perform really inverse design in microstructured fibers. It combines an analytical procedure to compute, for different wavelengths, the first derivative of the propagation constant with respect to the set of fiber parameters of interest and a gradient-based algorithm to find very quickly in the multidimensional design-parameter space the solution that meets the design goal.

**Keywords:** guided-wave optics design, photonic crystal fibers, chromatic dispersion

In this contribution we present a design technique based on an original analytical formulation to calculate the gradient of the propagation constant  $\beta$  with respect to the design photonic-crystal-fiber parameters. The same calculation procedure can be adapted to evaluate the gradient of other magnitudes as the group index and the group velocity dispersion. The above derivatives provide the trend of the magnitude under consideration, what allows us to capitalize on a gradient-based algorithm to model the properties of the guiding structure at issue.

First, our modal iterative Fourier algorithm [1] is used for the calculation of  $\beta$  for the reference value of the design parameters at different wavelengths. Next we obtain some closed relations for the first derivative of the propagation constant with respect to each selected optical-fiber parameter. Typical design parameters are the hole size for each ring, the hole shape, the lattice pitch, the refractive index of materials, etc. Likewise, analytical equations for the gradient of either the group-velocity or the group-velocity-dispersion parameter can be achieved with a similar procedure.

Second, we take advantage of a gradient-based algorithm to carry out the minimization process of a suitable merit function, which is defined within the design technique and involves the magnitude at issue. The information provided by the derivatives of such a function at a given point of the multidimensional parameter space is used to decide in which direction it is more convenient to move forward to find the final configuration that matches the design goal. Additionally, the above method is especially well adapted to the analysis of fabrication tolerances.

In this contribution we pay attention to the development of an optimization process to design photonic crystal fibers (PCFs) with a specific chromatic dispersion behavior [2]. In particular we will show some illustrative numerical simulations concerning ultraflattened dispersion in PCFs and PCFs for dispersion compensation.

[1] E. Silvestre, T. Pinheiro-Ortega, P. Andrés, J.J. Miret, *Opt. Lett.* **30**, 453–455, 2005.

[2] “Differential toolbox to shape the dispersion behavior in photonic crystal fibers”, E. Silvestre, T. Pinheiro-Ortega, P. Andrés, J.J. Miret, A. Coves, *Opt. Lett.* (submitted).

## Single-Polarization and Controllable Birefringence Guidance in Liquid-Crystal Microstructured Fibers

Dimitrios C. Zografopoulos, Emmanouil E. Kriezis, and Theodoros D. Tsiboukis  
 Department of Electrical and Computer Engineering, Aristotle University of Thessaloniki,  
 Thessaloniki GR-54124, Greece  
[dzogra@auth.gr](mailto:dzogra@auth.gr), [mkriezis@auth.gr](mailto:mkriezis@auth.gr), [tsibukis@auth.gr](mailto:tsibukis@auth.gr)

Numerical studies in the context of a planewave method demonstrate that infiltration of index- or bandgap-guiding microstructured fibers with liquid crystal nematic materials may allow for tunable operation, such as polarization preserving or controllable (low or high) birefringence guidance.

### Summary

Photonic crystal fibers (PCFs) or microstructured fibers, have been under intense study lately since they have shown remarkable, unattainable by their conventional counterparts, properties. Exhibiting a transversely periodic cladding around a guiding core region, such fibers are capable of confining light either by index-guiding, or by taking advantage of the full photonic bandgaps of the cladding [1]. Enhancing such fibers with nematic materials can lead to novel tunable properties [2] due to their intrinsic anisotropy, which can be dynamically addressed by an external static electric field. Proper selection of the glass index and the LC material, together with the structural design parameters and the application of external fields or anchoring conditions, can lead to both index-guiding (Fig. 1) or bandgap-guiding (Fig. 2) microstructured fibers operating in a single-polarization or controllable birefringence mode, with  $\Delta n$  from remarkably high values down to zero.

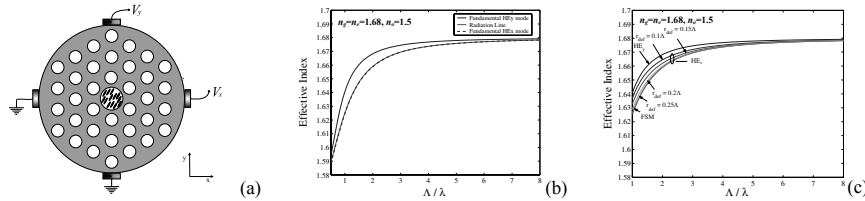


Figure 1: (a) Nematic-core index-guiding PCF. Subject to the fibre design and the external voltage the PCF can function [3] in: (b) single-polarization or (c) controllable birefringence.

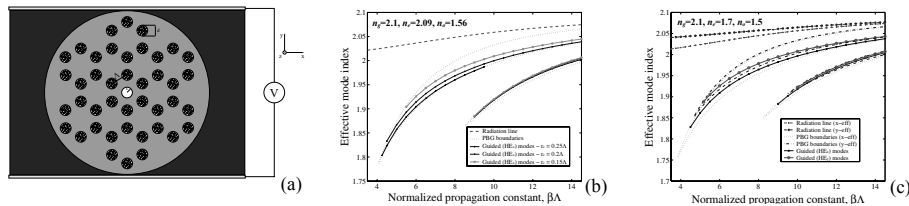


Figure 2: (a) Bandgap-guiding PCF with cladding holes filled with a nematic LC. By properly selecting the indices of the LC the fiber can operate in: (b) single-polarization or (c) high birefringence.

### References

- [1] J. Broeng, D. Mogilevstev, S.E. Barkou, and A. Bjarklev, *Opt. Fiber Technol.*, **5**, 305-330, 1999.
- [2] M.W. Haakestad, T.T. Alkeskjold, M.D. Nielsen *et al.*, *IEEE Phot. Tech. Lett.*, **17**, 819-821, 2005.
- [3] D.C. Zografopoulos, E.E. Kriezis, and T.D. Tsiboukis, *Opt. Express*, **14**, 914-925, 2006.

This work was supported by the Greek General Secretariat of Research & Technology (PENED03/Grant: 03ED936).

## Dynamics of the Long Period Grating in the Photonic Crystal Fibre with Bulk Cladding

Vladimir Mezentsev, Jovana S. Petrovic\*, Helen Dobb, David J. Webb  
 Photonics Research Group, Aston University, Aston Triangle, B4 7ET, Birmingham – United Kingdom  
[\\*petrovij@aston.ac.uk](mailto:*petrovij@aston.ac.uk)

Multiple period resonances and growth of long period gratings in photonic crystal fibres are described by generalised coupled-mode theory based on a representation of the mode amplitudes via harmonics of the lowest beat frequency. Fit to the measured grating growth was used to estimate induced index change.

### Summary

Long period gratings (LPG) fabricated in photonic crystal fibres (PCF) with bulk cladding may have interesting resonant properties (Petrovic et al, OWTNM 2005), [1]. Namely, in the silica-air fibres with undoped core the difference in propagation constants  $\Delta\beta$  of the core and bulk cladding modes is very small so that the phase difference required for the phase matching can be achieved only over multiple grating periods. We have proposed the following generalisation of the phase matching condition:  $M\Lambda = 2\pi N / \Delta\beta$ , where M is the number of the grating periods required and N is the grating order. Due to its inherent assumption that the fundamental frequency of the fibre-grating system equals one grating period, standard coupled mode theory [2] cannot explain this phenomenon. In an attempt to solve the problem we came up with a mathematical model that describes the resonant properties of a LPG and the dynamics of its growth.

If  $\Delta\beta < 2\pi / \Lambda$ , the slowly varying mode amplitudes can be expanded into the harmonics of

this beat frequency  $A(z) = \sum_{m=-\infty}^{\infty} A_m(z) e^{im\Delta\beta z}$ . For the M-period resonance of the 1<sup>st</sup> order LPG substitution of the above expansion to the coupled-mode equations gives:

$$\frac{dA_m^{co}}{dz} = i(k_{co} - m\Delta\beta)A_m^{co} + i\frac{k_{co}\sigma}{2}(A_{m+M}^{co} + A_{m-M}^{co}) + ikA_{m-1}^{cl} + i\frac{k\sigma}{2}(A_{m+M-1}^{cl} + A_{m-M-1}^{cl}) \quad (1)$$

$$\frac{dA_m^{cl}}{dz} = i(k_{cl} - m\Delta\beta)A_m^{cl} + i\frac{k_{cl}\sigma}{2}(A_{m+M}^{cl} + A_{m-M}^{cl}) + ikA_{m+1}^{co} + i\frac{k\sigma}{2}(A_{m+M+1}^{co} + A_{m-M+1}^{co}) \quad (2)$$

where  $k_{co}$ ,  $k_{cl}$ ,  $k$ , are coupling coefficients and depend on the induced index change. For M=1 system (1)-(2) reduces to the standard case given in [2]. The fit of the calculated transmission  $T(z) = |A^{co}(z)|^2$  to the experimental data (Fig.1) for the double period resonance of 500 $\mu$ m LPG in ESM-1550-01 PCF gave a considerably large index change of the order of  $10^{-3}$  in silica that might explain the possibility of fabrication of ultra-short LPGs in these fibres [3].

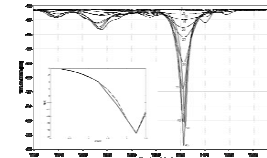


Figure 1 Measured growth of the 500 $\mu$ m LPG in ESM 1550-01 PCF. Inset: fit of the calculated transmission

### References

- [1] M.D. Nielsen et al, *Opt. Lett.* Vol. 28, No. 4, 236 (2003)
- [2] T. Erdogan, *J. Opt. Soc. Am. A* Vol. 14, No. 8, 1760 (1997)
- [3] S.H. Nam et al, *Optics Express* Vol. 13, No. 3, 731 (2005)

## Analysis of leaky photonic crystal fibers by means of an improved Fast-Fourier-based full-vectorial mode solver

Alejandro Ortega-Moñux, J. Gonzalo Wangüemert-Pérez, Iñigo Molina-Fernández  
Dpto. Ingeniería de Comunicaciones, E.T.S.I. Telecomunicación. Universidad de Málaga, Málaga, Spain  
[aom@ic.uma.es](mailto:aom@ic.uma.es)

In this work we improve the recently developed Fast-Fourier-based full-vectorial mode solver with the inclusion of PML absorbing boundary conditions. Its application to the modal analysis of photonic crystal fibers (PCFs) with a finite number of air holes gives an accurate description of their leaky nature.

### Summary

Application of Fourier Decomposition Methods (FDM) for optical dielectric waveguide analysis has been successfully done in a great variety of situations including modal analysis of dielectric waveguides [1], light propagation in z-variant structures [2], and characterization of optical waveguide discontinuities [3]. Advantages of this family of methods are their simplicity and flexibility, as they can be applied to any waveguide shape with no code modification, and that they yield accurate results even with a low number of terms. However, main limitation of these methods has been related to the maximum number of terms (harmonics) that can be used in the expansion of the fields. This is the reason why, although some results exist on application of FDM strategies to full vectorial situations, in practice they have been usually limited to the scalar description of dielectric structures. Other Fourier methods, not based on the Galerking strategy, have also been successfully applied to dielectric waveguide modal analysis [4]. These methods make use of the FFT to accelerate the computation and to avoid the explicit calculation of the involved matrix operators so that the number of harmonics can be greatly increased and accurate results can be obtained even in full-vectorial situations. Recently [5] authors have proposed a novel FFT based Fourier Beam Propagation Method for 3D full-vectorial situations, which retaining the Galerking nature of FDM, also takes advantage of the FFT to reduce the computational load and memory requirements. This approach has also been applied to obtain a 3D full-vectorial FFT based mode solver which allowed us to accurately analyze different strongly guiding waveguides of practical interest (photonic crystal fibers and trapezoidal rib waveguides in silicon-on-insulator (SoI) technology) with enhanced accuracy [6]. In this work we improve this recently developed technique with the inclusion of PML absorbing boundary conditions which allows the method to tackle with leaky situations, as for example for the study of finite size PCFs. Fig.1 shows the obtained results for a two ring PCF. Calculated confinement losses agree with recently reported ones [7].

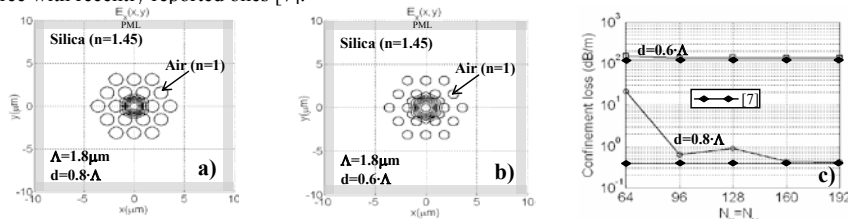


Fig.1. Photonic Crystal Fiber. a),b) Contour map of the fundamental mode. c) Convergence of the confinement loss.

### References

- [1] J.G. Wangüemert, I. Molina, IEEE J. of Lighthwave Tech. vol. 19, no. 10, 1614-1627, 2001.
- [2] J.G. Wangüemert-Pérez, I. Molina-Fernández, I. and M.A. Luque-Nieto, Optical and Quantum Electronics vol. 36, 285-301, 2004.
- [3] A. Ortega-Moñux, I. Molina-Fernandez, J.G. Wangüemert-Perez, Optical and Quantum Electronics, vol. 37, 213-228, 2005
- [4] E. Silvestre, T. Pinheiro-Ortega, P. Andrés, J.J. Miret, A. Ortigosa-Blanch, Optics Letters, vol. 30, 453-455, 2005.
- [5] J.M. López-Doña, J.G. Wangüemert-Pérez, I. Molina-Fernández, IEEE Photonics Tech. Lett., vol. 17, 2319-2321, 2005.
- [6] A. Ortega-Moñux, J.G. Wangüemert Pérez, I. Molina-Fernández, Enrique Silvestre, Pedro Andrés, submitted IEEE Photonics Tech. Lett, 2006.
- [7] S.S.A. Obayya, B.M.A. Rahman, K.T.V. Grattan, IEE Proc.-Optoelec., Vol. 152, no.5, 241-246, 2005.

## Numerical Analysis of Hollow Core Photonic Band Gap Fibers with Modified Honeycomb Lattice

Claudia Gazzetti\*, Moreno Maini\*, Luca Vincetti\*, Stefano Selleri°, Annamaria Cucinotta°, Federica Poli°

\*Dipartimento di Ingegneria dell'Informazione, Università di Modena e Reggio Emilia, Via Vignolese 905b, Modena - Italy

[vincetti.luca@unimore.it](mailto:vincetti.luca@unimore.it)

° Dipartimento di Ingegneria dell'Informazione, Università di Parma, Via Parco Area delle Scienze 181A, Parma - Italy

Hollow core photonic band gap fibers with a modified honeycomb lattice are investigated by a full vector complex modal solver based on the finite element method. Simulations show that confinement loss lower than  $0.1 \text{ dB/Km}$  and nonlinear coefficient lower than  $5 \cdot 10^{-3} (\text{WKm})^{-1}$  can be obtained over  $S$ ,  $C$  and  $L$  band of the third telecom window.

### Summary

Air-guiding is one of the most interesting possibility offered by Photonic Band Gap Fibers (PBGFs). The high guided mode confinement in air and not in silica allows to considerably reduce material absorption and nonlinear effects. In addition, air-guiding offers a new platform to study nonlinear optics in gases. Hollow core PBGFs with triangular lattice have been often employed. Unfortunately, the PBG crossed by the air line is quite narrow, causing guidance in a restricted band and high confinement losses. Recently air guiding into PBGFs with modified honeycomb lattice has been numerically demonstrated and their leakage loss and nonlinear properties analyzed [1]. Modified honeycomb lattice consists of a honeycomb lattice with an extra air hole in the center of the unitary cell. The extra hole provide an additional degree of freedom in tailoring PBGFs properties. In this work, dispersion, loss and nonlinear properties of modified honeycomb PBGFs have been numerically investigated by varying both core and cladding parameters. The numerical analysis has been performed by using a full-vector complex modal solver based on the finite element method with perfectly matched layer as boundary conditions [2]. In order to take into account both silica and air nonlinearity, the nonlinear parameter  $\gamma$  has been computed as follow:

$$\gamma_{\text{tot}} = \gamma_{\text{SiO}_2} + \gamma_{\text{air}} \quad \text{with} \quad \gamma_i = 2\pi n_{2i} / \lambda A_{\text{eff}} \quad i = \text{SiO}_2, \text{air}$$

being  $n_{2i}$  the nonlinear index coefficient and  $A_{\text{eff}}$  the effective area computed according to [3].

In the present analysis the hollow core is obtained by removing the silica inside a circle with radius  $R$ . Numerical results show that, by considering a normalized core radius  $R/A=3$  and a cladding with eight unitary cell rings, a pitch  $A=1.75 \mu\text{m}$ , a normalized hole diameter  $d/A=0.64$  and a normalized extra hole diameter  $dc/A=1.32$ , confinement loss lower than  $0.1 \text{ dB/Km}$  and nonlinear coefficient  $\gamma$  lower than  $5 \cdot 10^{-3} (\text{WKm})^{-1}$  can be obtained between  $\lambda=1.44 \mu\text{m}$  and  $\lambda=1.66 \mu\text{m}$  with eight unitary cell rings. The results highlight that, despite its very low nonlinear index, air plays a significant role in determining nonlinear coefficient of the fiber.

### References

- [1] L. Vincetti, F. Poli, and S. Selleri, to be published on IEEE Photon. Technol. Lett.
- [2] S. Selleri, L. Vincetti, A. Cucinotta, and M. Zoboli, Opt. Quantum Electron., 33, 359-371, 2001.
- [3] J. Laegsgaard, N. A. Mortensen, and A. Bjarklev, J. Opt. Soc. Am. B, 20, 2037-2045, 2003.

## Numerical modelling of the optical properties of infiltrated photonic crystals

Vasily Zabelin\* and Romuald Houdré

Institut de Photonique et d'Electronique Quantique, Ecole Polytechnique Fédérale, Lausanne, Switzerland  
\*vasily.zabelin@epfl.ch

The models of light propagation in 2D photonic crystal infiltrated by an anisotropic media are presented. The effect of the permittivity anisotropy and propagating light in-plane polarization on the tuning of the optical properties is discussed.

### Summary

Photonic crystals (PhC) offer many important possibilities to control light propagation. Present technologies allow us to produce high quality 2D PhC by etching a hole pattern in semiconductor structures. Nowadays there is a big interest in the fabrication of PhC-based devices with tuneable optical properties controlled by the operating conditions or an external field. One of the most promising ways to achieve such functionality is by filling the holes of 2D PhC with liquid crystals (LC) [1]. The permittivity of LC can be changed with the operating temperature because of the LC phase transition between ordered and disordered phases or by applying an external electric field, which affects LC molecules orientation. The latter case is much faster and seems more appropriate for application. In order to calculate the effect of LC molecule orientation and to estimate the tuning properties a model that takes into account anisotropic permittivity should be used.

Two different models of light propagation in a 2D heterogeneous media have been developed. The first of them is based on the well-known plane wave expansion method (PWE) [2] and considers an arbitrary 2D periodic structure with isotropic permittivities. The second one allows the description of light propagation in a media where permittivity is represented as an arbitrary second-rank tensor. This model is based on finite-difference discretization of Maxwell equations with high approximation order. The eigenvalue problem for either electric or magnetic field is derived (assuming the periodicity of the permittivity) and the solutions provide eigenfrequencies and field intensity distributions of the corresponding light modes. These models allow us to calculate PhC band structure and localized modes of PhC-based microcavities.

In this work we discuss application of both models and results obtained using these two approaches. PWE-based description of light propagation is more straightforward and quite fast for simple PhC lattices but the memory and computational requirements grows very fast with increasing the unit cell size, which makes this method hardly applicable for cavity mode calculation, where a large super-cell with high accuracy representation is required. The latter model, although it requires more calculations for simple PhC lattices, allows us to consider complex PhC structures with large unit cell with acceptable computational speed. It has been shown for both models that the light propagating through 2D PhC has, in general, elliptic in-plane polarization where the orientation of the main polarization axes and polarization ellipticity depend on position inside PhC lattice. This effect is especially important for LC-infiltrated PhC, because the elliptic polarization implies that the effect of the LC molecules orientation in the propagation plane is reduced and the efficiency of the optical tuning by the molecules rotation is decreased as well. The dependence of propagating light in-plane polarization on PhC parameters and operating frequency is discussed together with the PhC optical properties tuning.

### References

- [1] Ch. Schuller, J.P. Reithmaier, J. Zimmermann, et al., Appl. Phys. Lett., vol. 87, p. 121105, 2005
- [2] M. Plihal and A.A. Maradudin, Phys. Rev. B., vol. 44, no. 16, p. 8565, 1991

## Dissipative Solitons

F. Lederer

Institute of Condensed Matter Theory and Solid State Optics  
Friedrich-Schiller-Universität Jena, Max-Wien-Platz 1, 07743 Jena, Germany

In a strict sense only the solutions of integrable equations, such as the nonlinear Schrödinger equation, may be termed 'solitons'. However, this notion was early extended towards solitary waves, which are localized nonlinear objects in conservative and nonconservative (or dissipative) systems. *Dissipative solitons* have characteristics that are remarkably different from their conservative counterparts. In the last two decades they have attracted a considerable deal of interest, making this subject an almost independent area of research in nonlinear dynamics.

Optical solitons in conservative systems are formed as a result of a balance between nonlinearity and diffraction (spatial solitons) or dispersion (temporal solitons) and form families. By contrast, dissipative solitons require a continuous energy flow into the system, and, in particular, into the localized structure, in order to keep it "alive". Hence, a separate balance between energy input and output is alike important as that between the nonlinearity and dispersion (or diffraction). As a consequence the soliton properties are entirely determined by system's parameters and instead of forming families they represent strong attractors. Thus, a multitude of initial conditions will result in a unique soliton shape. This idea of viewing pattern formation and nonlinear localization as a consequence of energy flow introduced a new paradigm in many areas of physics, chemistry and biology.

As N. Akhmediev, one of the pioneers of dissipative solitons, pointed out there were forerunners of this idea dating from ancient times. For example, in the first Chinese medical text (500 B.C.), it is explained that the flow of *ch'i* (energy) produces a balance between the *yin* and *yang* organs of the body. Thus, these organs can be viewed as dissipative structures. If the flow stops, these organs cease to function correctly, and illness occurs. Isolated systems can only acquire entropy. Hence, non-equilibrium (or open) systems are required to allow spontaneous formation of structures. Thus, the formation of dissipative structures due to energy flow in nonlinear systems can be regarded as a fully new paradigm of dynamics where dissipative solitons are usually single (or bounded) objects, localized in space or/and time.

Representative optical systems with steady energy exchange are all types of open resonators, such as externally pumped Fabry-Pérot cavities and ring resonators, lossy waveguides structures with various kinds of amplifiers and mode-locked lasers.

A generic and simple mathematical model to describe dissipative soliton formation is the 1D Ginzburg-Landau equation

$$iu_z + \left(\frac{1}{2} + i\beta\right)u_n + (1 + i\varepsilon)|\psi|^2\psi + i\alpha\psi = 0$$

being essentially the nonlinear Schrödinger equation with complex coefficients. It describes e.g. pulse propagation in optical fibers with linear ( $\alpha$ ) and nonlinear ( $\varepsilon$ ) gain/loss as well as filtering ( $\beta$ ). Soliton solutions to this equation are essentially unstable but can be stabilized by adding a complex quintic nonlinear term.

Mean-field equations describing dissipative solitons in driven wide aperture cavities (or lasers) (frequently termed *cavity solitons*) are another mathematical model. They read in a cavity filled with a quadratic nonlinear material for the fundamental ( $u$ ) and second-harmonic field ( $v$ ) as [1]

$$iu_t + u_{xx} + u_{yy} (i + \Delta_1)u + u^*v = E,$$

$$iv_t + \alpha(v_{xx} + v_{yy}) + (i\gamma + \Delta_2)v + u^2 = 0,$$

where  $\Delta_{1,2}$  are the detunings from the cavity resonances,  $\alpha$  and  $\gamma$  account for the ratio of diffraction and radiation losses at both frequencies, respectively, and  $E$  is a homogeneous driving field.

In addition to these cavity solitons in the present talk we will report on theoretical and experimental results regarding stable temporal as well as spatial dissipative solitons in waveguide structures with semiconductor optical amplifiers (SOA). These amplifiers provide the required nonlinear gain to the system. The potentially unstable solitons can be stabilized by adding saturable absorption (SA) to the system. In the temporal case field ( $u$ ) and carrier dynamics ( $N_{\text{SOA},\text{SA}}$ ) are then governed by the more realistic (with respect to the Ginzburg-Landau equation) equations [2]

$$\begin{aligned} \left[ i\partial_z - \left( \frac{D}{2} + ig \right) \partial_t^2 + \chi_{\text{Kerr}} |u|^2 + i\alpha - (i + h_{\text{SOA}}) N_{\text{SOA}} + (i + h_{\text{SA}}) N_{\text{SA}} \right] u &= 0 \\ \partial_t N_{\text{SOA}} &= -\frac{1}{E_Q} [\exp(2N_{\text{SOA}}) - 1] \exp(-2\alpha) |u|^2 - \frac{N_{\text{SOA}} - \Pi_{\text{SOA}}}{\tau_Q} \\ \partial_t N_{\text{SA}} &= -[1 - \exp(-2N_{\text{SA}})] \exp(2N_{\text{SOA}} - 2\alpha) |u|^2 - (N_{\text{SA}} - \Pi_{\text{SA}}). \end{aligned}$$

We shall show how the system's parameters (small signal gain and loss  $\Pi_{\text{SOA},\text{SA}}$  and ratio of recovery times  $\tau_Q$ ) can be selected such that the bifurcation behaviour of the solution can be controlled (transition from supercritical to subcritical bifurcation) in order to obtain stable dissipative solitons. It is also shown that these solitons represent strong attractors of the nonlinear dissipative system.

Moreover, in the spatial domain we experimentally demonstrate soliton formation with mW peak power and study also the interactions of these objects [3].

#### References

1. Z. Bakonyi, D. Michaelis, U. Peschel, G. Onishchukov, and F. Lederer 'Dissipative Solitons and their Critical Slowing Down Near a Supercritical Bifurcation', J. Opt. Soc. Am. B19 (2002)487
2. C. Etrich, U. Peschel, and F. Lederer, "Solitary waves in quadratically nonlinear resonators", Phys. Rev. Lett. 79 (1997) 2454
3. 239) E. Ultanir, D. Michaelis, F. Lederer, and G. I. Stegeman, 'Stable Spatial Solitons in Semiconductor Optical Amplifiers', Opt. Lett. 28 (2003)251; 251) E. A. Ultanir, G. I. Stegeman, D. Michaelis, C. H. Lange, and F. Lederer, 'Stable Dissipative Solitons in Semiconductor Optical Amplifiers', Phys. Rev. Lett. 90 (2003) 253903

## Spatial solitons in optical fibres: a finite element analysis

F. Drouart, G. Renversez, A. Nicolet and C. Geuzaine<sup>+</sup>  
*Institut Fresnel (UMR CNRS 6133) and Université Paul Cézanne Aix-Marseille III*  
*Faculté des Sciences et Techniques de St Jérôme (case 161), 13397 Marseille Cedex 20, France*  
*e-mail: gilles.renversez@fresnel.fr*  
<sup>+</sup> *Case Western Reserve University, Cleveland, OH 44160, USA*

We propose an algorithm to find self-coherent solutions of the propagation equation, taking into account the fibre cross-section, in optical fibres with a Kerr medium core. We use a finite element method to compute the solutions. We find an unexpected behavior for the variations of the propagation constant versus the wavelength.

Ferrando *et al.* were able to take into account both the cross section of microstructured optical fibres[1] and a Kerr nonlinearity in the fibre matrix in the frame of the scalar approximation of the propagation equation. Consequently, they were able to define *spatial solitons* as solutions of the studied propagation problem. Due to the used numerical method, they were able to deal with only periodized structures in the transverse direction. We propose an algorithm allowing us to compute numerically the spatial solitons in conventional optical fibres but without any artificial periodization of the structure. We limit our study to the scalar approximation as in reference[1]. As a first example, we consider a conventional optical fibre made of a nonlinear Kerr type core in an homogeneous matrix. We seek for particular solutions of the usual scalar equation[2]:

$$\mathbf{E} = \Re e(\phi(x, y) \exp^{i(\omega t - \beta z)}) \hat{\mathbf{e}} \text{ such that } \Delta_t \phi + k_0^2 \varepsilon_r \phi = \beta^2 \phi \quad (1)$$

in which  $\omega = k_0 c$  is the angular frequency,  $\beta$  the propagation constant,  $\hat{\mathbf{e}}$  an arbitrary unit transverse vector, and  $\Delta_t$  the transverse Laplacian. In the case of Kerr material, the relative permittivity is itself a function of the electric field intensity and the following dependence is assumed[1]:

$$\varepsilon_r(\phi) = n_0^2 + n_2^2 |\phi|^2 \quad (2)$$

The solutions of the nonlinear propagation problem described by eqs. (1) and (2) are obtained through a simple Picard iteration scheme in which a propagation mode is computed in a linear fibre in which the refractive index profile is corrected by the field obtained at the previous iteration. The numerical method used to solve the successive linear problems is the finite element method[3] that is well adapted since it easily deals with the inhomogeneous permittivity of the core fibre induced by the Kerr medium. Two key steps whose one is included in the iteration scheme are used to solve the nonlinear problem. For the fundamental mode, we observe that the normalized difference between the  $\beta$  of the nonlinear self-coherent solution and the corresponding  $\beta$  of the linear problem increases with the wavelength. This result means that the nonlinear effect is in fact stronger for long wavelengths.

In our complete study, we will describe in details: the way we compute the self coherent nonlinear solutions, the results obtained for the fundamental mode and first higher order modes. We will also discuss the validity of the scalar approximation. In future works, we will focus on the development of a full-vectorial model and the study of finite size microstructured optical fibres.

#### References

- [1] A. Ferrando, M. Zacarés, P. Fernandez de Cordoba, D. Binosi, and J. A. Monsoriu. Spatial soliton formation in photonic crystal fibers. *Optics Express*, 11(5):452–459, 2003.
- [2] A. W. Snyder and J. D. Love. *Optical Waveguide Theory*. Chapman & Hall, New York, 1983.
- [3] F. Zolla, G. Renversez, A. Nicolet, B. Kuhlmeij, S. Guenneau, and D. Felbacq. *Foundations of Photonic Crystal Fibres*. Imperial College Press, London, 2005.

# Modeling Electromagnetically Induced Transparent Media Using the Finite-Difference Time-Domain Method

Curtis W. Neff, Mauritz Andersson, and Min Qiu

Department of Microelectronics and Information Technology, Royal Institute of Technology  
164 40 Kista, Sweden  
min@kth.se

A finite-difference time-domain method capable of modeling media exhibiting electromagnetically induced transparency is proposed, using an exact complex two-pole representation of the permittivity. The method is validated by comparing with existing results.

## Summary

Many interesting optical phenomena, such as ultra-slow light propagation [1], have been found in electromagnetically induced transparent (EIT) media. Modeling EIT poses certain challenges because of high dispersion in these materials. Using the finite-difference time-domain (FDTD) method, Soljačić et al. [2] approximately modeled an EIT medium as a Lorentz medium with two absorption lines sandwiching a gain line. This model is not exact, and it may cause instability in the FDTD method due to the existence of the gain line.

In this work, we propose to use an exact complex two-pole representation of the permittivity of a three-level EIT medium:

$$\epsilon_r = \epsilon_\infty + \sum_{l=1}^N \left( \frac{A_l}{B_l + i\omega} \right), \quad N = 2, \quad (1)$$

where  $\epsilon_\infty$  is the dielectric constant at infinite frequency and  $A_l$  and  $B_l$  are complex constants given by

$$A_l = \frac{iC}{2} \left( -1 + \frac{i^{(l+2)}\gamma_{ab}}{\sqrt{-\gamma_{ab}^2 + \Omega_c^2}} \right), \quad B_l = i \left[ -\omega_{ab} - \frac{1}{2} \left( i\gamma_{ab} + (-1)^l \sqrt{-\gamma_{ab}^2 + \Omega_c^2} \right) \right], \quad (2)$$

where  $\gamma_{ab}$  is the loss,  $\omega_{ab}$  is the frequency of the  $ab$  transition,  $\Omega_c$  is the Rabi frequency of the control field, and  $C$  is a materials constant related to the density of excitation centers and the dipole moment.

The frequency dependence of  $\epsilon$  is then linked to the electric flux density,  $\vec{D}$ , via the polarization,  $\vec{P}$ , which, in turn, introduces a phasor polarization current since  $\vec{J}_i(t) = \partial\vec{P}_i/\partial t$ . The standard FDTD implementations are then performed in combination with the auxiliary differential equation (ADE) method [3].

Our FDTD calculation procedure was tested by performing calculations on the corrugated waveguide system reported by Soljačić et al., to which we found good agreement.

## References

- [1] L. V. Hau, S.E. Harris, Z. Dutton, and C. H. Behroozi, *Nature* 397, 554 (1999).
- [2] M. Soljačić, E. Lidorikis, L. V. Hau, and J. D. Joannopoulos, *Phys. Rev. E* 71, 026602 (2005).
- [3] Allen Taflov and Susan C. Hagness. *Computational Electrodynamics: the Finite-difference Time-domain Method*. Artech House, Boston, second edition (2000).

# Possibility of Frequency Transformation in Time-Varying Dielectric Structures

Alexander Nerukh, Nataliya Sakhnenko

Kharkov National University of RadioElectronics, 14 Lenin Ave., Kharkov, 61166 - Ukraine  
nerukh@ddan.kharkov.ua

The process of an electromagnetic field transformation in a dielectric waveguide caused by changing its permittivity is analysed. Possibility of formation of a guided wave with new frequency is shown.

## Summary

It was shown long ago that time changing of the medium permittivity leads to change of a wave frequency [1]. This changing occurs immediately in the unbounded medium if the permittivity changes sharply. In the presence of boundaries as in the case of a waveguide or a resonator this process is more complex because of dispersion in such a structure. Such processes in a dielectric waveguide and in a dielectric resonator have been considered in [2] and [3]. Detailed consideration of evolution of the new guided wave is given in the present paper where the transformation of an initial Brillouin wave  $B^{(-)} = e^{i(\omega_0 t - \kappa_1 x - \Gamma z)}$  owing to the permittivity time jump is investigated. The initial wave is a constituent of any guided wave having the frequency  $\omega_0$  and the transverse wavenumber  $\kappa_1$  that corresponds to the permittivity  $\epsilon_1$  in the core and  $\epsilon$  in the cladding. The action of the core permittivity jump from  $\epsilon_1$  to  $\epsilon_2$  leads to the separation of wave fronts  $x = \pm(v_2 t - b/2)$  from the waveguide boundaries located at  $x = \pm b/2$ . Between these fronts the transformed field consists only of two waves  $A^{(\pm)} e^{\pm i\omega_2 t - i\kappa_1 x - i\Gamma z}$  where  $\omega_2 = \omega_0 v_2 / v_1$  is the new frequency and  $v_{1,2} = c/\sqrt{\epsilon_{1,2}}$  is the phase velocity. This field is the same as in an unbounded medium.

Behind the separated fronts the field structure containing guided waves as well as radiated ones becomes complicated as the fronts are reflected from the waveguide walls. There is the guided wave having the frequency  $\omega_0$  and the new wavenumber  $\kappa_2 = [(\omega/v_2)^2 - \Gamma^2]^{1/2}$ . The wave of the new frequency  $\omega_2$  has the old wavenumber  $\kappa_1$  and can be the guided one also. It depends on the behaviour of the wave amplitude which changes after each reflection of the fronts and are proportional to  $(R e^{-i\kappa_1 b/v_2})^m$  where  $m$  denotes the number of the front reflections. If the reflectivity module is  $|R|=1$  then the wave is the guided one that gives the corresponding criterion

$$\sin^2(\kappa_1 b/2) \leq (1 - v_1^2/v^2) / (1 - v_2^2/v^2). \quad (1)$$

This criterion says that the transformed wave of the new frequency is the guided wave for any value of the eigenwave number  $\kappa_1$  when the core medium becomes more optically dense. Similar transformation can occur with a whispering gallery wave in a circular resonator.

## References

- [1] F.R. Morgenthaler, *IRE Trans. Microwave Theory Techn.*, MTT-6, pp. 167-172, 1958.
- [2] A.G. Nerukh, P. Sewell, T. M. Benson, *Journal of Lightwave Technology*, vol. 22, No 5, pp. 1408-1419, 2004.
- [3] N. Sakhnenko, T. Benson, P. Sewell, A. Nerukh, *Proceeding of International Workshop on Optical Waveguide Theory and Numerical Modelling (OWTNM-2005)*, Grenoble, France.

## Account of the Active Region Shape in the Linear Modelling of Microcavity Lasers

A.I. Nosich\*, E.I. Smotrova\*, T.M. Benson<sup>o</sup>, P. Sewell<sup>o</sup>

\*Institute of Radio-Physics and Electronics NASU, Kharkov 61085, Ukraine - anosich@yahoo.com

<sup>o</sup>George Green Institute for Electromagnetics Research, University of Nottingham, NG7 2RD, UK

The paper reviews basic ideas and presents examples of the account of the shape of active region in the linear numerical modelling of thin microcavity lasers.

### Summary

Traditionally, cold-cavity linear modelling of microcavity lasers neglects the pedestal, which is assumed to have little effect on lasing modes, and nonuniformity in the direction of the normal to the cavity plane, due to the very small thickness of quantum-well layers. It also uses a reduction of dimensionality from 3-D to 2-D in the cavity plane, with the effective-index method. Further, the goal is finding the frequencies and Q-factors of the natural modes of the *passive cavities*. The methods applied range from the analytical WKB technique and the ray-tracing-based billiard theory to the all-numerical FDTD approximations. The important point, however, is that the lasing phenomenon is not addressed directly through the Q-factor – the specific value of threshold gain that is needed to force a mode to become lasing is not included in the formulation. Recent progress has been made in two directions. The first is the systematic use of the boundary integral equations to study the passive-cavity modes more accurately; the second is the development of a new model that macroscopically accounts for the presence of *active region* and enables one to find the lasing thresholds from the linear electromagnetic field equations.

On realising the above mentioned gap in the linear characterisation of lasers, one can modify the formulation of the cold-cavity electromagnetic problem by introducing macroscopic gain in the cavity material and extracting not only the frequencies but also the threshold values of gain as eigenvalues. The gain, say  $\gamma$ , can be introduced as the *active* imaginary part of the complex refractive index  $\nu$ : if the time convention is  $e^{-i\omega t}$ , then  $\nu = \alpha - i\gamma$ ,  $\alpha, \gamma > 0$ . Then, we may seek pairs of real numbers,  $(k, \gamma)$ ,  $k$  being a normalised frequency. Such a *lasing eigenvalue problem* (LEP) was suggested in [1] and developed further in [2]. Note that looking for a mode Q-factor in a cavity with an active region makes little sense, because it may become arbitrarily large depending on the nearness of the gain  $\gamma$  to the threshold value, at which the Q-factor turns to infinity.

A non-uniform distribution of gain across the cavity plane, due to either shaped pump beam or shaped electrodes, cannot be accounted for in the passive cavity model but is easily accounted for in LEP. To this end, one has to introduce the gain  $\gamma$  only inside the active region and impose an additional set of the field tangential components continuity conditions on the boundary of this region. In the presentation, we shall demonstrate the results of numerical modelling with the aid of LEP of a microdisk laser with a ring-like active region and other similar devices.

### References

- [1] E.I. Smotrova, A.I. Nosich, Optical and Quantum Electronics, 36, 1-3, 213-221, 2004.
- [2] E.I. Smotrova, A.I. Nosich, T.M. Benson, P. Sewell, IEEE J. Selected Topics in Quantum Electron, 11, 5, 1135-1142, 2005.

## A Non-iterative Bi-directional Wave Propagation Method based on the Split-Step Non-Paraxial (SSNP) Method

Anurag Sharma and Manmohan Singh Shishodia

Physics Department, Indian Institute of Technology Delhi, New Delhi-110016, India  
asharma@physics.iitd.ac.in

We describe a bidirectional wave propagation method based on the finite-difference split-step method. The method is applied to reflections from waveguide discontinuities and terminations.

### Summary

The problem of reflections in guided wave devices is either dealt with using FDTD methods, which are computationally intensive and time consuming, or using special bi-directional methods. The non-iterative bidirectional methods are generally transfer matrix type methods and differ in formation of the transfer matrix. To this end, the most commonly used approach has been the use of Padé approximants based finite-difference method [1,2]. Finite element in conjunction with the Taylor expansion for the square root of the propagation operator has also been used recently [3]. These methods are also, however, computationally intensive due to several matrix operations involving matrix inversion and/or series evaluation at each step of propagation.

We have recently developed a split-step non-paraxial (SSNP) method and have used it with the collocation method for wide-angle beam propagation [4]. This method, based on the unapproximated scalar wave equation, propagates waves in both directions. In this method, each propagation step requires only multiplications of a square matrix with a matrix vector and no inversion or diagonalization is required (except only once before the beginning of propagation). For the two-dimensional propagation case, this amounts to  $8N^2 + 6N$  multiplications of *real numbers* at each step,  $N$  being the number of transverse discretization points. This makes this method very efficient computationally.

In this presentation, we show this capability of the method. In particular, we have applied it to the problem of reflection from discontinuity. Figure 1 shows the reflected, transmitted and radiated power (for the incident TE<sub>0</sub> mode) from a junction between two waveguide, a problem treated in [3], while Figure 2 shows the reflected power from the end facet of a waveguide, a problem treated in [2]. These results show a good match with published results. More examples will be presented.

### References

- [1] H. El-Refaei, D. Yevick and I. Betty, IEEE Photon. Technol. Lett. 12, 389-391, 2000.
- [2] N.-N. Feng and W.-P. Huang, J. Lightwave Technol. 22, 664-668, 2004.
- [3] S.S.A. Obayya, J. Lightwave Technol. 22, 1420-1425, 2004.
- [4] A. Sharma and A. Agrawal, J. Opt. Soc. Am. A 21, 1082-1087, 2004.

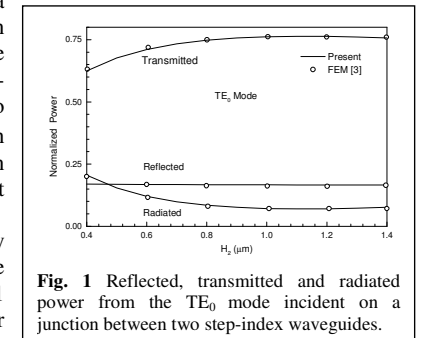


Fig. 1 Reflected, transmitted and radiated power from the TE<sub>0</sub> mode incident on a junction between two step-index waveguides.

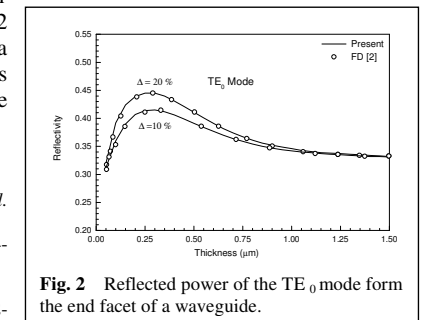


Fig. 2 Reflected power of the TE<sub>0</sub> mode from the end facet of a waveguide.

## Finite element-based numerical methods for Photonic Devices

B M A Rahman, A Agrawal, S S A Obayya, A K M S Kabir,  
K Namassivayane, M Rajarajan, and K T V Grattan

School of Engineering and Mathematical Sciences, City University, London EC1V 0HB, UK  
Tel: +44-20-7040-8123 Telefax: +44-20-7040-8568  
Email: B.M.A.Rahman@city.ac.uk

**Abstract:** Numerically simulated results for advanced photonic devices, such as microstructured photonic crystal fibers, high-speed modulators, spot-size converters and polarizers would be presented by using rigorous full vectorial finite element-based numerical approaches.

**Key words:** Finite element method, Beam propagation method, photonic devices.

The optimization of advanced photonic devices requires an accurate knowledge of their lightwave propagation characteristics and their dependence on the system fabrication parameters and has created significant interest in the development and use of rigorous and numerically efficient computational methods. Of the different numerical approaches for modal solutions reported so far, the finite element method (FEM) [1] has now been established as one of the most powerful and versatile methods. Over the last two decades this technique has been used to characterise a wide range of waveguides and guided-wave photonic devices.

Many important photonic devices, such as optical modulators, filters, polarization splitters, polarization rotators, power splitters, etc may be fabricated by combining several butt-coupled uniform waveguide sections. To design and analyse such photonic devices, it is important to use a junction analysis program in association with a modal analysis program. One of the most rigorous approaches, the least squares boundary residual (LSBR) method [2] has been developed by the authors. In this approach the continuity of the tangential electric and magnetic fields is imposed globally over the interface to obtain the scattering coefficients at the junction. Alternatively, to simulate the propagation of optical waves through a  $z$ -dependent linear or nonlinear structure, the finite element-based beam propagation method (BPM) has been developed [3] using a fully vectorial approach with a difference scheme along the axial directions. Imaginary distance BPM has also been developed [4] to study the evolution of a specific mode in such structures. Such a method is particularly useful in the characterization of tapered spot-size converters, high-power semiconductor amplifiers and nonlinear optical devices. More recently, a new time-domain beam propagation program is being developed for the design optimisation of various photonic devices, such as linear or nonlinear Bragg gratings.

Numerically simulated results for many important guided-wave photonic devices, using the full vectorial finite element-based approaches, will be presented, such as birefringence optimisation of photonic crystal fibers, high-speed modulators, spot-size converters, optical polarizers, single polarization guide, polarization rotators and Bragg gratings.

### References

- [1] B M A Rahman and J B Davies, *J. Lightwave Tech.*, **2**, pp.682-688, Oct. 1984.
- [2] B M A Rahman and J B Davies, *J. Lightwave Tech.*, **6**, pp.52-57, 1988.
- [3] S S A Obayya, B M A Rahman and H A El-Mikati, *J. Lightwave Technol.*, pp.409-415, 2000.
- [4] S S A Obayya *et al.*, *J Lightwave Technol.*, pp.1813-1819, Aug. 2003.

## A Domain Decomposition Method for Photonic Crystal Modeling

Yuxia Huang and Ya Yan Lu

Department of Mathematics, City University of Hong Kong, Hong Kong  
mayylu@math.cityu.edu.hk

The domain decomposition (DD) method has been extensively studied and applied to many different problems. For wave propagation problems in photonic crystal devices, DD can be useful because there are many identical unit cells. In this paper, we present a variant of the DD method based on the Dirichlet-to-Neumann (DtN) map of the unit cells. The DtN map of a unit cell maps the wave field at the boundary of the unit cell to its normal derivative. Using this map, we can establish a sparse system of equations that solves only the wave field on interfaces between the unit cells. For a 2-D square lattice of circular cylinders of radius  $r$  and dielectric constant  $\epsilon_1$  embedded in a material with dielectric constant  $\epsilon_2$ , the unit cell is the square given by  $0 < x < a$  and  $0 < y < a$  with a disk of radius  $r$  at the center. For the TE or TM polarizations, we have Helmholtz equations for a scalar function  $u$ , then the DtN map  $\Lambda$  is defined by

$$\begin{bmatrix} \partial_y u_0 \\ \partial_x v_0 \\ \partial_x v_1 \\ \partial_y u_1 \end{bmatrix} = \Lambda \begin{bmatrix} u_0 \\ v_0 \\ v_1 \\ u_1 \end{bmatrix},$$

where  $u_0 = u(x, 0)$ ,  $u_1 = u(x, a)$ ,  $v_0 = u(0, y)$  and  $v_1 = u(a, y)$ . The operator  $\Lambda$  is approximated by a  $4n \times 4n$  matrix, assuming that  $u_0$ ,  $u_1$ ,  $v_0$  and  $v_1$  are vectors of length  $n$  obtained from sampling at  $n$  points in the interval  $(0, a)$ , such that  $x_j = (j - 0.5)h$  for  $h = a/n$ . A partition of the matrix  $\Lambda$  gives 16 blocks of size  $n \times n$ . Meanwhile,  $\Lambda$  is actually obtained by assuming that the solution of the Helmholtz equation in the unit cell is given as a sum of  $4n$  exact solutions based on Bessel functions. Once  $\Lambda$  is obtained, a system of equations can be obtained for  $\{u_j, v_j\}$  (i.e.  $u$  on edges of the cells). These equations are obtained by imposing the continuity of the derivative of  $u$  on edges of the cells as computed from the DtN maps of the two opposite sides. Notice that such an equation is obtained from two neighboring cells and it involves seven unknown vectors (of length  $n$ ). Therefore, we obtain a sparse system of equations. As an application of the DD method based on the DtN map, we study the transmission problem of a 2-D photonic crystal of finite thickness. We have a square lattice of circular cylinders with radius  $r$  for  $0 < y < ma$  and  $-\infty < x < \infty$ , where  $a$  is the lattice constant,  $m$  is an integer representing the number of layers in the  $y$  direction. For  $y > ma$  and  $y < 0$ , we have a homogeneous medium of dielectric constant  $\epsilon_0$ . For  $m = 16$ ,  $r = a\sqrt{\pi}/2$ ,  $\epsilon_0 = \epsilon_1 = 1$ ,  $\epsilon_2 = 2.1$  and a normal incident wave, we are able to confirm the results in [1] using a very small  $n$  (5 or 9). The results in [1] are obtained based on a Fourier series of 2700 terms.

### References

- [1] K. Sakoda, *J. Opt. Soc. Am. B*, vol. 14, pp. 1961-1966, 1997.

## Grating and waveguide concepts in photonic crystal devices

**P. Lalanne and J.P. Hugonin**

Laboratoire Charles Fabry de l'Institut Optique, Centre National de la Recherche Scientifique et Université Paris Sud, 91 403 Orsay Cedex, France.

Clearly there is a conceptual link between “classical” grating- & waveguide-devices and “new” photonic-crystal-devices. This reflects in both the modeling and theory.

On the request of the organizers, we will try to illustrate through different examples taken from the photonic crystal (3D bandgap opening, one-row missing photonic-crystal waveguides in membrane, photonic crystal nanocavities) community how the knowledge from grating and waveguide may be used as an engineering tool to design photonic crystal devices.

## Controllable phaseshift in mirror based slab waveguides

D. Pietroy, M. Flury, A.V. Tishchenko, O. Parriaux  
*Laboratoire Traitement du Signal et de l'instrumentation, UMR CNRS 5516,*  
*18 Rue Benoît Lauras, F-42000 Saint-Etienne*  
[o.parriaux@univ-st-etienne.fr](mailto:o.parriaux@univ-st-etienne.fr)

A controllable phaseshift on a free space beam can be obtained by means of a resonant structure in reflection in the neighborhood of the resonance. The types of structures giving rise to this property will be discussed.

### Summary

Phase shifting is an important function in the optical processing of free space waves. A new way of performing a phase shift will be presented here. It uses the phase change taking place in the neighbourhood of the resonance of a grating coupled waveguide. It is well known that the abnormal or resonant reflection from a grating coupled slab waveguide is accompanied by a fast change of phase [1] of both the transmission and the reflection. The phase behaviour is however most often discarded since it is the possibly 100% reflection modulus which gives rise to applications [2]. Furthermore, the fact that the phase change takes place in conditions where the modulus has a fast and ample variation limits the usability of the phase change. This would be very different if the modulus could be kept constant. This condition can easily be fulfilled by placing the slab grating waveguide on top of a low loss or lossless mirror: the modulus of the reflection would remain essentially constant across the resonance (upon a scan of the wavelength or of the incidence angle) whereas the only change in the reflected field would be the phase. Such configuration would thus permit a fast and possibly controllable phase change in the neighbourhood of the resonance. The present contribution will demonstrate that the phase change across the resonance is 2D and that the slope of the phase change can be adjusted by the strength of the grating mode coupling resonance.

The possible applications will be discussed.

### References

- [1] T. Tamir, S. Zhang, J. Opt. Soc. Am. A, 14 (7), 1607-1616, 1997.
- [2] F. Pigeon, O.Parriaux, Y. Ouerdane, A.V. Tishchenko, IEEE Photonics Technol. Let., 12 (6), 648-650, 2000.

## Cancellation of the 0th order in a phase mask by mode interplay in a high contrast binary grating

E. Gamet, A.V. Tishchenko  
tishchen@univ-st-etienne.fr  
Laboratoire TSI, 18 Rue Benoît Lauras, F-42000 Saint-Etienne

### Summary

The grating fabrication technique using a phase mask is very attractive because the interferogram resulting from the transmitted +1st and -1st orders has half the period of the phase mask. The main difficulty for obtaining a high contrast interferogram is the suppression of the 0th transmitted order. The printing of gratings of the short periods needed for white light processing (down to about 150 nm period) by means of available short wavelength sources (325 or 244 or 193 nm) requires phase masks of period down to 300 nm with wavelength/period ratios close to 1. Under such conditions a standard silica grating the transmitted 0th order can by far not be suppressed.

We are showing here that the use of a high index grating layer on a silica substrate offers the possibility of cancelling the 0th transmitted order while keeping high the +1st and -1st order efficiency. The synthesis of the optimal structure is made explicitly by resorting to a modal representation of the true grating modes propagating up and down the binary grating and coupling and reflecting at its substrate and air interfaces [1]. The modal approach gives a vivid representation of the electromagnetic phenomena taking place in the grating layer and gives the possibility to solve the structure synthesis problem directly without resorting to an optimization process.

The talk will describe the modal interplay in the binary grating layer and explain the rationale of the synthesis process as well as the possibilities of generalization it offers.

### References

[1] A.V. Tishchenko, *Optical and Quantum Electronics*, 37, 309-330, 2005.

## Spectrally and spatially tunable microphotonic devices associating MOEMS and Photonic Crystal structures

Xavier Letartre, Salim Boutami, Jean-Louis Leclercq, Pierre Viktorovitch  
\*Laboratoire d'Electronique Optoélectronique et Microsystèmes LEOM, UMR CNRS 5512, Ecole Centrale de Lyon, 36 avenue Guy de Collongue, 69134 Ecully Cedex, FRANCE  
[xavier.letartre@ec-lyon.fr](mailto:xavier.letartre@ec-lyon.fr)

We propose a new kind of devices, combining MOEMS and Photonic Crystal (PC) technologies, which allows for wavelength and angular tunability through electromechanical actuation. Numerical and quasi-analytical methods are used to investigate the optical properties of these structures.

### Summary

Most of the devices using Photonic Crystals (PCs) explore either their photonic bandgap (microcavities) or their in-plane guided modes. The drawback of using solely waveguided modes in photonic crystals lies in the fact that they suffer from outcoupling losses due to diffractive coupling with radiated modes into free space, when operating above the light line [1]. However, this outcoupling can be usefully exploited for the design of devices which are meant to operate above the light line. The 2D PC can be deliberately opened to the third dimension of space by controlling the coupling between waveguided and radiated modes, leading to a significant extension of the operation of PCs, in the so-called "PCMOEMS" approach [2].

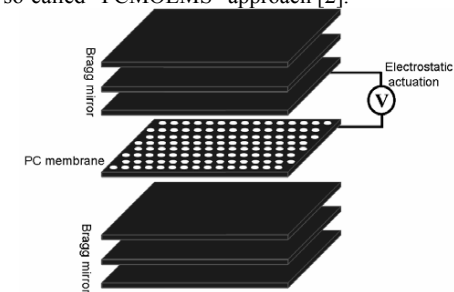


Figure 1 : Tunable PCMOEMS

In this paper, we design an original structure which combines an air gap Fabry-Perot vertical cavity (FP) and a PC membrane located inside the air cavity (figure 1). The strong coupling between the vertical resonant mode of the FP and the "quasi guided" resonant modes of the PC is exploited to obtain original mixed modes, which leads to wavelength selective and directive devices. Varying the thickness of the FP, via electrostatic actuation, allows for spectral and angular tunability. The specific case of an optical microsource is investigated using both analytical tools based on Temporal Coupled Modes Theory and numerical simulations (RCWA and FDTD). This work has been supported by the European Network Of Excellence Epix-Net.

### References

[1] W. Bogaerts, P. Bienstman, D. Taillaert, R. Baets, and D. De Zutter, *IEEE Photon. Technol. Lett* 13, 565 (2004)  
[2] X. Letartre, J. Mouette, J. L. Leclercq, P. Rojo-Romeo, C. Seassal, P. Viktorovitch, *J. Light. Technol* 21, 1691 (2003)

## An ARROW-based silicon-on-insulator photonic crystal waveguides with reduced losses

Andrei Lavrinenko\*,

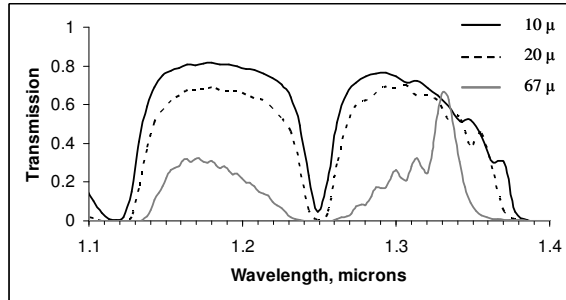
\* COM•DTU Department of Communications, Optics & Materials, NanoDTU, Technical University of Denmark, Building-345V, 2800 Kgs. Lyngby, - Denmark  
ala@com.dtu.dk

We employ an antiresonant reflecting layers arrangement for silicon-on-insulator based photonic crystal waveguides with thin cores. 3D FDTD numerical modelling reveals the reduction of losses with a promising potential for competing with membrane-like waveguides.

### Summary

The state-of-the-art results for transmission in photonic crystal waveguides (PCWs) evidently point out that the membrane-like configuration has provided ultimately low losses due to the highest possible index contrast at its interfaces [1]. Few attempts have been made so far to improve transmission of substrate-based PCWs. We have proposed recently to apply claddings with antiresonant reflection (a configuration known as ARROW) and showed that PCWs losses might be reduced [2]. However, the core thickness was assumed to be  $0.5\mu$  and that imposed very strict technological constraints on the layer deposition and holes etching processes.

Here we investigate a silicon-on-insulator PCW with a typical core thickness about  $250\text{ nm}$  based on the ARROW-type claddings arrangement. Transmission spectra are calculated by 3D FDTD method. Parameters of the system are the following: thickness of the silicon core  $240\text{ nm}$  ( $n = 3.5$ ), the first glass cladding –  $360\text{ nm}$  ( $n = 1.45$ ), the second silicon cladding –  $168\text{ nm}$  and a glass substrate underneath. Photonic crystal patterning is made with a triangular lattice of holes. The hole's diameter is  $185\text{ nm}$  and the lattice constant is  $336\text{ nm}$ . Lattice parameters and ARROW layers thicknesses are deliberately chosen to show the best performance in the silicon window around  $\lambda = 1.33\ \mu$ . The spectra for three different lengths of W1 PCW  $10, 20\ \mu$  and  $67\ \mu$  (200 lattice constants) are shown in the figure. The sharp transmission line for the longest PCW signals about resonant behavior of the claddings. We present numerous examples of thin-core ARROW platforms and dependence of losses on the holes depths. Transmission for pure silica cladding below the core is also calculated for comparison showing the half less transmitted flux. The memory requirements limit the lengths of PCWs we are able to simulate ( $70 - 80\ \mu$ ) and thus prevent from accurate evaluation of losses. However, low-loss propagation in such configuration is proved to be possible and might be ameliorated further to compete with membrane-like PCWs.



also calculated for comparison showing the half less transmitted flux. The memory requirements limit the lengths of PCWs we are able to simulate ( $70 - 80\ \mu$ ) and thus prevent from accurate evaluation of losses. However, low-loss propagation in such configuration is proved to be possible and might be ameliorated further to compete with membrane-like PCWs.

### References

- [1] E. Kuramochi, et al., Phys. Rev. B 72, 161318, 2005.
- [2] A. Lavrinenko, et al., ICTON, 03-07 July 2005, Barcelona, Spain, Proceedings, V.1, p.273-276.

## An Accurate Analytical Method for Simulating AWG Components

F.P. Payne\* and Stephane Paquet

\*Department of Engineering Science, University of Oxford, 17 Parks Road, Oxford OX1 3PJ,  
frank.payne@eng.ox.ac.uk

This paper describes an accurate analytical method for simulating AWG components. Our model shows very good agreement with experimental measurements on a flat-top AWG fabricated in silica on silicon.

The simulation of an AWG presents special problems for the component designer. The size and complexity makes it necessary to break the simulation down into smaller steps, consisting of

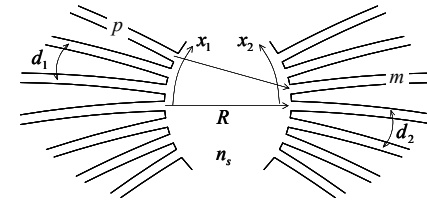


Figure 1 Geometry of star coupler. Separation between waveguides is  $d_1$ ; radius of star coupler is  $R$ ; refractive index of the free space region is  $n_s$ .

propagation through each of the two star couplers and the waveguide array. Accurate simulation of the star couplers is critical for the overall accuracy of the model. Figure 1 shows the geometry of a star coupler, and describes both input and output sides of the AWG. Coupling from waveguide  $p$  to waveguide  $m$  is given by the overlap integral of the far field radiated by waveguide  $p$  and the modal field of waveguide  $m$ . This is usually computed numerically, or approximated analytically using Gaussians to represent the waveguide fields. In this paper we present an accurate analytical equation for the overlap integral which uses the exact waveguide fields. We show that the coupling  $t_{pm}$  from waveguide  $p$  to  $m$  is given by

$$t_{pm} = 4\pi^2 \sqrt{\frac{n_s}{\lambda R}} \exp\left(-\frac{i n_s k_0 p d_1 m d_2}{R}\right) \cdot \left\{ \tilde{\psi}'_1\left(\frac{n_s k_0 m d_2}{R}\right) \tilde{\psi}_2\left(\frac{n_s k_0 p d_1}{R}\right) + i \frac{n_s k_0}{R} \tilde{\psi}'_1\left(\frac{n_s k_0 m d_2}{R}\right) \tilde{\psi}'_2\left(\frac{n_s k_0 p d_1}{R}\right) \right\} \quad (1)$$

where  $\tilde{\psi}_{1,2}$  are the Fourier transforms of the waveguide modal fields, and  $\tilde{\psi}'_{1,2}$  their derivatives. Comparison with exact numerical evaluation shows that equation (1) is very accurate. When combined with the phase shifts through the array waveguides equation (1) provides a very accurate model of an AWG. In Figure 2 we compare the predictions of our model with measurements made on a 40-channel flat top silica-on-silicon AWG designed for low loss with 100GHz channel spacing and maximal flatness in the passband. The solid line is the experimental measurement, and the dashed line is the model prediction. The results in Figure 2 confirm that our analytical model is capable of very high accuracy and suitable for detailed AWG design.

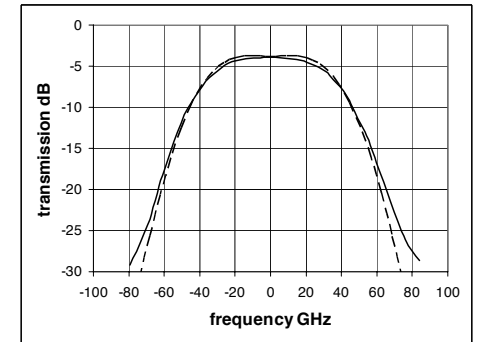


Figure 2 Transmission of centre output of a flat top silica on silicon AWG. Solid line shows measured response; dashed line shows model prediction.

# Analysis of Slot Characteristics in Single Mode Semiconductor Lasers using the Scattering Matrix Method (SMM)

Q. Y. Lu, W. H. Guo, R. Phelan, D. Byrne, and J. F. Donegan

Semiconductor Photonics Group, School of Physics, and Centre for Telecommunications Value-Driven Research (CTVR), Trinity College, Dublin 2, Ireland

Single mode semiconductor lasers can be fabricated by distributing reflective defects (slot as shown in Fig. 1 (a)) into conventional Fabry-Perot (FP) laser cavities [1]. By optimizing the slot reflection, position and slot number, a side mode suppression ratio (SMSR) of more than 40 dB can be achieved [2]. For optimization, firstly we need to make clear the characteristics of a single slot, most importantly the reflection and loss of this single slot. Traditionally, the analysis is done by the transfer matrix method (TMM), in which the 3D structure is simplified into a 1D model using the effective index method [2]. This kind of analysis is simple but not accurate enough, and in particular the scattering loss can not be analyzed. We present a 2D scattering matrix method (SMM) to simulate the single slot, in which the transverse direction and the propagation direction are considered simultaneously. In this model the plane wave expansion method is used to deal with the transverse direction. The perfectly matched absorption layer is introduced to absorb the out-scattering wave. At the interface between the slot and the waveguide region the mode matching condition is implemented. And finally the scattering matrix technique is used to deal with the multi-interface problem. Since the radiation modes are taken into account the scattering loss can be analyzed and the reflection calculated is more reliable. By the 2D SMM simulation we find that there is nearly no reflection at the interface from slot to waveguide while a large reflection exists at the interface from waveguide to slot, and the loss is much larger than the reflection. In the TMM, there is no loss at these interfaces, and the reflection at both interfaces is the same and much smaller than that calculated by SMM. For the single slot, the slot width has little influence on the slot reflection, which is completely different from that calculated by TMM as shown in Fig. 1 (b).

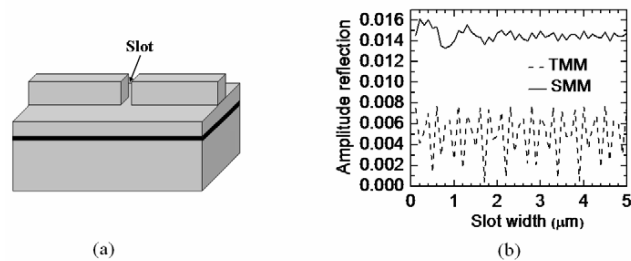


Fig. 1 (a) Schematic diagram of a FP laser with single slot (b) Amplitude reflection of single slot vs. slot width calculated by SMM and TMM

### References:

1. Corbett B. and McDonald D., Electronics Letters, 1995, **31**, 2181.
2. O'Brien S. and O'Reilly P. E., Applied Physics Letters, 2005, **86**, 20110-1.

# FDTD Modelling and Experimental Verification of FWM in Semiconductor Micro-Resonators

Masafumi Fujii\*, Christian Koos<sup>o</sup>, Christopher Poulton<sup>o</sup>, Juerg Leuthold<sup>o</sup>, Wolfgang Freude<sup>o</sup>

\*Department of Electrical and Electronic Eng., University of Toyama, Gofuku 3190, Toyama, Japan [mfujii@eng.toyama-u.ac.jp](mailto:mfujii@eng.toyama-u.ac.jp)

<sup>o</sup>Institute of High-Frequency and Quantum Electronics, University of Karlsruhe, 76131 Karlsruhe, Germany

We have modelled for the first time to our knowledge parametric four-wave mixing (FWM) in an actual InP/InGaAsP micro-resonator device using a nonlinear FDTD code which models strong material dispersion of the semiconductor optical waveguide. The numerical results have been verified by accurate experiments.

### Summary

Four-wave mixing (FWM) in a micro-resonator structure (Fig. 1) has been investigated numerically and experimentally. We have implemented a 2D and 3D nonlinear finite-difference time-domain (FDTD) analysis code, which was executed on a parallel computer XC6000 at the University of Karlsruhe [1]. Strong material dispersion and the optical Kerr effect have been considered in the analysis. The resonance frequencies of the resonator were analyzed first (Fig. 2), and then pump (denoted as 'p') and signal ('s') waves were entered from port 1 of the bus-waveguide for the FWM analysis. The optical field in the resonator is enhanced by the resonance, and is observed to be much stronger than that in the bus-waveguide as in Fig. 3. The converted wave ('c') is seen in the computed FWM spectrum of Fig. 4. The optical wavelength conversion efficiencies for various pump powers are plotted in Fig. 5. The numerical results exhibit similar efficiencies for 2D and 3D results including or excluding the material dispersion, and are compared to measurements in Fig. 5. We observe differences of about 7 dB between the numerical and the measured results, which are due to the radiation from the slight roughness of the waveguide sidewalls and fabrication tolerances.

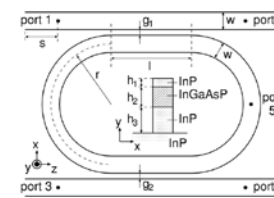


Fig. 1 Racetrack resonator under investigation.

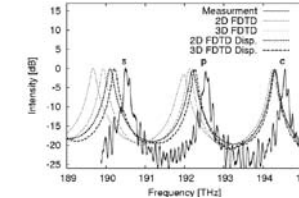


Fig. 2 Computed resonance spectrum of the resonator.

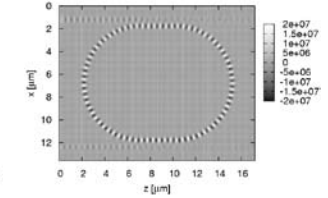


Fig. 3 Optical field distribution in the resonator.

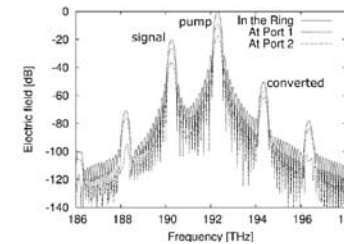


Fig. 4 Typical computed FWM spectrum.

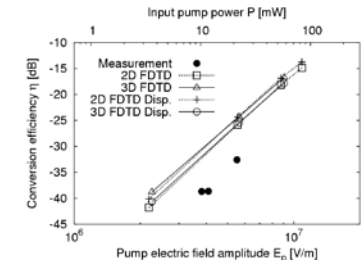


Fig. 5 Computed and measured wavelength conversion efficiencies.

### References

- [1] M. Fujii, C. Koos, C. Poulton, J. Leuthold, W. Freude, IEEE Photon. Tech. Letters, Feb. 2000.

## Time-domain analysis of parametric frequency conversion

Michele Lauritano\*, Stefano Trillo, Gaetano Bellanca

Dipartimento di Ingegneria, Università di Ferrara, Via Saragat 1, 44100 Ferrara, Italy

\*michele.lauritano@unife.it

M. Conforti, A. Locatelli, C. De Angelis

Dip. di Elettronica per l'Automazione, Università di Brescia, via Branze 38, 25123 Brescia, Italy

Frequency doubling is analyzed in the framework of time-domain Maxwell equations. Special emphasis is posed on critical phenomena occurring in the counter-propagating geometry, as well as the impact of numerical dispersion comparing FDTD with pseudo-spectral methods.

### Summary

Time domain methods such as the well known FDTD are a powerful tool in the analysis of linear and nonlinear propagation phenomena [1]. However, the limitations imposed by the numerical dispersion artificially introduced by finite differences may affect the accuracy of the description. While in many cases this results in a mere error on the phase constant that can be reduced by choosing a sufficiently thin grid, this problem becomes particularly bad in the description of nonlinear parametric processes such as second harmonic generation (SHG). In this case the errors on the propagation constants may result through a smearing effect in a large error on the wave-number mismatch which directly affect quantitatively (conversion efficiency and spatial period) and qualitatively the description of the process. Our results suggest that this is indeed the case in the FDTD analysis of SHG in the standard forward configuration (F-SHG) both in homogeneous materials and QPM nonlinear gratings (obtained by modulating the nonlinear susceptibility). Comparisons with coupled-mode-theory (CMT) show that the numerical dispersion critically corrupts the theoretical predictions. Viceversa, a far better description can be obtained by means of an alternative pseudo-spectral time-domain (PSTD) method involving spectral representation of spatial derivatives [2]. We report comparisons between FDTD and PSTD simulations and show that the latter are in better agreement with the CMT.

We have also tested the ability of FDTD to reproduce critical phenomena described by CMT. To this end the case of SHG occurring in the backward direction (B-SHG, obtained in short period QPM gratings [3]) is more intriguing because CMT tells us that the built-in distributed feedback is responsible for the onset of several instability mechanisms encompassing bistability, limiting, filamentation and self pulsing, all originating from a critical phenomenon (a type bifurcation) in the underlying CMT dynamical system. We apply here for the first time (to the best of our knowledge) the FDTD method to give a qualitative and quantitative description of a BSHG converter with the aim of validating the scenarios originating from CMT, while going beyond the approximations (finite number of frequencies, rotating-wave approximation, slowly varying evolution) that are implicit in the CMT approach. The importance of such analysis is also in view of envisaging experimental demonstration of such phenomena, which have never been reported to date.

### References

- [1] A. Taflov, Computational Electrodynamics, The Finite-Difference Time-Domain Method, (Artech House Boston-London, 1995)
- [2] Q. H. Liu, "The PSTD Algorithm: a Time-Domain Method Requiring only two Cells per Wavelength", Microwave And Opt. Tech. Lett. 15, 158 (1997).
- [3] J.U. Kang, Y.J. Ding, W.K. Burns and J.S. Melinger, "Backward second-harmonic generation in periodically poled bulk LiNbO<sub>3</sub>", Opt. Lett. 22, 862 (1997).

## An all-optical switching structure based on the decoupling property of two parallel photonic crystal waveguides

Ivan S. Maksymov, Lluís F. Marsal and Josep Pallarès

D.E.E.E.A., Universitat Rovira i Virgili, Avda. Paisos Catalans 26, 43007 Tarragona, Spain

lluis.marsal@urv.net

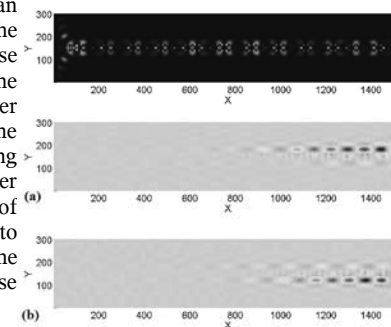
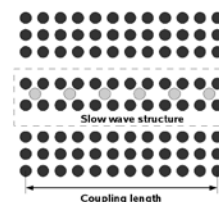
An all-optical switching structure based on a nonlinear 2-D photonic crystal (PC) decoupler is presented and analyzed. The finite-difference time-domain (FDTD) method is used to calculate and discuss the optical properties of the device.

### Summary

In the future, the electronic chips may be substituted by their optical analogs based on the photonic crystal technology. In such chips, active elements can be realized using the possibility to control the light with light by means of nonlinearities of the propagation medium. Here, one of the main problems is connected with the fact that the nonlinearities of materials used in fabrication are weak, which means that very long devices or very high optical power are required. In many respects, this problem can be solved using optical slow wave structures [1] similar to those used in microwave devices and masers. An optical slow wave structure can be made by introducing defects in a PC [2]. The main feature of slow wave structures is the strong reduction of the group velocity and, therefore, the enhancement of the propagation parameters by a factor called the slowing ratio [1].

In this study, we propose an all-optical switching structure based on a nonlinear 2-D PC decoupler [3]. Unlike the all-optical structures based on nonlinear directional couplers, our device functions in the bar state when its working regime is linear and it switches to the cross state in the nonlinear regime. We take a special care in modifying the coupling region between two PC waveguides. We introduce a line of defects made of a Kerr-like nonlinear material (gray rods) and change the distance between them. Thus, we obtain a slow wave structure that is used to enhance the nonlinear effect and improve the efficiency of the device.

The pictures show the calculated field distributions in the slow wave system and in the waveguides. A modulated Gaussian pulse is launched into the upper waveguide. If the power of the control signal is small, this pulse propagates only in the upper waveguide because the waveguides are decoupled in this regime. If the power is high enough to cause a considerable increase in the refractive index of the nonlinear rods, the coupling becomes possible and the pulse enters to the lower waveguide and then propagates in it. The estimation of the power needed to achieve such a device takes into consideration the impact of the group velocity in the slow wave system and the influence of cross-phase modulation (XPM).



### References

- [1] A. Melloni, F. Morichetti and M. Martinelli, Opt. Quantum. Electron. 35, 365-379, 2003.
- [2] A. Yariv, Y. Xu, R. K. Lee, A. Scherer, Opt. Lett. 24, 711-713, 1999.
- [3] S. Boscolo, M. Midrio and C. G. Someda, IEEE J. Quantum. Electron. 38, 47-53, 2002.

## Time resolved numerical simulation of a single laser beam in a photorefractive semi-conductor for telecommunications applications

Delphine Wolfersberger\*, Naima Khelfaoui\*, Cristian Dan\*, Nicolas Fressengeas\*,

\* *Laboratoire Matériaux Optiques, Photonique et Système (LMOPS), CNRS UMR-7132, Unité de recherche commune à Supélec et à l'université de Metz, 2 Rue Edouard Belin, Metz, France*

[Delphine.Wolfersberger@supelec.fr](mailto:Delphine.Wolfersberger@supelec.fr)

Hervé Leblond°

° *Laboratoire Propriétés Optiques des Matériaux et Applications (POMA), CNRS UMR 6136, Université d'Angers, 2 Bd Lavoisier, Angers, France*

The simulation of the fast self-trapping of an infrared laser beam in a photorefractive semi-conductor crystal has been modeled : the calculations are performed using two different analytical and numerical methods for describing the space charge field masking, coupled with a Beam Propagation Method (BPM).

### Summary

Photorefractive insulators as propagation media of low power laser beams have been the object of intense theoretical and experimental research regarding the screening of an externally applied electric field and its influence on the self-focusing properties of the incident beam [1,2], in the visible wavelength range both in continuous and pulsed regime. In such materials the build up of this kind of solitons can take up to seconds owing to the carriers moving and trapping in the photorefractive medium. Till nowadays, in the semi-conductor InP, only the case of steady state self-trapping of optical beams has been studied [3].

We propose here a new calculation of the propagation of a single laser beam in the photorefractive semiconductor InP:Fe crystal taking into account the temporal regime at infrared wavelengths. The model is based on the rate and charge transport equations under the adiabatic approximation where the densities of electrons and holes are considered to reach instantaneously their equilibrium value. Furthermore, we suppose the electrons to be excited thermally and the holes optically. We calculate the space charge field versus time and space by two different methods : one is an analytic method considering further assumptions, the second one is a numerical resolution based on a finite difference scheme with a Runge-Kutta algorithm. This calculation of the space charge field has been coupled to the simulation of the propagation of a beam in a non linear medium using a Beam Propagation Method.

For both methods, we analyze the influence of different parameters such as the externally applied electric field, the beam intensity, the entrance beam waist. The theoretical numerical simulations show the possibility for a single laser beam to be self-focused in the millisecond range which is very promising for applications in optical communication component (optical logic gates, optical routing...).

### References

- [1] M. Wesner, C. Herden, D. Kip, E. Krätzig, and P. Moretti. Photorefractive steady state solitons up to telecommunication wavelengths in planar SBN waveguides. *Opt.Comm.*, 188, 69–76, 2001.
- [2] M. Morin, G. Duree, G. Salamo, and M. Segev. Waveguides formed by quasi-steady-state photorefractive spatial solitons. *Opt. Lett.*, 20, 2066, 1995.
- [3] M. Chauvet, S. A. Hawkins, G. J. Salamo, M. Segev, D. F. Bliss, G. Bryant, *Opt. Lett.*, 21, 1333 (1996).

## Continuation method applied to the bifurcation analysis of polarization dynamics in vertical-cavity surface-emitting lasers

Marc Sciamanna\*, Ignace Gatare\*, and Krassimir Panajotov°

\* *Supélec, Laboratoire Matériaux Optiques, Photonique et Système (LMOPS), CNRS UMR-7132, 2 Rue Edouard Belin, F-57070 Metz, France*

[Marc.Sciamanna@supelec.fr](mailto:Marc.Sciamanna@supelec.fr)

° *TW-TONA Department, Vrije Universiteit Brussel (VUB), Pleinlaan 2, B-1050 Brussels, Belgium.*

Modern continuation techniques are applied to bring new physical insight into the polarization dynamics of vertical-cavity surface-emitting lasers subject to time-delayed optical feedback or to optical injection.

### Summary

Vertical-Cavity Surface-Emitting Lasers (VCSELs) are interesting devices considering their numerous advantages with respect to the conventional edge-emitting lasers but also their unique polarization properties. VCSELs usually emit linearly polarized (LP) light but may switch between two orthogonal LP modes depending on the injection current or temperature. Time-delayed optical feedback or external light injection may be used either to control the VCSEL light polarization [1] or, on the other hand, to induce nonlinear polarization dynamics of interest for all-optical signal processing or telecommunication applications (e.g. secure chaos communications) [2].

We report here on the use of recently developed continuation techniques (DDE-BIFTOOL) to numerically investigate the polarization dynamics of VCSELs. In the case of a time-delayed optical feedback, new steady-states called external-cavity modes (ECMs) are successively created as the feedback strength is increased. ECMs may be either linearly polarized along the VCSEL eigenaxes or elliptically polarized, but switching between different polarization states is possible as we change the feedback parameters. The continuation method allows following the cascading branches of ECMs irrespective of their stability, and to analyze the ECM stability. It therefore helps to connect the polarization switching to primary or secondary bifurcations on the ECMs.

We have recently unveiled experimentally a period doubling route to chaos and different nonlinear polarization dynamics (wave mixing, time-periodic oscillations) in VCSELs with orthogonal optical injection [3], i.e. when external light is injected with a polarization orthogonal to that of the free-running VCSEL. The use of continuation techniques allows us to analyze in detail the injection locked steady-states and their stability. Of particular interest is the report of a two-mode injection locked steady-state, with the two x-and y-LP modes of the VCSEL locked to the external laser polarization and frequency. As we modify the frequency detuning or injection strength, the two-mode injection locked steady-state destabilize with a Hopf or with a saddle-node bifurcation. The continuation techniques also allow to unveil bistability between different injection-locked solutions.

### References

- [1] M. Sciamanna, K. Panajotov, H. Thienpont, I. Veretennicoff, P. Mégret, M. Blondel, *Opt. Lett.* 28, 1543-1545, 2003.
- [2] Y. Hong, M. W. Lee, P. S. Spencer, K. A. Shore, *Opt. Lett.* 29, 1215-1217, 2004.
- [3] J. Buesa Altès, I. Gatare, K. Panajotov, H. Thienpont, M. Sciamanna, *IEEE J. Quantum Electron.* QE-42, 198-207, 2006.

## All-Optical AND Gate based on Raman effect in Silicon-on-Insulator Waveguide

Vittorio M. N. Passaro\* and Francesco De Leonardis<sup>o</sup>

\*Dipartimento di Elettrotecnica ed Elettronica, Politecnico di Bari, Via E. Orabona 4, Bari - Italy  
passaro@deemail.poliba.it

<sup>o</sup>Dipartimento di Ingegneria dell'Ambiente e per lo Sviluppo Sostenibile, Politecnico di Bari, Taranto, Italy

An all optical AND gate based on Raman effect in SOI waveguide with nano-scale cross section is presented. Various modelling techniques have been applied, including time-space nonlinear partial differential equations, collocation method, and finite element method.

### Summary

Recently an amount of research has been focused on Silicon Photonics, due to the high quality of commercial silicon wafers driven by Microelectronics industry, and high compatibility with silicon integrated circuits manufacturing and silicon Micro-Electro-Mechanical Systems (MEMS) technology. In addition, silicon-on-insulator (SOI) waveguides can confine the optical field to an area that is approximately 100 times smaller than the modal area in a standard single-mode optical fiber, inducing much higher nonlinear effects. The cross section and the architecture of a high performance all optical AND gate based on Raman effect is shown in Fig. 1 and 2, respectively. The SOI waveguide, with a nano-scale cross section ( $H \sim 500$  nm,  $W \sim 390$  nm,  $H_s \sim 150$  nm), has been designed to be polarization insensitive at the Stokes wavelength ( $\lambda_s = 1.65$   $\mu$ m). The curves in Fig. 3 represent the pulse signals applied at the inputs A and B ("1" logic), using a pump wavelength of 1.5450  $\mu$ m and pulse width of 1 ps. In Figs. 4 and 5 3D plots of space-time behaviour of the all-optical AND gate are sketched in terms of combined inputs after Y-junction and Stokes pulse excitation at the output, respectively. A large sidelobe suppression ratio of about -18 dB can be so achieved.

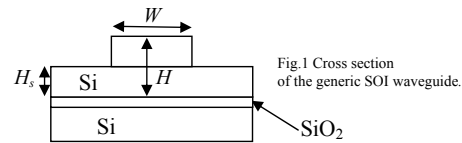


Fig.1 Cross section of the generic SOI waveguide.

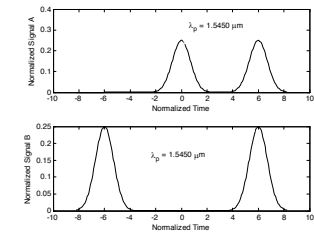


Fig.3 Input pulses (signals A and B, respectively).

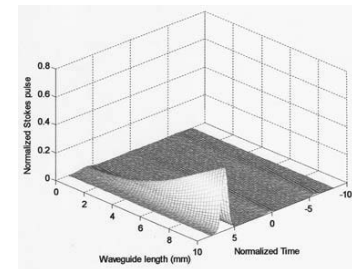


Fig. 5. Time-space evolution of resulting Stokes waves at the output,  $\lambda_p = 1.65$   $\mu$ m.

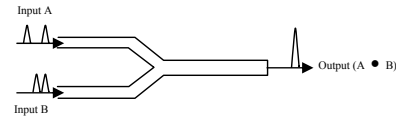


Fig.2. Schematic structure of the all-optical AND gate.

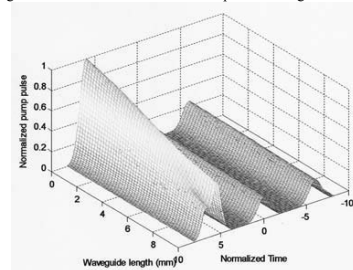


Fig. 4. Time-space evolution of input signals interfering after the Y-junction..

## Abstracts Index

- |  |           |
|--|-----------|
| <b>Nanostrip and Photonic Crystal Waveguides: The Modelling of Imperfections</b><br><i>Wolfgang Freude, Christopher G. Poulton, Christian Koos, Jan Brosi, Masafumi Fujii, Andreas Pfrang, Thomas Schimmel, Manfred Müller, Juerg Leuthold</i> | <b>1</b>  |
| <b>Impairment of Photonic-Crystal Waveguide Taper due to Hole Inaccuracy</b><br><i>Lorenzo Rosa, Federica Poli, Matteo Foroni, Annamaria Cucinotta, Stefano Selleri</i>  | <b>3</b>  |
| <b>Damping of TE Waves in an InP Based Photonic Crystal Waveguide</b><br><i>Zsolt Szabó, György Kádár</i>  | <b>4</b>  |
| <b>Modelling lossy photonic wires: a mode solver comparison</b><br><i>P. Bienstman, S. Selleri, H.P. Uranus, W.C.L. Hopman, A. Melloni, R. Costa, L.C. Andreani, P. Lalanne, J.P. Hugonin, D. Pinto, S.S.A. Obayya</i>                         | <b>5</b>  |
| <b>Design optimisation for a generic planar scattering platform</b><br><i>Carl Styan, Ana Vukovic, Phillip Sewell, Trevor Benson</i>   | <b>6</b>  |
| <b>Modeling of Membrane Photonic Crystal Defect Cavities for Semiconductor Quantum Wire Laser Applications</b><br><i>K.F. Karlsson, K.A. Atlasov, E. Kapon</i>   | <b>7</b>  |
| <b>Ultrashort Vectorial Pulse Propagators</b><br><i>J.V. Moloney</i>   | <b>8</b>  |
| <b>Strong Control of Radiation States in a Slab Waveguide sandwiched between two Omni-Directional Mirrors</b><br><i>H.J.W.M. Hoekstra, D. Yudistira, R. Stoffer</i>  | <b>10</b> |
| <b>Time-Domain Full-Wave Solver for Integrated Optical Waveguides</b><br><i>Luca Pierantoni, Alessandro Massaro, Andrea Di Donato, Davide Mencarelli, Tullio Rozzi</i>   | <b>11</b> |
| <b>Frequency-domain modeling of photonic crystal and plasmonic devices</b><br><i>Georgios Veronis, Shanhui Fan</i>   | <b>12</b> |
| <b>Guiding Light in Plasmon-Polariton Waveguides</b><br><i>A.N.Kireev, Olivier J.F. Martin</i>   | <b>13</b> |
| <b>Improved ASR convergence for the simulation of Surface Plasmon Waveguide Modes</b><br><i>Peter Debackere, Peter Bienstman, Roel Baets</i>   | <b>14</b> |
| <b>Efficient simulation of metals in the finite-difference time-domain method</b><br><i>W.H.P. Pernice, F.P. Payne, D.F.G. Gallagher</i>   | <b>15</b> |
| <b>Numerical optimization of cascaded Y-branches in Ti:LiNbO3</b><br><i>Andrea Guglielame, Stefano Balsamo</i>   | <b>16</b> |

<b>The Modelling of Segmented MMI Structures</b> <i>Laurence Cahill</i>	17	<b>Time Domain Modelling of Nonlinear Optical Waveguides</b> <i>S.S.A. Obayya, D.Pinto</i>	31
<b>Imaginary distance BPM as an efficient tool for modelling optical waveguide fabrication by ion diffusion</b> <i>G. Lifante, E. Cantelar, F. Cussó, M. Domenech, A.C. Busacca, A. Cino, S. Riva Sanseverino</i>	18	<b>Modeling of an Optical Ring Resonator Electric Field Sensor</b> <i>Francesco De Leonardis, Vittorio M. N. Passaro</i>	32
<b>Single-Mode Volume Waveguides in Ferroelectrics Written by Bright Soliton Beams: Towards 3D Integrated Circuits</b> <i>Eugenio Fazio, Federico Pettazzi, Grigore Leahu, Massimo Alonzo, Mathieu Chauvet, Adrian Petris, Valentin Ionel Vlad, Nicola Argiolas, Marco Bazzan, Paolo Mazzoldi, Cinzia Sada</i>	19	<b>Simulation of Thermo-Optic Reconfigurable Optical Add/Drop Multiplexers in SOI Technology</b> <i>Vittorio M. N. Passaro, Francesca Magno, Andrei V. Tsarev</i>	33
<b>Balancing the grating excitation of slab waveguide modes for the highest accuracy retrieval of the slab parameters</b> <i>M. Flury, N. Destouches, A.V. Tishchenko, O. Parriaux</i>	20	<b>Efficient Phase Matched Second Harmonic Generation through Rotated Periodic Poling in LiNbO3 Waveguides</b> <i>F.M. Pigozzo, E. Autizi, A.D. Capobianco, C. Sada, M. Bazzan, N. Argiolas, P. Mazzoldi</i>	34
<b>Oblique Coordinates for Computing Band-Diagrams in Photonic Crystals with Hexagonal Lattice</b> <i>Stefan F. Helfert</i>	21	<b>Solving Boundary Problem for Nonlinear Elliptic Equation By Successive Approximations Method</b> <i>S.V. Kolosova, S. Ruzhytska</i>	35
<b>A simple coupled mode model for near band-edge phenomena in grating waveguides</b> <i>H.J.W.M. Hoekstra, W.C.L. Hopman, J. Kautz, R. Dekker, R.M. de Ridder</i>	22	<b>Spontaneous Parametric Down Conversion Process in a Guided Wave Photonic Crystal</b> <i>Letizia Sciscione, Marco Centini, Concita Sibilìa, Mario Bertolotti, Micheal Scalora</i>	36
<b>Molding the Emission of Photonic Nanojets by Different Particle Shapes</b> <i>Tahmineh Jalali, Daniel Erni, Christian Hafner</i>	23	<b>Square-lattice photonic crystal fiber cut-off analysis</b> <i>Federica Poli, Matteo Foroni, Lorenzo Rosa, Annamaria Cucinotta, Stefano Selleri</i>	37
<b>Measurements of effective index in channel SiON waveguides</b> <i>Yu. Larionov, S.Kuzmin, V.Svetikov, V. Sychugov</i>	24	<b>Analytical Computation of the Propagation Matrix for the Finite-Difference Split-Step Non-Paraxial Method</b> <i>Anurag Sharma, Debjani Bhattacharya, Arti Agrawal</i>	38
<b>Finite Difference Time Domain (FDTD) studies of an electrically pumped integrated microdisk laser</b> <i>Xavier Letartre, Pedro Rojo-Romeo, Christian Seassal</i>	25	<b>Scale-Length Invariant Guided Modes in 1D Metamaterial Photonic Crystal Waveguides</b> <i>Juan A. Monsoriu, Ricardo A. Depine, Maria L. Martinez-Ricci, Enrique Silvestre, Pedro Andrés</i>	39
<b>Improved Finite-Difference Time-Domain Modelling of Surface Plasmons</b> <i>Ahmad Mohammadi, Mario Agio</i>	26	<b>A simple low-dimensional model and efficient FEM calculations to determine the quality of photonic crystal cavities</b> <i>A. Sopaheluwakan, E. van Groesen</i>	40
<b>Self-Phase Modulation in Slow-Wave Structures: a comparative numerical analysis</b> <i>Francesco Morichetti, Andrea Melloni, P. Bienstman, G. Priem, J. Petráček</i>	27	<b>Numerical Approaches for the Analysis of Injection Locked Lasers</b> <i>Giovanni Tartarini, Lorenzo Rosa, Stefano Selleri, Pier Faccin, Enrico Maria Fabbri</i>	41
<b>Hurst's Index and Complexity of Wave in Modulated Dielectric Medium</b> <i>Alexander Nerukh, Nataliya Ruzhytska, Dimitry Nerukh</i>	28	<b>Limited buffer waveguides: impact on leakage and coupling loss</b> <i>R. Costa, G. Cusmai, A. Melloni, M. Martinelli</i>	42
<b>Semi-analytical diagnostics and design of gradient refractive index profile waveguides</b> <i>Nikolai Nikolaev, Victor V. Shevchenko</i>	29	<b>Simulation of New Integrated Optic Polarisation Controller in SOI Technology</b> <i>Andrei V. Tsarev</i>	43
<b>Bragg Diffraction in Bounded Homogeneous System of Coupled Channel Waveguides</b> <i>J. Kh. Nurligareev, V.A. Sychugov, K.M. Golant</i>	30	<b>Fabry-Perot Interferometer With Two Waveguide Grating Mirrors</b> <i>B.A.Usievich, V.A.Sychugov</i>	44

<b>Numerical Model of S-band depressed cladding EDFAs</b>	<b>45</b>	<b>Numerical modelling of the optical properties of infiltrated photonic crystals</b>	<b>62</b>
<i>Stefano Selleri, Annamaria Cucinotta, Federica Poli, Matteo Foroni, Moreno Maini, Luca Vincetti</i>		<i>Vasily Zabelin, Romuald Houdré</i>	
<b>Hybrid and network methods in electromagnetic simulations</b>	<b>46</b>	<b>Dissipative Solitons</b>	<b>63</b>
<i>Mauro Mongiardo</i>		<i>F. Lederer</i>	
<b>Dual resonance in a waveguide-coupled ring microresonator</b>	<b>48</b>	<b>Spatial solitons in optical fibres: a finite element analysis</b>	<b>65</b>
<i>Jiri Ctyroky, Ivan Richter, Milan Šinor</i>		<i>F. Drouart, G. Renversez, A. Nicolet, C. Geuzaine</i>	
<b>Hybrid analytical / numerical coupled-mode modeling of guided wave devices</b>	<b>49</b>	<b>Modeling Electromagnetically Induced Transparent Media Using the Finite-Difference Time-Domain Method</b>	<b>66</b>
<i>Manfred Hammer</i>		<i>Curtis W. Neff, Mauritz Andersson, Min Qiu</i>	
<b>Fabrication Tolerant Design of Bent Singlemode Rib Waveguides on SOI</b>	<b>50</b>	<b>Possibility of Frequency Transformation in Time-Varying Dielectric Structures</b>	<b>67</b>
<i>R. Halir, A. Ortega-Moñux, J.G. Wangüemert-Pérez, I. Molina-Fernández, P. Cheben</i>		<i>Alexander Nerukh, Nataliya Sakhnenko</i>	
<b>High index-contrast multi-layer waveguides</b>	<b>51</b>	<b>Account of the Active Region Shape in the Linear Modelling of Microcavity Lasers</b>	<b>68</b>
<i>F. Morichetti, R. Costa, A. Melloni, R.G. Heideman, M. Hoekman, A. Borreman, A. Leinse</i>		<i>A.I. Nosich, E.I. Smotrova, T.M. Benson, P. Sewell</i>	
<b>Analysis of Propagation in Multimode Fibre and Waveguide Devices</b>	<b>52</b>	<b>A Non-iterative Bi-directional Wave Propagation Method based on the Split-Step Non-Paraxial (SSNP) Method</b>	<b>69</b>
<i>John Love</i>		<i>Anurag Sharma, Manmohan Singh Shishodia</i>	
<b>Cladding Mode Coupling Suppression in Bent Single-Mode Slab Waveguides</b>	<b>53</b>	<b>Finite element-based numerical methods for Photonic Devices</b>	<b>70</b>
<i>Céline Durniak, John Love</i>		<i>B.M.A. Rahman, A. Agrawal, S.S.A. Obayya, A.K.M.S. Kabir, K. Namassivayane, M. Rajarajan, K.T.V. Grattan</i>	
<b>Rigorous analysis of the coupling between two non-parallel optical fibers</b>	<b>54</b>	<b>A Domain Decomposition Method for Photonic Crystal Modeling</b>	<b>71</b>
<i>Ioannis Chremmos, Nikolaos Uzunoglu, George Kakarantzas</i>		<i>Yuxia Huang, Ya Yan Lu</i>	
<b>A source model technique (SMT) for the analysis of the modal fields of Photonic Crystal Fibers</b>	<b>55</b>	<b>Grating and waveguide concepts in photonic crystal devices</b>	<b>72</b>
<i>Yehuda Leviatan</i>		<i>P. Lalanne, J.P. Hugonin</i>	
<b>Differential toolbox to model microstructured-fiber behaviour</b>	<b>57</b>	<b>Controllable phaseshift in mirror based slab waveguides</b>	<b>73</b>
<i>J.J. Miret, E. Silvestre, T. Pinheiro-Ortega, P. Andrés</i>		<i>D. Pietroy, M. Flury, A.V. Tishchenko, O. Parriaux</i>	
<b>Single-Polarization and Controllable Birefringence Guidance in Liquid-Crystal Microstructured Fibers</b>	<b>58</b>	<b>Cancellation of the 0th order in a phase mask by mode interplay in a high contrast binary grating</b>	<b>74</b>
<i>Dimitrios C. Zografopoulos, Emmanouil E. Kriezis, Theodoros D. Tsiboukis</i>		<i>E. Gamet, A.V. Tishchenko</i>	
<b>Dynamics of the Long Period Grating in the Photonic Crystal Fibre with Bulk Cladding</b>	<b>59</b>	<b>Spectrally and spatially tunable microphotonic devices associating MOEMS and Photonic Crystal structures</b>	<b>75</b>
<i>Vladimir Mezentsev, Jovana S. Petrovic, Helen Dobb, David J. Webb</i>		<i>Xavier Letartre, Salim Boutami, Jean-Louis Leclercq, Pierre Viktorovitch</i>	
<b>Analysis of leaky photonic crystal fibers by means of an improved Fast-Fourierbased full-vectorial mode solver</b>	<b>60</b>	<b>An ARROW-based silicon-on-insulator photonic crystal waveguides with reduced losses</b>	<b>76</b>
<i>Alejandro Ortega-Moñux, J. Gonzalo Wangüemert-Pérez, Iñigo Molina-Fernández</i>		<i>Andrei Lavrinenko</i>	
<b>Numerical Analysis of Hollow Core Photonic Band Gap Fibers with Modified Honeycomb Lattice</b>	<b>61</b>		
<i>Claudia Gazzetti, Moreno Maini, Luca Vincetti, Stefano Selleri, Annamaria Cucinotta, Federica Poli</i>			

<b>An Accurate Analytical Method for Simulating AWG Components</b>	<b>77</b>
<i>F.P. Payne, S. Paquet</i>	
<b>Analysis of Slot Characteristics in Single Mode Semiconductor Lasers using the Scattering Matrix Method (SMM)</b>	<b>78</b>
<i>Q. Y. Lu, W. H. Guo, R. Phelan, D. Byrne, J. F. Donegan</i>	
<b>FDTD Modelling and Experimental Verification of FWM in Semiconductor Micro-Resonators</b>	<b>79</b>
<i>Masafumi Fujii, Christian Koos, Christopher Poulton, Juerg Leuthold, Wolfgang Freude</i>	
<b>Time-domain analysis of parametric frequency conversion</b>	<b>80</b>
<i>Michele Lauritano, Stefano Trillo, Gaetano Bellanca</i>	
<b>An all-optical switching structure based on the decoupling property of two parallel photonic crystal waveguides</b>	<b>81</b>
<i>Ivan S. Maksymov, Lluís F. Marsal, Josep Pallarès</i>	
<b>Time resolved numerical simulation of a single laser beam in a photorefractive semi-conductor for telecommunications applications</b>	<b>82</b>
<i>Delphine Wolfersberger, Naima Khelifaoui, Cristian Dan, Nicolas Fressengeas</i>	
<b>Continuation method applied to the bifurcation analysis of polarization dynamics in vertical-cavity surface-emitting lasers</b>	<b>83</b>
<i>Marc Sciamanna, Ignace Gatare, Krassimir Panajotov</i>	
<b>All-Optical AND Gate based on Raman effect in Silicon-on-Insulator Waveguide</b>	<b>84</b>

## Authors Index

M.	Agio	26	S.	Fan	12
A.	Agrawal	38, 70	E.	Fazio	19
M.	Alonzo	19	M.	Flury	20, 73
M.	Andersson	66	M.	Foroni	3, 37, 45
P.	Andrés	39, 57	N.	Fressengeas	82
L.C.	Andreani	5	W.	Freude	1, 79
N.	Argiolas	19, 34	M.	Fujii	1, 79
K.A.	Atlasov	7	D.F.G.	Gallagher	15
E.	Autizi	34	E.	Gamet	74
R.	Baets	14	I.	Gatare	83
S.	Balsamo	16	C.	Gazzetti	61
M.	Bazzan	19, 34	C.	Geuzaine	65
G.	Bellanca	80	K.M.	Golant	30
T.M.	Benson	6, 68	K.T.V.	Grattan	70
M.	Bertolotti	36	A.	Gugliera	16
D.	Bhattacharya	38	W.H.	Guo	78
P.	Bienstman	5, 14, 27	C.	Hafner	23
A.	Borreman	51	R.	Halir	50
S.	Boutami	75	M.	Hammer	49
J.	Brosi	1	R.G.	Heideman	51
A.C.	Busacca	18	S.	Helfert	21
D.	Byrne	78	M.	Hoekman	51
L.	Cahill	17	H.J.W.M.	Hoekstra	10, 22
E.	Cantelar	18	W.C.L.	Hopman	5, 22
A.D.	Capobianco	34	R.	Houdré	62
M.	Centini	36	Y.	Huang	71
M.	Chauvet	19	J.P.	Hugonin	5, 72
P.	Cheben	50	T.	Jalali	23
I.	Chremmos	54	A.K.M.S.	Kabir	70
A.C.	Cino	18	G.	Kádár	4
M.	Conforti	80	G.	Kakarantzas	54
R.	Costa	5, 42, 51	E.	Kapon	7
J.	Ctyroký	48	K.F.	Karlsson	7
A.	Cucinotta	3, 37, 45, 61	J.	Kautz	22
G.	Cusmai	42	N.	Khelifaoui	82
F.	Cussò	18	A.N.	Kireev	13
C.	Dan	82	S.V.	Kolosova	35
C.	De Angelis	80	C.	Koos	1, 79
F.	De Leonardis	32, 84	E.	Kriezis	58
R.M.	de Ridder	22	S.	Kuzmin	24
P.	Debackere	14	M.L.	Martinez-Ricci	39
R.	Dekker	22	P.	Lalanne	5, 72
R.A.	Depine	39	Y.	Larionov	24
N.	Destouches	20	M.	Lauritano	80
A.	Di Donato	11	A.	Lavrinenko	76
H.	Dobb	59	G.	Leahu	19
M.	Domenech	18	H.	Leblond	82
J.F.	Donegan	78	J.L.	Leclercq	75
F.	Drouart	65	F.	Lederer	63
C.	Durniak	53	A.	Leinse	51
D.	Erni	23	X.	Letarte	25, 75
E.M.	Fabbri	41	J.	Leuthold	1, 79
P.	Faccin	41	Y.	Leviatan	55

G.	Lifante	18	G.	Priem	27
A.	Locatelli	80	M.	Qiu	66
J.	Love	52, 53	B.M.A.	Rahman	70
Y.Y.	Lu	71	M.	Rajarajan	70
Q.Y.	Lu	78	G.	Renversez	65
F.	Magno	33	I.	Richter	48
M.	Maini	45, 61	S.	Riva Sanseverino	18
I.	Maksymov	81	P.	Rojo-Romeo	25
L.	Marsal	81	L.	Rosa	3, 37, 41
O.J.F.	Martin	13	T.	Rozzi	11
M.	Martinelli	42	N.	Ruzhytska	28
A.	Massaro	11	S.	Ruzhytska	35
P.	Mazzoldi	19, 34	C.	Sada	19, 34
A.	Melloni	5, 27, 42, 51	N.	Sakhnenko	67
D.	Mencarelli	11	M.	Scalora	36
V.	Mezentsev	59	T.	Schimmel	1
J.J.	Miret	57	M.	Sciamanna	83
A.	Mohammadi	26	L.	Sciscione	36
I.	Molina-Fernández	50, 60	C.	Seassal	25
J.V.	Moloney	8	S.	Selleri	3, 5, 37, 41, 45, 61
M.	Mongiardo	46	P.	Sewell	6, 68
J.A.	Monsoriu	39	A.	Sharma	38, 69
F.	Moricchetti	27, 51	V.V.	Shevchenko	29
M.	Müller	1	M.	Shishodia	69
K.	Namassivayane	70	C.	Sibilia	36
C.	Neff	66	E.	Silvestre	39, 57
A.	Nerukh	28, 67	M.	Šinor	48
D.	Nerukh	28	E.I.	Smotrova	68
A.	Nicolet	65	A.	Sopaheluwakan	40
N.	Nikolaev	29	R.	Stoffer	10
A.I.	Nosich	68	C.	Styan	6
J.Kh.	Nurligareev	30	V.	Svetikov	24
S.S.A.	Obayya	5, 31, 70	V.A.	Sychugov	24, 30, 44
A.	Ortega-Moñux,	50, 60	Z.	Szabó	4
J.	Pallarès	81	G.	Tartarini	41
K.	Panajotov	83	A.V.	Tishchenko	20, 73, 74
S.	Paquet	77	S.	Trillo	80
O.	Parriaux	20, 73	A.V.	Tsarev	33, 43
V.M.N.	Passaro	32, 33, 84	T.	Tsiboukis	58
F.P.	Payne	15, 77	H.P.	Uranus	5
W.H.P.	Pernice	15	B.A.	Usievich	44
J.	Petráček	27	N.	Uzunoglu	54
A.	Petris	19	E.	van Groesen	40
J.	Petrovic	59	G.	Veronis	12
F.	Pettazzi	19	P.	Viktorovitch	75
A.	Pfrang	1	L.	Vincetti	45, 61
R.	Phelan	78	V.I.	Vlad	19
L.	Pierantoni	11	A.	Vukovic	6
D.	Pietrozy	73	J.G.	Wangüemert-Pérez	50, 60
F.M.	Pigozzo	34	D.	Webb	59
T.	Pinheiro-Ortega	57	D.	Wolfersberger	82
D.	Pinto	5, 31	D.	Yudistira	10
F.	Poli	3, 37, 45, 61	V.	Zabelin	62
C.	Poulton	1, 79	D.	Zografopoulos	58